新 制
工
932
京大附図

Theoretical Studies on the Electronic Structures of Molecules in Excited, Ionized, and High-Spin States

Masahiro Ehara

1993

Theoretical Studies on the Electronic Structures of Molecules in Excited, Ionized, and High-Spin States

Masahiro Ehara

1993

PREFACE

Advances in various fields of molecular spectroscopies are remarkable in recent years and they have clarified fine details of excited and ionized states in wide energy regions of various molecules. In addition to the determinations and assignments of the electronic states, they have been applied to predict or to design new chemical reactions which utilize the characteristic properties of the excited and ionized states. The time resolved technique has made it possible to directly observe the transient species of the chemical reactions and has opened new fields. According to these developments of precise and fine experimental techniques, accurate theoretical informations, as represented by the *ab initio* potential energy surfaces and dynamical calculations including excited states, have become considerably important for the analyses of these experiments and for the designs of new experimental systems.

The quantum chemistry has also developed so much in recent years and has become to be able to deal with large molecular systems and to provide highly accurate results. It has been considerably applied to clarify the electronic structures of molecules and to elucidate the mechanism of the chemical reactions. These extensive applications may be attributed to the developments of both the theoretical methodologies and computational facilities. Attempt to obtain quantitative results with accurate description of electron correlations has been one of the major subjects in quantum chemistry. Various kinds of refined methods have been proposed and applied to the molecular spectroscopies, however, the method which is applicable to open shell systems and to large number of solutions seems to have been limited. The difficulties exist in the electronic structure of open-shell system itself and the theoretical treatment of the open-shell model.

The SAC/SAC-CI method developed by H. Nakatsuji in 1978, which has been used in this thesis, is based on the cluster expansion theory and describes electron correlation accurately and effectively. The method is applicable to open-shell systems, to large number of states, and to the systems with different number of electrons. The theory and the program systems of the method have been established before the author started the present works. The extension of the method to quasi-degenerate case has also been already accomplished as the EGCI and MEG4/MEG4-CI methods. The author has extended these methods to high-spin multiplicity. He has also performed

highly accurate calculations on the excited and ionized states of transition metal complexes and chemical reaction of weak interacting systems in optical field.

In part I, the methods, which are accurate and efficient for calculating the high-spin states of molecules, are investigated. Firstly, the SAC-CI(symmetry adapted cluster-configuration interaction) method is extended to high-spin multiplicity in chapter 1. The method is originally formulated for arbitrary spin multiplicity, however, its implementation has been limited up to triplet so far. The program is extended to high-spin multiplicities from quartet to septet and the SAC-CI(SD-R, DT-R, TQ-R) method is applied to several high-spin states of the N_2, N_2^+, OH, m-PBM molecules at their equilibrium geometries of the ground states. The results show good agreements with those of the full-CI reference calculations.

The SAC-CI(SD-R) method has been successfully applied to the calculations of hyperfine splitting constants (hfsc's) of various doublet radicals. In chapter 2, the accuracy and usefulness of the SAC-CI method for calculating the hfsc's are examined. Two kinds of the SAC-CI expansion are performed: SAC-CI(SD-R, DT-R) method, in which lower-order excitation operators are included in R operators and SAC-CI(general-R) method, in which higher-order ones are also included. The hfsc's for the doublet, triplet, and quartet states of small radicals are calculated by the SAC-CI method and the results are compared with the full-CI ones. Another topic in this study is to propose a configuration selection method in which both energy and hfsc are used as criteria. The method, which is applicable to ordinal CI method, is shown to be effective for accurate calculation of the hfsc's especially for large systems and high-spin systems, where large number of CFS's are required.

High-spin molecules often have quasi-degenerate characters with various spin multiplet states owing to their highly-degenerate open-shell structure. In chapter 3, theoretical method for investigating the energetics and the properties of these quasi-degenerate high-spin states is developed. The $\mathscr{EXP}$ operator, which is suitable for describing the quasi-degenerate system, is adopted and the EGCI method is adopted among the several methodologies because of its conceptual and computational simplicity. The method is applied to large numbers of the quasi-degenerate high-spin states such as potential curves of C_2 and C_2^+, quasi-degenerate states of N_2 and N_2^+,

and low-lying states of m-PBM. The accuracy of the EGCI wave function is also examined in terms of the hfsc's of C_2^+ and the spin density distributions of m-PBM.

In part II, the electronic structures of the excited and ionized states of titanium tetraharides are studied theoretically by the SAC/SAC-CI method. The electronic spectra of these metal complexes are complicated because (1) five valence shells lie in very narrow energy region and (2) spin-orbit interactions of the ligands are strong. In chapter 4, $TiCl_4$ is investigated in terms of the excitation spectrum both in UV and VUV regions and ionization spectrum both in outer and inner valence regions. The parallel calculation using MRD-CI method is also performed and the results show essentially consistent assignments of the spectrum.

The excitation and ionization spectra of TiX_4 (X=Br, I) are studied by the SAC/SAC-CI method in chapter 5. The valence excited states and the ionized states in the outer valence region of these molecules are investigated and the assignments of the spectra are systematically performed in comparison with the study on $TiCl_4$. The inclusion of the spin-orbit interaction of the ligands is shown to be very important for the assignments or interpretations of the spectra.

In part III, collision induced absorption process of Cs-Rg (Rg= Ne, Ar, Kr, and Xe) system is investigated. Dipole forbidden transitions of alkali or alkali-earth atoms are transformed into dipole allowed ones when perturbed by rare gas atoms. This phenomenon so-called collision induced absorption process has important meaning because it is a basic and primary example of the advanced photo-assisted chemical reactions. In chapter 6, collision induced absorption spectra of the CsXe system associated to dipole-forbidden 5D and 7S line of the Cs atom are investigated by ab-initio potential curves and induced dipole moments. The weak open-shell vdw interaction between Cs and Xe is accurately described by the SAC-CI method and therefore, the calculated induced absorption spectra reproduce well the experimental spectra. However, the quality of basis sets is not satisfactory for getting the proper ordering between 5D and 7S level of the Cs atom in this calculations.

In chapter 7, we overcome this problem with refined basis sets and then investigate this phenomenon systematically with the perturber substituted by other rare gas atoms. The potential energy curves which correlate to 6S, 6P, 5D, and 7S states of the Cs atom and the oscillator strengths of corresponding electronic transitions are

calculated. Experimental spectra show systematic changes of the peaks and absorption intensities as the rare gas atoms are substituted. The origins of these systematical changes of the spectra are discussed in detail. The results of the calculated shift values and intensities show good agreements with the experimental data. The broadening of 6P resonance line is also considered and is shown to be explained in the same way.

Masahiro Ehara

Kyoto,
September, 1993

ACKNOWLEDGMENTS

The present thesis is the summary of the author's studies carried out at the Faculty of Engineering of Kyoto University from 1988 to 1993. The author studied at the Division of Molecular Engineering for the first term of the course (1988-1990) and at the Department of Synthetic Chemistry for the latter term (1991-1993). The author is indeed happy to express his cordial gratitude to Professor Hiroshi Nakatsuji for his continuous guidance, valuable discussions, and warm encouragements throughout the course of this study.

The part of this thesis is summarized at the Institute for Fundamental Chemistry (IFC). The author would like to express his sincere gratitude to Professor Kenichi Fukui, the director of IFC, for his warm understanding and encouragements. He is also obliged to Dr. Koichi Yamashita for his warm encouragements and for giving him new fields of quantum chemistry.

The author would like to thank Professor Ken-ichi Honda and Professor Isao Morishima for their warm encouragements and precious suggestions at the beginning of this study.

The author wishes to thank Dr. Masahiko Hada and Dr. Hiromi Nakai for their suggestions and encouragements. He is indebted to Dr. Yoshihiro Mizukami, Dr. Taketoshi Nakao and Mr. Masaru Izawa. He thanks Mr. Manabu Sugimoto and Mr. Shinji Saito for their valuable discussions on the quantum chemistry. He thanks Mr. Yoshifumi Fukunishi, Mr. Shinya Jitsuhiro and Miss Masami Yoshimoto. Thanks are also due to the other members of our group and the members of IFC.

During the course of the study, the author has many opportunities of valuable collaborations with other research groups. He is obliged to Professor Micheal F. Palmer for the collaboration of the research presented in Part II. He is also indebted to Dr. Kiyoshi Ueda and Professor Noriyuki Sato for valuable discussions and suggestions in the course of the study presented in Part III. He would like to express his gratitude to Dr. Takamasa Momose for kindly letting him use full-CI program, which was quite useful for the studies in Part I, and for severe encouragements. He also thanks Dr. Hidetoshi Suemitsu and Professor Takashi Fugimoto for the collaborative studies not presented in this thesis.

The numerical calculations were carried out with FACOM M780/30 and VP400E computers at the Data Processing Center of Kyoto University, HITAC M680H and S810/10 computers at the Institute for Molecular Science, and the power stations of Nakatsuji's laboratory and those of IFC.

Finally, the author expresses his sincere gratitude to his parents, Mr. Masanao Ehara and Mrs. Yoko Ehara, and to his brother, Mr. Kouji Ehara, and to his fiancee, Miss Kumiko Tsuji, for their continuous understanding, hearty encouragements and financial supports.

CONTENTS

PREFACE ..... (i)
ACKNOWLEDGMENTS ..... (v)
CONTENTS ..... (vii)

PART I. Theoretical Studies on the High-Spin States of Molecules

Chapter 1. SAC-CI method applied to high-spin multiplicity 3

Chapter 2. Hyperfine splitting constants studied by the SAC-CI method 19

Chapter 3. EGCI method applied to high-spin multiplicity 37

PART II. Theoretical Studies on the Excited and Ionized States of Titanium Tetraharides

Chapter 4. Theoretical study on the excited and ionized states of titanium tetrachloride 63

Chapter 5. Theoretical study on the excited and ionized states of $TiBr_4$ and TiI_4 93

PART III. Theoretical Studies on the Collision Induced Absorption Spectra of CsRg System (Rg=Xe, Kr, Ar, Ne)

Chapter 6. Collision induced absorption spectra of CsXe system calculated by the SAC-CI method with ECP potentials 129

Chapter 7. Collision induced absorption spectra of CsRg system (Rg=Xe, Kr, Ar, Ne) calculated by the SAC-CI method with all-electron basis sets 139

LIST OF PUBLICATIONS 165

PART I

Theoretical Studies on the High-Spin States of Molecules

Chapter 1

SAC-CI method applied to high-spin multiplicity

ABSTRACT

The SAC-CI(symmetry adapted cluster-configuration interaction) method is extended to high-spin multiplicity and applied to the quartet, quintet, sextet, and septet states of N_2, N_2^+, OH, and m-phenylenebis(methylene) (m-PBM) molecules. The results show good agreements with those of the full-CI reference calculations, though the dimensions of the calculations are much smaller than those of the full-CI method. The smallness of the calculational efforts and the excellent agreement with the full-CI results assure that the SAC-CI method is useful and accurate not only for singlet, doublet, and triplet states but also for high-spin multiplet states.

I. INTRODUCTION

High-spin states sometimes occur for molecules with degenerate or near-degenerate orbital structures. Some transition metal complexes and clusters have high-spin states in their ground and excited states. For linear molecules, high-spin states often play a significant role in predissociation and recombination processes.[1-5] For example, $1^5\Sigma_g^+$ state of N_2 is known to be responsible for the predissociation of $a^1\Pi_g$ and $B^3\Pi_g$ states and for the recombination of the two $N(^4S)$ atoms.[2] The predissociation observed for the $A^2\Sigma^+(v=2)$ state of OH radical is attributed to the existence of the repulsive $1^4\Sigma^-$ state.[3-5] Other interesting examples of high-spin states are organic ferromagnetic molecules:[6-14] several organic π-conjugated molecules composed of methylene and phenylene fragments show ferromagnetism in their ground state due to "topological degeneracy": Molecules of high-spin ground states up to tridecet (S=6) state have been synthesized.[11] For some ferromagnetic molecules, several different spin states lie closely together,[12] so that accurate theoretical information on the relative stability is very important for definite identifications. However, these molecules are sometimes so large that the calculations including spin and electron correlations with large basis sets are difficult. In this sense, we need a theory which is useful and yet accurate for all the low- and high-spin multiplicities.

The SAC(symmetry adapted cluster)/SAC-CI theories are based on the cluster expansion method and are designed to describe electron correlations efficiently.[15-18] The method has been applied successfully to various systems of excited, ionized, and electron attached states and has been confirmed to be simple and accurate enough to be useful.[18] The SAC-CI theory was originally formulated for arbitrary spin multiplicity,[16] though the implementation has been limited so far up to triplet-spin multiplicity.[19] The method has been extended to arbitrary multi-reference cases.[20,21] In the present article, we apply the SAC-CI method to the calculations of several high-spin multiplet states, namely, quartet, quintet, sextet, and septet states. Benchmark calculations have been performed for the high-spin states of N_2, N_2^+, OH, and m-phenylenebis(methylene) molecules. The accuracy of the SAC-CI results is examined by comparing with the full-CI results.

II. METHOD AND CALCULATIONS

The SAC wave function is expressed as[15]

$$\Psi_g^{SAC} = Q \exp\left(\sum_I C_I S_I^\dagger\right)|0\rangle$$

where $|0\rangle$ is a single determinant (usually Hartree-Fock), $S_I^\dagger$ a symmetry adapted excitation operator, and Q a symmetry projector. The SAC-CI wave function is constructed by applying the reaction operator $\mathfrak{R}$ to the SAC wave function as[16]

$$\Psi_e^{SAC\text{-}CI} = \mathfrak{R}\, \Psi_g^{SAC}$$

where the excitator $\mathfrak{R}$ generates excited, ionized, and electron-attached states. The excitator $\mathfrak{R}$ is expanded by a linear combination of the excitation operators as

$$\mathfrak{R} = \sum_K d_K P\, R_K^\dagger$$

where P is the projector that projects out the space of the SAC wave function, and $R_K^\dagger$ is the excitation, ionization, or electron attachment operator.[16] In the present SAC-CI method for high-spin multiplicity, the $R_K^\dagger$ operator is defined to generate the corresponding high-spin multiplicity.

In the program SAC85,[19] the $R_K^\dagger$ operators represent single and double excitations. Recently, we reported that the inclusion of higher excitation operators is effective for improving the accuracy for multiple-electron excitation processes.[22] In the present calculation, we follow the spirit of the program SAC85: we include two- and three-electron excitation operators, R(2) and R(3), for $R_K^\dagger$ of the quartet and quintet states. Namely, as shown in Table I, the symmetry adapted 2h-1p, 3h-2p and 2h-2p, 3h-3p operators are included for quartet and quintet states, respectively. Three- and four-electron excitation operators, R(3) and R(4), are used for sextet and septet states. We include all independent spin-functions, except for the case stated later. The explicit forms of these linked operators are given in Table I. For the unlinked operators, we include the products of the double excitation operators $S_I^\dagger$ of Ψ_g^{SAC} and the lower-excitation operators of $R_K^\dagger$, which are R(2) for quartet and quintet states and R(3) for sextet and septet states; for quartet, for example, $\{S_i^a S_j^b \times R_{kl}^c\}$ operators are included, but $\{S_i^a S_j^b \times R_{klm}^{cd}\}$ operators are not included except

for the calculations of the quartet states of OH radical. The unlinked operators included in the present calculation are also summarized in Table I.

The present method is applied to the several lower states of the singlet to septet states of N_2, N_2^+, OH, and m-phenylenebis(methylene) (m-PBM) molecules. The internuclear distances of N_2 and N_2^+ are taken to be 1.09768Å for all the states, which is the equilibrium distance of the ground state of the N_2 molecule. The OH distance of 0.96966Å, which is again the equilibrium distance for the ground state, is used for all the states of OH. The molecular structure of m-PBM is depicted in Fig. 1. The phenylene and methylene geometries are borrowed from those of the free benzene and methylene: the C-C and C-H lengths in benzene ring are set to 1.397Å and 1.084Å, respectively, and the C-C-H angle and the C-H length of methylene group are 140° and 1.08Å, respectively. The basis set of N is the [4s2p] set of Huzinaga and Dunning[23] plus Rydberg s function with ζ_s=0.028. The basis set for OH is the [4s2p/2s] set.[23] For m-PBM molecule, the STO-6G basis is used. The resultant SCF dimensions are 22, 12, and 46 for N_2, OH, and m-PBM, respectively.

The SAC/SAC-CI calculations are performed without configuration selection. The high-spin calculations are carried out by modifying the SAC85 program.[19] The RHF MOs are calculated by the program HONDO7[24] and are used as the reference orbitals. The full-CI calculations are performed for examining the accuracy of the present method. In order to keep the size of the full-CI calculation to be practical, the active space is limited to be very small: five occupied and five unoccupied MOs are adopted for N_2; $(2s\sigma_g)^2(2s\sigma_u)^2(p\pi_u)^4(p\sigma_g)^2$(Rydberg s, σ_g)(Rydberg s, σ_u)($p\pi_g$)($p\sigma_u$), and four occupied and seven unoccupied MOs for m-PBM. For OH radical, all 12MOs are included in the active space. The full-CI calculation of OH radical is performed by using the slater-determinant-based algorithm of Knowles et al.[25] coded by Momose.[26] Other full-CI calculations are done using the program HONDO7.[24]

III. RESULTS

A. N_2 and N_2^+

First, we investigate the accuracy of the present method for N_2 and N_2^+. They have a number of excited states of various spin-multiplicity. The valence MO of N_2 is

TABLE I. Linked and unlinked operators included in the present calculation.

Spin multiplicity	Linked operator[a,b]			Unlinked operator[c]
Quartet	R(2)	$= R_{ij}^{a}$ $= a_{a\alpha}^{\dagger}a_{i\beta}a_{j\beta}$	$R(3) = S_i^{a}R_{jk}^{b}$	$S(2)R_{ij}^{a}$
Quintet	R(2)	$= R_{ij}^{ab}$ $= a_{a\alpha}^{\dagger}a_{b\alpha}^{\dagger}a_{i\beta}a_{j\beta}$	$R(3) = S_i^{a}R_{jk}^{bc}$	$S(2)R_{ij}^{ab}$
Sextet	R(3)	$= R_{ijk}^{ab}$ $= a_{a\alpha}^{\dagger}a_{b\alpha}^{\dagger}a_{i\beta}a_{j\beta}a_{k\beta}$	$R(4) = S_i^{a}R_{jkl}^{bc}$	$S(2)R_{ijk}^{ab}$
Septet	R(3)	$= R_{ijk}^{abc}$ $= a_{a\alpha}^{\dagger}a_{b\alpha}^{\dagger}a_{c\alpha}^{\dagger}a_{i\beta}a_{j\beta}a_{k\beta}$	$R(4) = S_i^{a}R_{jkl}^{bcd}$	$S(2)R_{ijk}^{abc}$

[a] The operator S_i^{a} denotes singlet-type single excitation operator; $S_i^{a} = (a_{a\alpha}^{\dagger}a_{i\alpha} + a_{a\beta}^{\dagger}a_{i\beta})/\sqrt{2}$

[b] Values in parentheses denote excitation levels relative to the closed-shell Hartree-Fock configuration.

[c] The operator S(2) denotes double excitation operators like $S_i^{a}S_j^{b}$ of Ψ_g^{sac}.

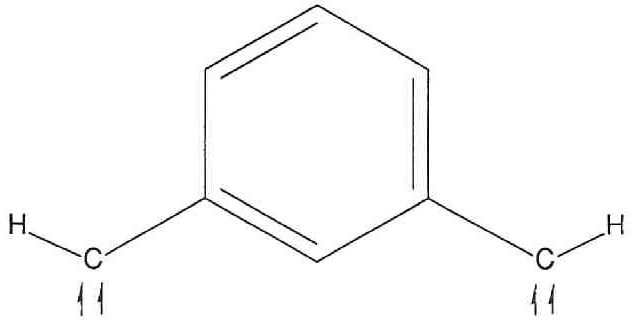

FIG. 1 m-Phenylenebis(methylene) molecule

$(p\sigma_g)^2(p\pi_u)^4(p\pi_g)(p\sigma_u)$ in its ground state. Six or five electrons distribute among these orbitals, and therefore high-spin states up to septet state exist for N_2 and those up to sextet state for N_2^+. Some of these high-spin states are important in the predissociation and recombination processes. Potential curves of these high-spin states cross those of the low-spin states and lead to predissociations. For example, $1^5\Sigma_g^+$ state is a predissociation path of $a^1\Pi_g$ and $B^3\Pi_g$ states, and $1^7\Sigma_u^+$ state dissociates into $N(^4S^0) + N(^4S^0)$ which is the same atomic limit as the $X^1\Sigma_g^+$ state.

We carry out full-CI and SAC/SAC-CI calculations of N_2 and N_2^+ at the equilibrium geometry (R=1.09768Å) of the ground state of N_2. The results are summarized in Tables II and III, which show the leading configurations, total energies, and the size of calculations. 'Excitation level' denotes the number of electrons involved in the excitation from the HF closed-shell configuration. The present choice of the linked operators corresponds to that of the SAC-CI (SD) method[22], and therefore the present calculations give reliable energies for the states whose main configurations are generated by the lower-level excitation operators of the linked term; i.e., single excitations for the states up to triplet-spin multiplicity, double excitations for quartet and quintet states, and triple excitations for sextet and septet states. Tables II and III include only such states. In order to describe the states generated by many-electron processes, higher multiple-excitation operators should be included in the $R_K^\dagger$ operators.[22]

The results for the ground and low-lying excited states of low-spin multiplet states of N_2 and N_2^+ molecules, namely singlet, doublet(ionized), and triplet states are summarized in Table II: the SAC-CI and full-CI results are compared to each other. Three singlet and doublet states and five triplet states are calculated. The SAC-CI method reproduces the correct ordering of these states calculated by the full-CI method. The deviations of the SAC-CI results from the full-CI ones are within 7.5 mhartree in the total energy and within 0.15 eV in the excitation energy. The average discrepancies in the total energy and the excitation energy are 3.92 mhartree and 0.08 eV, respectively. The sizes of the SAC-CI calculation are quite small, less than 100, and two orders of magnitude smaller than the full-CI ones. Thus, the SAC-CI method is very effective for these low-spin states, as already confirmed by many calculations.[16,18,27]

TABLE II. Full-CI and SAC-CI results for singlet, doublet, and triplet states of N_2 and N_2^+.

State	Exitation level	Main configuration[a]	SAC-CI			Full-CI			Exptl. (eV)
			Size	Total energy (Δ[b]) (au)	Excitation energy(Δ[c]) (eV)	Size	Total energy (au)	Excitaion energy (eV)	
Singlet states									
$X^1\Sigma_g^+$	0	0.97(22222)	72	-108.96314 (1.78)	0.0 -	2640	-108.96492	0.0	
$a^1\Pi_g$	1	0.95(222211)	34	-108.61413 (3.90)	9.50 (0.07)	2408	-108.61803	9.43	9.39[d]
$a'^1\Sigma_u^-$	1	0.70(222121)+0.70(2212201)	26	-108.57018 (6.96)	10.69 (0.14)	2296	-108.57714	10.55	10.15-10.45[d]
Average discrepancy				(4.21)	(0.11)				
Doublet states (Ionized)									
$X^2\Sigma_g^+$	1	0.95(22221)	21	-108.38866 (-0.49)	15.63 (-0.06)	3596	-108.38817	15.69	15.60[e]
$A^2\Pi_u$	1	0.97(22122)	13	-108.31827 (5.47)	17.55 (0.10)	3460	-108.32374	17.45	16.98[e]
$B^2\Sigma_u^+$	1	0.91(21222)	27	-108.26169 (7.38)	19.09 (0.15)	3596	-108.26907	18.94	18.78[e]
Average discrepancy				(4.45)	(0.07)				
Triplet states									
$A^3\Sigma_u^+$	1	0.70(221221)+0.70(2221201)	63	-108.65943 (2.98)	8.26 (0.03)	3788	-108.66241	8.23	7.86[d]
$B^3\Pi_g$	1	0.96(222211)	50	-108.66070 (2.96)	8.23 (0.03)	3720	-108.66366	8.20	8.12[d]
$W^3\Delta_u$	1	0.70(222121)-0.70(2212201)	63	-108.61270 (5.65)	9.54 (0.11)	3788	-108.61835	9.43	9.15-9.3[d]
$C^3\Pi_u$	1	0.93(2122201)	58	-108.53963 (5.09)	11.52 (0.09)	3720	-108.54472	11.43	11.25[d]
$E^3\Sigma_g^+$	1	0.94(222210001)	62	-108.51327 (-0.44)	12.24 (0.06)	3688	-108.51283	12.30	(11.95-12.0)[d,f]
Average discrepancy				(3.42)	(0.05)				

[a] The MO ordering is $(\sigma_g)(\sigma_u)(p_x\pi_u)(p_y\pi_u)(p\sigma_g)(p_x\pi_g)(p_y\pi_g)(p\sigma_u)$(Rydberg s,$\sigma_g$)(Rydberg s,$\sigma_u$)
[b] Deviation from the full-CI results (in mhartree).
[c] Deviation from the full-CI results (in eV).
[d] Reference 28-30
[e] Reference 31
[f] Uncertainty in the experimental value is 0.2 eV[29]; the T_0 value is 11.89 eV.[28]

TABLE III. Full-CI and SAC-CI results for quartet, quintet, sextet, and septet states of N_2 and N_2^+.

State	Excitation level	Main configuration[a]	SAC-CI Size	SAC-CI Energy	Full-CI Size	Full-CI Energy	Difference (mhartree)
Quartet states (Ion)[b]							
$1^4\Sigma_u^+$	2	0.68(222110001)+0.68(22121001)	89	-108.07606	2416	-108.07561	-0.45
$1^4\Delta_u$	2	0.68(22211001)+0.68(221210001)	87	-108.02787	2524	-108.03024	2.37
$1^4\Pi_u$	2	0.96(212210001)	87	-108.00566	2480	-108.01184	6.18
$1^4\Sigma_u^-$	2	0.68(22211001)-0.68(221210001)	87	-108.00257	2524	-108.00787	5.30
$1^4\Pi_g$	2	0.98(221120001)	89	-107.97544	2480	-107.97792	2.48
$1^4\Sigma_g^+$	2	0.66(21122001)+0.66(212120001)	85	-107.96563	2524	-107.96668	1.05
$1^4\Delta_g$	2	0.66(21122001)-0.66(212120001)	87	-107.91663	2416	-107.91995	3.32
$1^4\Sigma_g^-$	2	0.66(21212001)-0.66(211220001)	85	-107.89388	2524	-107.90043	6.55
Average discrepancy							3.46
Quintet states[c]							
$1^5\Pi_u$	2	0.98(221210011)	128	-108.37714	1540	-108.37756	0.42
$1^5\Sigma_g^+$	2	1.00(221120011)	124	-108.35819	1540	-108.35838	0.19
$1^5\Sigma_u^-$	2	0.98(212210011)	128	-108.34024	1580	-108.34665	6.41
$1^5\Pi_g$	2	0.95(212120011)	120	-108.26921	1540	-108.26999	0.78
$1^5\Sigma_u^+$	2	0.68(22121101)+0.68(222111001)	116	-108.20347	1515	-108.20611	2.64
$2^5\Sigma_g^+$	2	0.65(222110101)+0.65(22121011)	124	-108.16790	1540	-108.17082	2.92
$1^5\Delta_u$	2	0.68(22211101)+0.68(221211001)	116	-108.16048	1515	-108.16045	-0.03
$2^5\Pi_u$	2	0.96(212211001)	128	-108.13264	1540	-108.13890	6.26
$1^5\Delta_g$	2	0.65(222110101)-0.65(22121011)	124	-108.12478	1540	-108.12485	0.07
$2^5\Pi_g$	2	0.90(221121001)-0.38(21221011)	120	-108.10537	1540	-108.10831	2.94
Average discrepancy							2.27
Sextet states (Ion)[d]							
$1^6\Pi_g$	3	0.99(212110011)	98	-107.76082	615	-107.76120	0.38
$1^6\Sigma_g^+$	3	0.97(221110011)	98	-107.74308	629	-107.74322	0.14
$1^6\Sigma_u^+$	3	0.99(211120011)	96	-107.62994	629	-107.62988	-0.06
Average discrepancy							0.19
Septet state[e]							
$1^7\Sigma_u^+$	3	0.91(221110111)	80	-107.84480	287	-107.84498	0.18

[a] The MO ordering is $(\sigma_g)(\sigma_u)(p_x\pi_u)(p_y\pi_u)(p\sigma_g)$(Rydberg s,$\sigma_g$)(Rydberg s,$\sigma_u$)$(p_x\pi_g)(p_y\pi_g)(p\sigma_u)$.
[b] Quartet states which dissociate to $N(^4S^0) + N^+(^3P)$ and $N(^4S^0) + N^+(^1D)$.
[c] Quintet states which dissociate to $N(^4S^0) + N(^4S^0)$, $N(^4S^0) + N(^2D^0)$, and $N(^4S^0) + N(^2P^0)$.
[d] Sextet states which dissociate to $N(^4S^0) + N^+(^3P)$.
[e] Septet state which dissociates to $N(^4S^0) + N(^4S^0)$.

The excitation energies for the low-spin states are also compared with the experimental values.[28-31] Because of the insufficiency in the basis set and the active space, the present results do not necessarily reproduce the experimental values. However, the ordering of the excited states is properly reproduced except for the $A^3\Sigma_u^+$ state and the excitation characters are the same as those reported in the previous calculations using extend basis set.[30] The deviations from the experimental values are to within 0.3 eV. Further, the ionization potentials are calculated as 15.63, 17.55, and 19.09 eV for the $X^2\Sigma_g^+$, $A^2\Pi_u$, and $B^2\Sigma_u^+$ states, respectively, which are compared with the experimental values, 15.69, 16.98, and 18.78 eV, respectively.[31]

Next, we examine the results for the high-spin multiplicities. Eight quartet states of N_2^+ are calculated. These quartet states dissociate into $N(^4S^0) + N^+(^3P)$ and $N(^4S^0) + N^+(^1D)$ in their atomic limits. $2^4\Pi_u$ and $2^4\Pi_g$ states whose main configurations are described by three-electron excitation operators are omitted. These eight quartet states exist in a narrow energy region (within 0.18 au.); nevertheless, the present SAC-CI calculation gives the same correct ordering as the full-CI one. The average deviations from the full-CI results are 3.46 mhartree for total energy and 0.06 eV for the ionization energy. These deviations are very small, though the dimensions of the SAC-CI calculations are only 85 ~ 89, very small in comparison with the full-CI ones, 2400 ~ 2500. This shows the efficiency of the SAC-CI method for the quartet states. Among these states, some quartet states are lower than the shake-up states like $C^2\Sigma_u^+$ and $D^2\Pi_g$ states.

We calculate ten quintet spin states and they dissociate into $N(^4S^0) + N(^4S^0)$, $N(^4S^0) + N(^2D^0)$, and $N(^4S^0) + N(^2P^0)$ in the atomic limits. These high-spin states of N_2 molecule lie in a higher-energy region than the first ionized state ($X^2\Sigma_g^+$): a reason is that the present calculation gives the vertical excitation energy. The lowest four states, $1^5\Pi_u$ to $1^5\Pi_g$, have valence excitation nature, while the following six states have the Rydberg components at the present geometry. Again the SAC-CI calculation gives a correct ordering for all of these ten quintet states. The average discrepancy of the SAC-CI results from the full-CI ones is only 2.27 mhartree, though the dimensions of the SAC-CI calculation are very small in comparison with the full-CI ones.

Next, three states of the sextet spin multiplicity are calculated: they dissociate into $N(^4S^0) + N^+(^3P)$. The errors for these sextet states are within 0.4 mhartree and the average error is only 0.19 mhartree. Finally, only one septet state $1^7\Sigma_g^+$ is calculated. This state is described by a three-electron operator and has a Rydberg nature at this geometry. Since the excitation level increases as the spin multiplicity increases, the number of independent spin functions, and therefore the dimensions of the SAC-CI calculation, increase relative to that of the full-CI method: the ratio is ~ 0.04 for quartet and 0.28 for septet. However, when we introduce the configuration selection method[32] or the method described below, we can much reduce the size of the SAC-CI calculation.

We thus conclude that the SAC-CI method gives accurate and efficient descriptions of not only the low-spin multiplicities, singlet, doublet, and triplet, but also the high-spin ones, quartet, quintet, sextet, and septet of the N_2 and N_2^+ molecules.

B. OH radical

Next, we investigate the low-lying electronic states of the OH radical at the equilibrium geometry (R=0.96966 Å) of the ground state. We summarize the result in Table IV. The ground state $X^2\Pi$ and the first excited state $A^2\Sigma^+$ of OH are well described by the one-electron excitation operators, so that these states are properly described by the present SAC-CI (SD) method. The errors of the SAC-CI results are within 2 mhartree. The smallness of the SAC-CI calculation is remarkable: the SAC-CI dimensions are only 44 and 77 in comparison with the full-CI dimensions of 98044 and 97616, respectively.

Two quartet states, $1^4\Sigma^-$ and $1^4\Pi$, exist in a low energy region and have the electronic configurations, $(p\sigma)^2(p\pi)^2(\sigma^*)^1$ and $(p\sigma)^1(p\pi)^3(\sigma^*)^1$, respectively. The total energy of the $1^4\Sigma^-$ state calculated by the SAC-CI method is somewhat worse (the error is 13.9 mhartree) than the preceding results. This SAC-CI calculation is the same as before and includes only $S(2)R_{ij}^a$ type unlinked operators as shown in Table I. We denote this calculation as 'without H35' in Table IV. Examining the calculated result, we find that the $1^4\Sigma^-$ state has some nature of three-electron excitation at this geometry. Therefore, we examine the effect of the unlinked terms of the form $\{S_i^a S_j^b$

TABLE IV. Full-CI and SAC-CI results for doublet and quartet states of OH radical.

State	Excitation level	Main config.[a]	SAC-CI						Full-CI			Exptl. (eV)
			Without H35[b]			With H35[b]						
			Size	Total energy (au) (Δ[c])	Excitation energy (Δ[d]) (eV)	Size	Total energy (au) (Δ[c])	Excitation energy (Δ[d]) (eV)	Size	Total energy (au)	Excitation energy (eV)	
Doublet states												
$X^2\Pi$	1	0.96(2221)	44	-75.49296 (1.67)	-	-	-	-	98,044	-75.49463	-	
$A^2\Sigma^+$	1	0.96(2122)	77	-75.33780 (1.73)	4.22(0.0)	-	-	-	97,616	-75.33953	4.22	4.05[e]
Quartet states												
$1^4\Sigma^-$	2	0.90(22111)	328	-75.17813 (13.93)	8.57(0.34)	328	-75.18734 (4.72)	8.31(0.08)	66,351	-75.19206	8.23	
$1^4\Pi$	2	0.92(21121)	356	-75.07075 (5.82)	11.49(0.11)	356	-75.07738 (-0.81)	11.31(-0.07)	50,904	-75.07657	11.38	

[a] The MO ordering is $(2s)(p\sigma)(p_X\pi)(p_Y\pi)(\sigma^*)$.
[b] H35 means the unlinked integrals of the form <0|R(3)HS(2)R(3)|0>.
[c] Deviation from the full-CI results (in mhartree).
[d] Deviation from the full-CI results (in eV).
[e] Experimental value is term energy.; Reference 34

$\times R_{klm}^{cd}\}$. For saving computer time, we include only such unlinked terms of the R_{klm}^{cd} operators whose CI coefficients in the $\{R_K^\dagger|0\rangle\}$ space is larger than 0.1. The result is given in the column under 'with H35': the deviation from the full-CI is reduced to 4.72 mhartree. We are sure that a better improvement will be obtained if we adopt the SAC-CI(R-general) method reported previously.[22]

The vertical excitation energy of the $A^2\Sigma^+$ state is calculated to be 4.22 eV, which is compared with the experimental term energy, 4.05 eV.[33] Two quartet states are calculated at 8.23 and 11.38 eV, which are lower in energy than the first ionization potential, 12.9 eV, though they are unstable states. The deviations from the full-CI results in the excitation energy are within 0.08 eV.

C. m-Phenylenebis(methylene) (m-PBM)

Last, we investigate the ground state of m-phenylenebis(methylene) (m-PBM). This molecule is the smallest unit of a series of the organic high-spin molecules synthesized in Itoh's[6-12] and Iwamura's[13,14] laboratories. The ground state of m-PBM is calculated to be 1^5A_1 state, the same result as that obtained by Teki et al. using the Heizenberg Hamiltonian.[9] The total energy of this 1^5A_1 state is calculated by different methods and shown in Table V. The SD-CI calculation with the same excitation operators as in the SAC-CI calculation gives a deviation from the full-CI energy by 47.81 mhartree, very large. On the other hand, the SAC-CI result, denoted as 'full' in Table V, deviates only 6.73 mhartree. The 1^5A_1 state of m-PBM is properly described by the two-electron excitation operators of the quintet spin multiplicity, so that the present SAC-CI calculation gives a good description.

Here, we consider a convenient method of reducing the number of linked operators in the SAC-CI calculation. The choice of the excitation operators described in section II has an advantage of giving a large configuration space including various kinds of excitation nature, and therefore, is suitable for solving many roots in a wide energy region. However, the calculation of high-spin multiplicity involves many independent spin functions, and therefore the resultant number of excitation operators becomes large. It is impossible to handle all triple- and quadruple-excitation operators when the active space is large. One possible method is to limit the excitation operators to those that interact with the leading configurations of the reference states, namely

TABLE V. Full-CI and SAC-CI results of 1^5A_1 state for m-phenylenebis(methylene).

Method	Main configuration[a]	Size	Energy(au)	Difference (mhartree)
Full-CI	0.68(221111) +0.41(2211101) -0.38(22110101) -0.23(22110011)	5462	-305.52729	0.0
SD-CI[b]		354	-305.47948	47.81
SAC-CI (Full)		354	-305.52056	6.73
SAC-CI (1-ref.)[c]		122	-305.51920	8.09
SAC-CI (4-ref.)[d]		216	-305.52050	6.79

[a] The MO ordering is (core)(a_2)(b_1)(a_1)(b_2)(a_2)(b_1)(b_1)(a_2)(b_1)(a_1)(a_1).
[b] With 2h-2p and 3h-3p configurations from closed-shell HF.
[c] Reference configuration is (221111).
[d] Four main configurations shown for full-CI are adopted as reference configurations.

single- and double-excitation operators relative to the reference configurations within the symmetry-adapted 2p-2h and 3p-3h operators. This procedure is also performed automatically by the configuration selection method.[32] However, this method makes it possible to omit the generation of a large number of unimportant excitation operators prior to the configuration selection step.

We test this procedure for the 1^5A_1 state of m-PBM. First, we adopt only one main configuration of the 1^5A_1 state as a reference (denoted as SAC-CI (1-ref.)) The dimension is reduced to 122, in comparison with that of the SAC-CI (full) calculation, 354. The energy error is 8.09 mhartree compared with 6.73 mhartree. Next we adopt four configurations given in Table V as reference configurations: this SAC-CI (4-ref.) calculation describes most of the electron correlations obtained by the SAC-CI (full) method. The energy error of the former is 6.79 mhartree in comparison with that of the latter 6.73 mhartree. The usefulness of this method would become more remarkable as the active space becomes larger.

IV. CONCLUSION

The SAC-CI method is extended to high-spin multiplicity and the calculation is carried out for the quartet, quintet, sextet, and septet states. The present results for the several high-spin states of N_2, N_2^+, OH, and m-phenylenebis(methylene) (m-PBM) show good agreements with the full-CI results, though the calculational dimensions of the SAC-CI method are much smaller than those of the full-CI method. We have confirmed that the SAC-CI method is simple enough to be useful and accurate enough to be useful not only for the singlet, doublet, and triplet states,[18] but also for the high-spin quartet, quintet, sextet, and septet states. We have introduced a convenient procedure to omit the generation of a large number of unimportant excitation operators before the configuration selection step. This method is useful for high-spin states.

Higher multiple-electron processes sometimes become important for high-spin states of quasi-degenerate systems. We are now examining the EGCI and MR-SAC methods[20,21,34,35] for describing the quasi-degeneracy in high-spin states.

ACKNOWLEDGMENTS

The authors wish to thank Dr. T. Momose for kindly letting us use his slater-determinant-based full-CI program. The full-CI calculations have been carried out with the HITAC M-680H and S-820 computer at the Institute for Molecular Science. This study has been supported by the Grant-in-Aid for Scientific Research from the Japanese Ministry of Education, Science, and Culture.

REFERENCES

1 F. R. Gilmore, J. Quant. Spectrosc. Radiat. Transfer **5** 369 (1965).

2 M. Krauss and D. B. Neumann, Mol. Phys. **32** 101 (1976).

3 H. H. Michels and F. E. Harris, Chem. Phys. Lett. **3** 441 (1969).

4 I. Easson and M. H. L. Pryce, Can. J. Phys. **51** 518 (1973).

5 K. R. German, J. Chem. Phys. **63** 5252 (1975).

6 K. Itoh, Chem. Phys. Lett. **1** 235 (1967).

7 K. Itoh, in *Magnetic Molecular Materials*, edited by D. Gatteschi *et al.* (Kluwer Academic Dordrecht, the Netherlands, 1991).

8 Y. Teki, T. Takui, K. Itoh, H. Iwamura, and K. Kobayasi, J. Am. Chem. Soc. **108** 2147 (1986).

9 Y. Teki, T. Takui, M. Kitano, and K. Itoh, Chem. Phys. Lett. **142** 181 (1987).

10 I. Fujita,Y. Teki, T. Takui, T. Kinoshita, K. Ito, F. Miko, Y. Sawaki, H. Iwamura, A. Izuoka, and T. Sugawara, J. Am. Chem. Soc. **112** 4074 (1990).

11 K. Furukawa, T. Matsumura, Y. Teki, T. Kinoshita, T. Takui, and K. Itoh, Mol. Cryst. Liq. Cryst. (in press);
K. Furukawa, T. Kinoshita, T. Matsumura, Y. Teki, T. Takui, and K. Itoh, in the proceeding for "The Second Japan-China Symposium on Theoretical Chemistry", September 1992, Institute for Fundamental Chemistry, Kyoto.

12 M. Matsushita, T. Nakamura, T. Momose, T. Shida, Y. Teki, T. Takui, T. Kinoshita, and K. Itoh, J. Am. Chem. Soc. **114** 7470 (1992).

13 T. Sugawara, H. Tukada, A. Izuoka, and H. Iwamura, J. Am. Chem. Soc. **108** 4272 (1986).

14 A. Izuoka, S. Murata, T. Sugawara and H. Iwamura, J. Am. Chem. Soc. **109** 2631 (1987).

15 H. Nakatsuji and K. Hirao, J. Chem. Phys. **68** 2053 (1978).

[16] H. Nakatsuji, Chem. Phys. Lett. **59** 362 (1978); **67** 329, 334 (1979).

[17] H. Nakatsuji, Intern. J. Quantum Chem. Symp. **17** 241 (1983).

[18] H. Nakatsuji, Acta Chim. Hungarica **129** 719 (1992).

[19] H. Nakatsuji, Program system for SAC and SAC-CI calculations, Program Library No.146(Y4/SAC), Data Processing Center of Kyoto University, 1985;
H. Nakatsuji, Program Library SAC85 (No.1396), Computer Center of the Institute for Molecular Science, Okazaki, 1986.

[20] H. Nakatsuji, J. Chem. Phys. **83** 713 (1985); Theoret. Chim. Acta **71** 201 (1987).

[21] H. Nakatsuji, J. Chem. Phys. **95** 4296 (1991).

[22] H. Nakatsuji, Chem. Phys. Lett. **177** 331 (1991).

[23] S. Huzinaga, J. Chem. Phys. **42** 1293 (1965).
T. H. Dunning Jr., J. Chem. Phys. **53** 2823 (1970).

[24] M. Dupuis, J. D. Watts, H. O. Viller, and G. J. B. Hurst,
Program System HONDO7, Program Library No. 544,
Computer Center of the Institute for Molecular Science, (1989).

[25] P. J. Knowles and N. C. Handy, Chem. Phys. Lett. **111** 315 (1984).

[26] T. Momose, Slater-determinant-based Full-CI program based on Knowles algorithm.

[27] K. Hirao and Y. Hatano, Chem. Phys. Lett. **100** 519 (1983); **111** 533 (1984);
H. Nakatsuji, K. Hirao, and Y. Mizukami, *ibid.* **179** 555 (1991).

[28] A. Lofthus and P. H. Krupenie, J. Phys. Chem. Ref. Data. **6** 113 (1977).

[29] F. R. Gilmore, Potential Energy Curves for N_2, NO, O_2 and Corresponding Ions,
RAND Corporation Memorandum R-4034-PR, June, 1964.

[30] S. Shih, W. Butscher, R. J. Buenker, and S. D. Peyerimhoff, Chem. Phys. **29** 241 (1978).

[31] D. W. Turner, C. Baker, A. D. Baker, and C. R. Brundle, *Molecular photoelectron spectroscopy* (Wiley, New York, 1970).

[32] H. Nakatsuji, Chem. Phys. **75** 425 (1983).

[33] G. Herzberg, *Spectra of Diatmic Molecules* (Van Nostrand, New York, 1950).

[34] H. Nakatsuji, J. Chem. Phys. **83**, 5743 (1985).

[35] H. Nakatsuji, J. Chem. Phys. **94**, 6716 (1991).

Chapter 2

Hyperfine splitting constants studied by the SAC-CI method

ABSTRACT

The accuracy and usefulness of the SAC-CI (symmetry adapted cluster-configuration interaction) method for calculating hyperfine splitting constants (hfsc's) are examined. Two kinds of the SAC-CI expansion are performed: SAC-CI(SD-R, DT-R) method, in which single and double(double and triple) excitation operators are included in $R^{\dagger}$ operators and SAC-CI(general-R) method, in which higher-order ones are also included. The hfsc's for the doublet, triplet, and quartet states of small radicals calculated by these two method compare very well with the full-CI results. A convenient configuration selection method, in which both energy and hfsc are used as criteria, is shown to be useful. This method, which is also applicable to ordinal CI method, is effective for accurate calculations of the hfsc's especially for large systems and high-spin systems, where a large number of configurations are required.

I. INTRODUCTION

The hyperfine splitting constant (hfsc) is an important quantity which gives the information of the unpaired electron spin distribution in molecule. It is experimentally observed by ESR and ENDOR techniques. For reliable description of this quantity by ab-initio method, the spin polarization and electron correlation effects and the cusp condition are necessarily included in the calculation.[1-9] This indicates that the theoretical description of the hfsc's requires highly accurate and yet useful method of calculating correlated wavefunctions.

There are some studies[10-12] that report cancelation between incompleteness of the basis sets and neglect of the higher order terms gives accidental agreements of the calculated hfsc's with the experimental values. However, in the sense of general applications, it is important to establish the methods which describe the spin correlations and electron correlations in high accuracy and to discuss the improvements of the basis sets and the importance of cusp condition.

The SAC-CI(symmetry adapted cluster-configuration interaction) method[13] has been successfully applied to the spectroscopy of excited and ionized states and also to the calculations of the hfsc's of various doublet radicals.[3-9] The SAC-CI method, which properly includes both of the spin polarization and electron correlation corrections, gives reliable estimation of the hfsc's. The method, in which higher-order correction terms are described by the unlinked terms, is computationally useful especially for large systems. The SAC-CI method is applicable to arbitrary spin multiplicity[13] and its implementation to high-spin multiplicities of quartet up to septet states has been performed recently.[14] The method would be effective for evaluating the hfsc's of high-spin systems, as well as lower-spin systems. The first purpose of this paper is to examine the accuracy and usefulness of the SAC-CI method for calculating the hfsc's by comparing with the full-CI method. The hfsc's for doublet, triplet, and quartet states of small radical species are examined by two types of the method reported elsewhere, ie. SAC-CI(SD-R, DT-R)[13,14] and SAC-CI(general-R) method.[15] The former method includes lower-order excitation operators in $R^{\dagger}$ operators, while the latter one includes higher-order operators as well.

Accurate calculations of the hfsc's including electron correlation often require large calculational dimensions for the following reasons. (1) Since the inner core

polarization is extremely important for the hfsc's, the calculation should be performed with the active space including both core and valence MO's. (2) Extended basis set including flexible AO's is necessary for obtaining quantitative estimation. (3) The excitation configurations which are important for describing the hfsc's do not necessarily give a large energy contribution and therefore, the configuration selection using only energy threshold is dangerous for the calculation of the hfsc's. Another purpose of this paper is to propose a convenient configuration selection method which avoids discarding such important configurations and guarantees the calculational quality of the hfsc's.

II. METHOD

The SAC-CI wavefunction is constructed by applying the reaction operator to the SAC wavefunction as[13]

$$\Psi_e^{\text{SAC-CI}} = \Re\, \Psi_g^{\text{SAC}}, \tag{1}$$

where the excitator $\Re$ generates excited, ionized, or electron-attached states from the ground state. The excitator is expanded as

$$\Re = \sum_K d_K\, P\, R_K^{\dagger}, \tag{2}$$

where P is a projector which projects out the Ψ_g^{SAC} component, and $R_K^{\dagger}$ is an excitation, ionization, or electron attachment operators of the corresponding spin multiplicity. The Ψ_g^{SAC} usually represents totally symmetric singlet closed-shell system and therefore, the projector P is unnecessary for the $\Psi_e^{\text{SAC-CI}}$ of different spin multiplicity.

There exist two ways of expansion for $R_K^{\dagger}$ operators in the SAC-CI calculation.[15] One choice is to limit $R_K^{\dagger}$ operators to the lower-order electron operators, such as single- and double-excitation operators for up to triplet multiplicities[13] and double- and triple-excitation operators for quartet and quintet multiplicities.[14] The other is to include further the higher-order excitation operators for $R_K^{\dagger}$ operators.[15] The former is designated as SAC-CI(SD-R or DT-R) and the latter as SAC-CI(general-R) method. The latter method is found to be effective for

the quantitative description of the states characterized by multiple excitations. Explicit forms[13,14] of the excitation operators and the method[15] of generating higher-order excitation operators are given elsewhere.

We examine two different configuration selection methods in the present calculations. First is the usual selection method[16] based on the energy selection alone and second is the method proposed here for the calculation of the hfsc's. In the SAC-CI(SD-R, DT-R) calculation for large systems, double-(triple-)excitation operators are usually selected according to their perturbation energy in the following way.[16] Let $\Psi^{(p)}$ be a primary configuration and be expanded as

$$\Psi^{(p)} = \sum_i \alpha_i^{(p)} \phi_i^{(p)} \qquad (p=1,...,N), \tag{3}$$

where $\phi_i^{(p)}$ is single-(double-)excitation operator and N is the number of solutions considered. Double-(Triple-)excitation configuration to be selected is denoted as ϕ_s and $\Delta E_{si}^{(p)}$ is defined as

$$\Delta E_{si}^{(p)} = \frac{|H_{si}^{(p)}|^2}{H_{ii}^{(p)} - H_{ss}^{(p)}}, \tag{4}$$

where $H_{si}^{(p)} = \langle \phi_s | H | \phi_i^{(p)} \rangle$, $H_{ii}^{(p)} = \langle \phi_i^{(p)} | H | \phi_i^{(p)} \rangle$, and $H_{ss}^{(p)} = \langle \phi_s | H | \phi_s \rangle$. Double-(Triple-)excitation configurations are selected for those which satisfy

$$\Delta E_{si}^{(p)} \geq \lambda_e \tag{5}$$

with at least one of the configurations $\phi_i^{(p)}$.

The configurations which involve the excitations from the inner most core MO's, are very important for the description of the hfsc, though they usually give only a small energy contributions. In order not to discard such important configurations in the configuration selection step, the selection should be done on the basis of the contributions not only to the energy but also to the hfsc. Such configuration selection is performed in the following manner. Again let $\Psi^{(p)}$ be a primary configuration defined by eq. (3). Adopting the first order perturbation method, the coefficient c_{si} of the double-(triple-)excitation configuration ϕ_s contributing to the reference function $\phi_i^{(p)}$ is written as

$$c_{si} = \frac{H_{si}^{(p)}}{H_{ii}^{(p)} - H_{ss}^{(p)}} . \tag{6}$$

On the other hand, the integral necessary for the hfsc is written as

$$\lim_{r \to R_A} X_k X_l, \tag{7}$$

where X_k is basis function used and this integral is stored beforehand in MO basis. Then, the contributions of ϕ_s to the spin density and the hfsc of the nucleus A are approximated as

$$D_{kl} = \alpha_i^{(p)} c_{si} \langle \phi_s | s_z | \phi_i^{(p)} \rangle \tag{8}$$

and

$$\Delta V_{hfsc,A} = \sum_{k,l} | \lim_{r \to R_A} D_{kl} X_k X_l | , \tag{9}$$

respectively. Double-(Triple-)excitation configurations are selected for those which satisfy

$$\Delta V_{hfsc,A} \geq \lambda_{hfsc} \tag{10}$$

with at least one of the configurations $\phi_i^{(p)}$ and one of the nuclei A in molecule. The resultant selected configurations are the sum of those which satisfy eqs. (5) and (10).

III. CALCULATION

The present methods are applied to the calculation of the hfsc's of the doublet, triplet, and quartet states of small radicals, that is OH, CH_2, BH_2, CH_3, and H_2O^+. The ground states of these radicals and low lying excited states of OH radicals are examined. The geometries of these radicals are due to experimental values; namely, R_{OH} = 0.96966Å[17] for all the states of OH, R_{CH} = 1.08Å and θ_{HCH} = 134° for $^3B_1$ state of CH_2, R_{BH} = 1.18Å and θ_{HBH} = 131° for $^2A_1$ state of BH_2,[18] R_{CH} = 1.079Å for $^2A_2$" state of CH_3,[19] R_{OH} = 0.999Å and θ_{HOH} = 110.5° for $^2B_1$ state of H_2O^+.[20] The basis sets are limited to double-zeta quality, [4s2p] set for B, C, and O atoms and [2s] set for H atom of Huzinaga and Dunning,[21] in order to keep the size of the full CI

to be practical. The closed-shell RHF MOs of the ground states are calculated by the program HONDO7[22] and are used as the reference orbitals. All MOs are included in the active space without frozen MOs. The SAC/SAC-CI calculations are performed by the modified version of the SAC85 program[23] and the MEG4/EX-MEG4 program.[24] The full-CI calculations are carried out by using the slater-determinant-based algorithm of Knowles et al.[25] coded by Dr. Momose.[26]

In the SAC-CI calculation, all single- and double-(double- and triple-)excitation operators are included without configuration selection both in the SD-R(DT-R) and general-R method. Higher-order terms in the general-R method are produced with reference functions whose SD-CI coefficients are larger than c_{ref}=0.1, which is slightly modified from the original scheme.[15] Configuration selection using perturbation energy is performed for these higher-order terms due to eq. (5) with the threshold of λ_e=1.0X10^{-5}. The primary configurations $\Phi_i^{(p)}$ of the selection are adopted identical to the reference functions. Since the higher-order excitation operators are included for the $R^\dagger$ operators in the general-R method, some of the excitation configurations are described by both linked and unlinked terms. In the present calculation, unlinked terms which give such identical excitations are neglected.

In the examination of the configuration selection methods, the threshold λ_{hfsc} is set to 3G for all the nuclei.

IV. COMPARISON WITH FULL-CI CALCULATIONS

The doublet, triplet, and quartet states of the OH, CH_2, BH_2, CH_3, and H_2O^+ radicals are investigated by the SAC-CI(SD-R, DT-R), SAC-CI(general-R), and full-CI methods in order to examine the accuracy and usefulness of the SAC-CI method. The CI calculation with the same variational space as $\{R^\dagger|0\rangle\}$ space of the SAC-CI method is also performed for comparison. The SAC-CI method is performed with systematic inclusion of the $R^\dagger$ operators; namely, SAC-CI(SDT-R) method includes up to triple-excitation operators (denoted as N=1-3) and SAC-CI(SDTQ-R) method includes up to quadruple ones (denoted as N=1-4). The calculational dimensions are given in Table I. The total energies and the hfsc's calculated by these methods are summarized in Table II and III, respectively.

TABLE I. Dimension of the CI, SAC-CI(SD-R, DT-R), SAC-CI(general-R) and full-CI methods.

Molecule	State	CI, SAC-CI			full CI
		N=1,2	N=1-3	N=1-4	
OH	$X^2\Pi$	44	292	814	97,616
	$A^2\Sigma^+$	70	295	676	98,044
	$1^4\Sigma^-$	328	893	1,452	66,351
	$1^4\Pi$	356	658	896	50,904
CH_2	$^3B_1$	190	576	981	181,760
BH_2	$^2A_1$	71	288	484	94,128
CH_3	$^2A_2''$	60	496	1,466	1,955,576
H_2O^+	$^2B_1$	48	388	1,133	500,638

TABLE II. Total energy of small radicals calculated by the SAC-CI(SD-R, DT-R), SAC-CI(general-R) and full-CI methods.[a]

Molecule	State	N=1,2		N=1-3		N=1-4		full CI
		CI	SAC-CI(R-SD[b])	CI	SAC-CI(R-SDT[b])	CI	SAC-CI(R-SDTQ[b])	
OH	$X^2\Pi$	-75.41247 (82.16)	-75.49296 (1.67)	-75.47861 (16.02)	-75.49495 (-0.32)	-75.49049 (4.14)	-75.49507 (-0.44)	-75.49463
	$A^2\Sigma^+$	-75.25840 (81.13)	-75.33780 (1.73)	-75.32579 (13.74)	-75.33962 (-0.09)	-75.33556 (3.97)	-75.34013 (-0.60)	-75.33953
	$1^4\Sigma^-$	-75.15044 (41.62)	-75.18734 (4.72)	-75.18085 (11.21)	-75.19203 (0.03)	-75.19041 (1.65)	-75.19091 (1.15)	-75.19206
	$1^4\Pi$	-75.03885 (37.72)	-75.07738 (-0.81)	-75.06522 (11.35)	-75.07498 (1.59)	-75.07198 (4.59)	-75.07314 (3.43)	-75.07657
CH_2	$^3B_1$	-38.93627 (61.72)	-38.99509 (2.90)	-38.99279 (5.20)	-38.99573 (2.26)	-38.99456 (3.43)	-38.99702 (0.97)	-38.99799
BH_2	$^2A_1$	-25.74720 (57.74)	-25.80046 (4.48)	-25.79799 (6.95)	-25.80361 (1.33)	-25.79947 (5.47)	-25.80363 (1.31)	-25.80494
CH_3	$^2A_2''$	-39.56705 (90.69)	-39.65294 (4.80)	-39.64658 (11.16)	-39.65847 (-0.73)	-39.65235 (5.39)	-39.65863 (-0.89)	-39.65774
H_2O^+	$^2B_1$	-75.63716 (85.70)	-75.72129 (1.57)	-75.70586 (17.0)	-75.72322 (-0.36)	-75.71728 (5.58)	-75.72271 (0.15)	-75.72286
Average discrepancy		(67.31)	(2.84)	(11.58)	(0.84)	(4.28)	(1.12)	

[a] Daviations from the full-CI values are given in the parenthesis (in mhartree).
[b] For quartet states, SD-R, SDT-R and SDTQ-R methods correspond to DT-R, DTQ-R and DTQQ-R methods, respectively.

TABLE III. Hyperfine splitting constants of small radicals calculated by the SAC-CI(SD-R, DT-R), SAC-CI(general-R) and full-CI methods.[a]

Molecule Atom	RHF	N=1,2		N=1-3		N=1-4		full CI	Exptl.
		CI	SAC-CI(R-SD[b])	CI	SAC-CI(R-SDT[b])	CI	SAC-CI(R-SDTQ[b])		
OH									
$X^2\Pi$									
O	-	-5.28 (13.42)	-12.23 (6.47)	-15.41 (3.29)	-20.28 (-1.58)	-17.56 (1.14)	-20.88 (-2.18)	-18.70	-
H	-	-23.48 (8.39)	-25.61 (6.26)	-29.74 (2.13)	-31.72 (0.15)	-30.58 (1.29)	-31.50 (0.37)	-31.87	-26.1[c]
$A^2\Sigma^+$									
O	-161.47	-221.69 (-8.45)	-214.78 (-1.54)	-207.82 (5.42)	-215.81 (-2.57)	-212.53 (0.71)	-215.87 (-2.63)	-213.24	-
H	247.48	276.00 (-8.82)	273.24 (-11.58)	290.89 (6.07)	285.96 (1.14)	287.18 (2.36)	285.79 (0.97)	284.82	-
$1^4\Sigma^-$									
O	-35.55	-64.05 (14.12)	-73.40 (4.77)	-80.40 (-2.23)	-81.67 (-3.50)	-81.87 (-3.70)	-82.40 (-4.23)	-78.17	-
H	0.63	29.92 (0.94)	29.67 (0.69)	29.16 (0.18)	29.02 (0.04)	28.63 (-0.35)	29.04 (0.06)	28.98	-
$1^4\Pi$									
O	-89.38	-101.85 (6.61)	-105.56 (-2.90)	-110.72 (-2.26)	-112.49 (-4.03)	-111.73 (-3.27)	-112.14 (-3.68)	-108.46	-
H	83.13	112.37 (-2.51)	115.06 (0.18)	115.64 (0.76)	113.77 (-1.11)	114.35 (-0.53)	114.42 (-0.46)	114.88	-
CH_2 $^3B_1$									
C	53.43	92.57 (-10.33)	96.45 (-6.45)	96.91 (-5.99)	104.54 (1.64)	98.69 (-4.21)	102.88 (-0.02)	102.90	(85.2)[d]
H	9.58	-13.36 (-4.45)	-15.75 (-2.06)	-16.11 (-1.70)	-17.40 (-0.41)	-16.66 (-1.15)	-17.48 (-0.33)	-17.81	-7.2[e]
BH_2 $^2A_1$									
B	72.57	130.30 (-1.05)	123.80 (-7.55)	123.55 (-7.80)	131.34 (-0.01)	125.83 (-5.52)	130.86 (-0.49)	131.35	128[f]
H	11.70	1.64 (0.06)	0.93 (-0.65)	1.41 (-0.17)	1.64 (0.06)	1.42 (-0.16)	1.73 (0.15)	1.58	±13.6[f]
CH_3 $^2A_2''$									
C	-	25.77 (-15.80)	28.69 (-12.88)	31.46 (-10.11)	42.06 (0.49)	35.12 (-6.45)	42.45 (0.88)	41.57	28.7[g]
H	-	-26.80 (8.51)	-28.67 (6.64)	-31.68 (3.63)	-35.18 (0.13)	-32.85 (2.46)	-34.90 (0.41)	-35.31	-24.7[g]
H_2O^+ $^2B_1$									
O	-	-15.20 (18.43)	-20.09 (13.54)	-28.94 (4.69)	-34.09 (-0.46)	-34.55 (-0.92)	-34.64 (-1.01)	-33.63	±29.7[h]
H	-	-23.81 (11.00)	-28.23 (6.58)	-32.17 (2.64)	-34.68 (0.13)	-34.31 (0.50)	-34.49 (0.32)	-34.81	±26.1[h]

[a] Daviations from the full-CI values are given in the parenthesis (in Gauss).
[b] For quartet states, SD-R, SDT-R and SDTQ-R methods correspond to DT-R, DTQ-R and DTQQ-R methods, respectively.
[c] Reference 26
[d] MRD-CI calculation with extended basis sets; Reference 28
[e] Reference 27
[f] Reference 28
[g] Reference 29
[h] Reference 30

A. OH radical

Two doublet ($X^2\Pi$ and $A^2\Sigma^+$) and two quartet ($^4\Sigma^-$ and $^4\Pi$) states of the OH radical are investigated. The results of the total energies calculated by the SAC-CI(SD-R, DT-R) were already discussed in the preceding paper.[14] We note here that $1^4\Sigma^-$ state has some nature of triple-excitation and therefore, the unlinked terms of the form $\{S_i^a S_j^b \times R_{klm}^{cd}\}$ are important for an appropriate description in the SAC-CI(DT-R) method. On the other hand, the SAC-CI(SDT-R, DTQ-R) method gives accurate results of the total energies for all the states, though the calculated values slightly overshoot the full-CI ones: the average discrepancy is only 0.51 mhartree. The effects of the unlinked terms are estimated to be 11-16 mhartree in the SAC-CI(SDT-R, DTQ-R) method.

The hfsc's of the ground and excited states of the OH radical are examined. In the present calculational condition, the full-CI method gives the hfsc's of the $X^2\Pi$ state as -18.70G and -31.87G for the O and H atoms, respectively. Experimental value of -26.1G for the H atom is reported.[26] The SD-CI calculation underestimates the hfsc's of this state as -5.28G (O) and -23.48G (H), while the SAC-CI(SD-R) method improves the values as -12.23G (O) and -25.61G (H), but the difference from the full-CI values are still -6.47 and -6.26 gauss, respectively. Since the linked configurations of the SAC-CI(SD-R) method are identical with the CI configurations of the SD-CI, this improvement is purely attributed to the inclusion of the unlinked terms in the SAC-CI method. Similar improvements are also obtained for the hfsc's of the excited states: improvement is more remarkable for the hfsc's of the O atom than for those of the H atom. The SAC-CI(SDT-R) method, in which excitation operators up to triple-ones are included in the $R^\dagger$ operators, gives more accurate values as -20.28G (O) and -31.72G (H) for the $X^2\Pi$ state: the errors are only -1.58G and 0.15G, respectively. Comparing the results of the CI method with those of the SAC-CI method, the effect of the higher order terms is recognized as to increase the spin density at nucleus especially of the radical center.

Two quartet states, $^4\Sigma^-$ and $^4\Pi$, have the electronic configurations of $(p\sigma)^2(p\pi)^2(\sigma^*)^1$ and $(p\sigma)^1(p\pi)^3(\sigma^*)^1$, respectively. Firstly, analysis of spin appearing mechanism for these states is performed: ie. decomposition to spin delocalization, spin polarization, and electron correlation effects. The RHF contributions which

correspond to the spin-delocalization ones are calculated to be -35.55G (O) and 0.63G (H) for the $^4\Sigma^-$ state and -89.38G (O) and 83.13G (H) for the $^4\Pi$ state. Reflecting two and one unpaired spin in π orbitals of the $^4\Sigma^-$ and $^4\Pi$ states, respectively, total correlation contributions are large for these states; -42.6G (O) and 28.4G (H) for the $^4\Sigma^-$ state and -19.1G (O) and 31.75G (H) for the $^4\Pi$ state. The accuracy of the SAC-CI(DT-R) method is excellent for the quartet states. The deviations from the full-CI results are only -4.77G (O) and 0.69G (H) for the $1^4\Sigma^-$ state, which correspond to 6.1% and 2.4% of the exact values. Those for the $1^4\Pi$ state are -2.90G (O) and 0.18G (H), which are 2.7% and 0.2% of the exact values. The hfsc's of the quartet states calculated by the SAC-CI(general-R) are almost in the same accuracy as those calculated by the SAC-CI(DT-R) method. The result of the SAC-CI(DT-R) method is very accurate because (1) these quartet states have some RHF contributions and (2) $\{R^\dagger|0>\}$ space of quartet multiplicity covers wider variational space than that of doublet one.

The present examination shows that the SAC-CI method gives quantitative values not only for the energies but for the hfsc's in spite of the smallness of the calculational dimensions: 44 (SD-R) and 292 (SDT-R) compared with the full-CI dimension 97616 for the $X^2\Pi$ state. Especially, the SAC-CI(SD-R) method largely improves the result of the SD-CI method. Quantitative agreements of the hfsc's guarantee the accuracy of the fine details of the SAC-CI wave function in terms of the spin correlations and electron correlations.

B. CH_2 and BH_2 radicals

The ground states of the CH_2 and BH_2 radicals, $^3B_1$ and $^2A_1$, are examined. The total energies of these states are calculated to be -38.99799 au. for CH_2 and -25.80494 au. for BH_2, respectively In all cases of the excitation levels of the $R^\dagger$ operators, the SAC-CI method reproduces well the values of the full-CI method. The errors are reduced as the higher-order operators are included in the $R^\dagger$ operators. The errors of the SAC-CI(SDTQ-R) is only 0.97 au and 1.31au for CH_2 and BH_2, respectively.

The full-CI method estimates the hfsc's of 102.90G (C) and -17.81G (H) for the $^3B_1$ state of CH_2 using [4s2p/2s] basis sets. Experimental value of -7.2G is available for the H atom.[27] The MRD-CI calculation with extended basis sets gives the hfsc of

85.2G for the C atom.[28] The RHF contributions are estimated to be 53.43G (C) and 9.58G (H), where value for the H atom has opposite sign to the full-CI results. The effects of the total correlation contributions are as large as 49.5G (O) and -27.4G (H). For this state, the results of the SAC-CI method are excellent; the SAC-CI method improves the hfsc values estimated by the CI method in all cases of the excitation levels for both the C and H atoms. The effects of the unlinked terms are approximately 4G for the C atom and 1-2G for the H atom, respectively. The deviations from the full-CI results are only 1.54G (C) and -0.41G (H) in the SAC-CI(SDT-R) method.

The hfsc of the B atom for the $^2A_1$ state of BH_2 is calculated to be 131.35G by the full-CI method in good agreement with the experimental value of 128G.[28] There are large RHF contributions estimated as 72.57G (B) and 11.70G (H). In this case, the SD-CI method accidentally gives good value of 130.30G for B. However, inclusion of the higher order terms reduces the spin density at B and the calculations with these terms give worse results; the hfsc's of 123.80G and 123.55G are calculated by the SAC-CI (SD-R) method and the CI method of N=1-3 level, respectively. Therefore, the SAC-CI(SD-R) method shows reasonable behavior. Again the SAC-CI(SDT-R) method gives excellent results with the errors of -0.01G (B) and 0.06G (H).

C. CH_3 and H_2O^+ radicals

The CH_3 and H_2O^+ radicals are π-radicals and therefore, their spin distributions are determined by the spin polarization and electron correlations. The $^2A_2''$ state of the CH_3 radical is investigated. The total energy is calculated to be -39.65774 au. and the dimension of the full-CI calculation is as large as 1,955,576. The SAC-CI method gives -39.65294 au. and -39.65847 au. with the dimension of 60 and 496 by the SD-R and SDT-R methods, respectively. The hfsc's of CH_3 are calculated to be 41.57G(C) and -35.31G (H) by the full-CI method, which are estimated larger than the experimental values of 28.7G (C) and -24.7G (H).[29] The CI calculation of N=1-3 level gives the values of 31.46G (C) and -31.68G (H): the errors are as large as 10.11G (C) and 3.63G (H). The SAC-CI(SDT-R) method improves the values as 42.06G (C) and -35.18G (H), whose deviations from the full CI are 0.49G and 0.13G for C and H, respectively.

The results of the $^2B_1$ state of H_2O^+ are very similar to those of the $X^2\Pi$ state of OH; the results of the SAC-CI method show same tendencies. The total energy of the $^2B_1$ state of H_2O^+ is calculated to be -75.72286 au. by the full-CI method. Even the CI calculation of N=1-3 level gives the error of 17 mhartree, and the effect of the unlinked terms is still large. The SAC-CI method shows good agreement in all cases of the excitation levels; the errors are within 2 mhartree. The hfsc's of H_2O^+ are calculated to be -33.63G (O) and -34.81G (H) by the full-CI method. Experimental values are reported as ±29.7G (O) and ±26.1G (H),[30] whose signs cannot be determined. As for the hfsc of the O atom, it is difficult to reproduce the full-CI value and the inclusion of the higher order terms is indispensable for accurate description. The CI calculations of N=1,2 and N=1-3 levels give -15.20G and -28.94G for the hfsc of O atom, whose errors are as large as 18.43G and 4.69G, respectively. The SAC-CI method improves these values as -20.09G and -34.09G, where the effects of the unlinked terms are 4.9G and 5.2G, respectively. The result of the SAC-CI(SDT-R) method is satisfactory and the errors are negligible as -0.46G (O) and 0.13G (H).

V. CONFIGURATION SELECTION METHOD FOR THE HFSC'S

Next we consider the effect of the configuration selection on the calculation of the hfsc's. Two configuration selection methods described in sec. II are examined through the SAC-CI(SD-R, DT-R) and SAC-CI(general-R) calculations and the results are summarized in Table IV. First one named as 'method I' corresponds to usual selection method, in which only the energy is used for the criterion of the selection according to the eq. (5). In the second method (method II), the contribution to the hfsc of each atom is also taken into accounts: selected configurations are sum of those which satisfy eqs. (5) and (10). The results of these two methods are compared with those obtained without doing configuration selection, which are shown in column under 'full'.

The effectiveness of method II is discussed in terms of the results of the SAC-CI(SD-R, DT-R) method. The difference of the two methods is remarkable for the hfsc's of the radical center atoms. For the $^2\Pi$ state of OH radical, for example, the hfsc of O atom is calculated as -12.23G without configuration selection. Method I whose criterion is only perturbation energy ($\lambda e = 5X10^{-5}$ au) gives -56.12G. This

Table IV. Calculated size, energy, and hyperfine splitting constants (hfsc's) of small radicals by the SAC-CI method. Two types of the configuration selection methods are examined.

			SAC-CI (SD-R, DT-R)			SAC-CI (SDTQ-R, DTQQ-R)		
			Method I[a]	Method II[b]	full[c]	Method I[a]	Method II[b]	full[c]
OH								
$X^4\Pi$	Size		26	29	44	525	528	814
	Energy (au)		-75.49285	-75.49288	-75.49296	-75.49427	-75.49430	-75.49507
	Hfsc (G)	O	-56.12	-11.24	-12.23	-68.98	-25.62	-20.88
		H	-25.60	-25.61	-25.61	-30.85	-30.86	-31.50
$1^2\Sigma^+$	Size		36	39	70	422	425	676
	Energy (au)		-75.33677	-75.33763	-75.33780	-75.33881	-75.33882	-75.34013
	Hfsc (G)	O	-221.76	-202.72	-214.78	-224.11	-206.04	-215.87
		H	273.71	273.70	273.24	286.92	286.91	285.79
$1^4\Sigma^-$	Size		132	164	328	833	865	1452
	Energy (au)		-75.17787	-75.17795	-75.17813	-75.18971	-75.18978	-75.19091
	Hfsc (G)	O	-97.17	-74.44	-73.79	-107.36	-85.78	-82.40
		H	30.37	30.37	30.35	28.96	28.96	29.04
$1^4\Pi$	Size		108	124	356	447	463	896
	Energy (au)		-75.07035	-75.07039	-75.07075	-75.07171	-75.07175	-75.07314
	Hfsc (G)	O	-122.41	-106.17	-104.81	-130.81	-114.93	-112.14
		H	116.05	116.05	116.00	114.51	114.52	114.42
CH_2								
$^3B_1$	Size		77	89	190	562	575	981
	Energy (au)		-38.99424	-38.99431	-38.99509	-38.99406	-38.99413	-38.99702
	Hfsc (G)	C	124.61	98.95	96.45	132.99	107.98	102.88
		H	-16.43	-16.43	-15.75	-17.31	-17.31	-17.48
BH_2								
$^2A_1$	Size		32	36	71	334	338	481
	Energy (au)		-25.79986	-25.79988	-25.80046	-25.80165	-25.80166	-25.80363
	Hfsc (G)	B	128.26	125.11	123.80	137.81	134.70	130.86
		H	2.50	2.50	0.93	3.09	3.09	1.73
CH_3								
$^2A_2''$	Size		34	38	60	840	844	1466
	Energy (au)		-39.65286	-39.65289	-39.65294	-39.65771	-39.65774	-39.65863
	Hfsc (G)	C	63.32	30.99	28.69	83.00	51.29	42.45
		H	-28.67	-28.68	-28.67	-34.43	-34.44	-34.90
H_2O^+								
$X^2\Pi$	Size		29	34	48	272	277	1133
	Energy (au)		-75.72114	-75.72119	-75.72129	-75.72228	-75.72233	-75.72271
	Hfsc (G)	O	-71.13	-18.93	-20.09	-87.75	-37.26	-34.64
		H	-28.17	-28.18	-28.23	-34.46	-34.49	-34.49

[a] Configuration selection is performed with the criterion of the energy (eq. (5)).
[b] Configuration selection is performed with the criterion of the energy and hfsc (eqs. (5) and (10)).
[c] Without configuration selection.

degradation is caused by the fact that method I discards the important excitation configurations which describe the inner core polarization. On the other hand, method II, in which the contributions of the configurations to the hfsc of each atom is taken into account, gives reliable value as -11.24G. For the hfsc's of the quartet states, method II is also reliable. The hfsc's of O atom calculated by method II deviate only by 0.65G and 1.36G for the $1^4\Sigma^-$ and $1^4\Pi$ states, respectively, from those obtained without the selection, while those by method I deviate as large as by 23.38G and 17.6G, respectively. The excitation configurations, which are important for describing the hfsc's of H atom, give large contributions of perturbation energies to the reference functions. Therefore, method I also gives good description for those values. These trends hold good for other radicals except for the $^2A_1$ state of BH_2 in which core MO's of the B atom are not so much deeply bounded. The deviations of method I for the hfsc's of the radical centers are calculated to be 28.16G, 34.63G, and 51.04G for CH_2, CH_3, and H_2O^+, respectively, while those of method II are only 2.5G, 2.3G, and 1.16G. The effectiveness of the method II is also observed in the SAC-CI(general-R) method as shown in Table IV.

The increment of the dimension from method I to method II would be just as required for the accurate description of the hfsc's. The efficiency of the present method would increase as the system becomes large, heavy atoms are included in the system, and basis sets are qualified.

VI. SUMMARY

The accuracy and the usefulness of the SAC-CI method for calculating hyperfine splitting constants (hfsc's) are examined for the doublet, triplet, and quartet states of several small radicals. The results of the SAC-CI method show good agreements with those of the full-CI ones. The SAC-CI(general-R) method is performed for the high-spin states for the first time and is found to give an accurate description of the hfsc's. For the present examples, whose main configurations of the states are described by one-electron process, the SAC-CI(SDT-R) method gives highly accurate results of the hfsc's. A convenient configuration selection method which keeps the quality of the calculated hfsc's is proposed. This method, in which both energy and hfsc are used as the criteria of the configuration selection procedure, is applicable also to ordinal CI

method and is effective for accurate calculation of hfsc's especially for large systems and for high-spin system, where a large number of CFS's are required.

ACKNOWLEDGMENTS

The authors wish to thank Dr. T. Momose for kindly letting us use his Slater-determinant-based full-CI program. The full-CI calculations have been carried out with the HITAC M-680H and S-820 computer at the Institute for Molecular Science. This study has partially been supported by the Grant-in-Aid for Scientific Research from the Japanese Ministry of Education, Science, and Culture, and by CIBA-GEIGY Foundation (Japan) for the Promotion of Science.

REFERENCE

[1] H. Nakatsuji, H. Kato, and T. Yonezawa, J. Chem. Phys. **51** 3175 (1969): H. Nakatsuji, J. Chem. Phys. **59** 2586 (1973).

[2] H. Nakatsuji and K. Hirao, J. Chem. Phys. **68** 4279 (1978).

[3] H. Nakatsuji, K. Ohta, and T. Yonezawa, J. Phys. Chem. **87** 3068 (1983).

[4] T. Momose, T. Shida, and H. Nakatsuji, J. Chem. Phys. **89** 4185 (1988).

[5] H. Nakatsuji and M. Izawa, J. Chem. Phys. **91** 6205 (1989).

[6] T. Momose, M. Yamaguchi, and T. Shida, J. Chem. Phys. **93** 7284 (1990).

[7] L. B. Knight, Jr., B. W. Gregory, D. W. Hill, C. A. Arrington, T. Momose, and T. Shida, J. Chem. Phys. **94** 67 (1991).

[8] H. Nakatsuji and M. Izawa, J. Chem. Phys. **97** 435 (1992).

[9] H. Nakatsuji, Acta Chim. Hungarica **129** 719 (1992).

[10] D. Feller and E. R. Davidson, J. Chem. Phys. **97** 435 (1992); Theor. Chim. Acta **68** 57 (1985).

[11] B. Engels and S. D. Peyerimhoff, Mol. Phys. **67** 583 (1989).

[12] T. Nakano, K. Morihashi, and O. Kikuchi, Chem. Phys. Lett. **186** 572 (1991).

[13] H. Nakatsuji, Chem. Phys. Lett. **59** 362 (1978); **67** 329, 334 (1979).

[14] H. Nakatsuji and M. Ehara, J. Chem. Phys. **98** 7179 (1993).

[15] H. Nakatsuji, Chem. Phys. Lett. **177** 331 (1991).

[16] H. Nakatsuji, Chem. Phys. **75** 425 (1983).

[17] G. Herzberg, *Spectra of Diatmic Molecules* (Van Nostrand, New York, 1950).

[18] G. Herzberg, *Molecular Spectra and Molecular Structure* (Van Nostrand, New York, 1966);
G. Herzberg and J. W. C. Johns, Proc. R. Soc. (London) Ser. **A298**, 142 (1967).

[19] G. Herzberg, Proc. R. Soc. (London) Ser. **A262**, 291 (1961).

[20] H. Lew and I. Heiber, J. Chem. Phys. **58** 1246 (1973).

[21] S. Huzinaga, J. Chem. Phys. **42** 1293 (1965).
T. H. Dunning Jr., J. Chem. Phys. **53** 2823 (1970).

[22] M. Dupuis, J. D. Watts, H. O. Viller, and G. J. B. Hurst,
Program System HONDO7, Program Library No. 544,
Computer Center of the Institute for Molecular Science, (1989).

[23] H. Nakatsuji, Program system for SAC and SAC-CI calculations, Program Library No.146 (Y4/SAC), Data Processing Center of Kyoto University, 1985;
H. Nakatsuji, Program Library SAC85 (No. 1396), Computer Center of the Institute for Molecular Science, Okazaki, 1986.

[24] H. Nakatsuji, Program system for the MEG4/EX-MEG4
for ground, excited, ionized, and electron attached states (to be published).

[25] P. J. Knowles and N. C. Handy, Chem. Phys. Lett. **111** 315 (1984).

[26] T. Momose, Slater-determinant-based Full-CI program based on Knowles algorithm.

[26] E. Hirota, *High-Resolution Spectroscopy of Transient Molecules* (Springer, Berlin, 1985).

[27] T. J. Sears, P. R. Bunker, A. R. W. McKellar, K. M. Evenson, D. A. Jennings, and J. M. Brown, J. Chem. Phys. **77** 5348 (1982).

[28] L. B. Knight, Jr., M. Winiski, P. Miller, C. A. Arrington, and D. Feller,
J. Chem. Phys. **91** 4468 (1989).

[29] D. Chipman, J. Chem. Phys. **78** 3112 (1983).

[30] L. B. Knight and J. Steadman, J. Chem. Phys. **78** 5940 (1983).

Chapter 3

EGCI method applied to high-spin multiplicity

ABSTRACT

The exponentially generated configuration interaction (EGCI) method is extended to high-spin multiplicity. This method, in which excited, ionized, and electron attached states are calculated on the basis of the correlated wave function of the ground state, is applicable to quasi-degenerate states of various spin multiplicity and various number of excitation processes. The accuracy and efficiency of the EGCI method is examined for the high-spin quasi-degenerate states with multiple excitation nature. Test calculations are performed for several high-spin states of C_2, C_2^+, N_2, N_2^+, and m-phenylenebis(methylene) (m-PBM) molecules. The EGCI method reproduces well the full-CI results in total energy, spectroscopic constants, and spin density distributions. The EGCI method is confirmed to be accurate and useful not only for investigating the energetics involved in the study of dynamics and reactions but also for studying spin density distributions of various spin multiplet states.

I. INTRODUCTION

High-spin states have received much attention in many fields of science.[1-20] They play an important role in reaction dynamics and energy relaxation processes, and in the design of ferromagnetic materials. They appear in the ground and excited states of molecules with degenerate or near degenerate orbital structure, such as diatomics, metal complexes and clusters and well-designed organic high-spin compounds et ecetra. For example, the ground state of C_2^+ is identified as quartet state $X^4\Sigma_g^+$.[1-8] Furthermore, these high spin molecules often have quasi-degenerate characters with various spin multiplet states owing to their highly-degenerate open-shell structure. Therefore, theoretical method for investigating the properties and dynamics of these high-spin molecules should be able to deal with not only one high-spin state but also all of the related high-spin states in a same accuracy.

Recently, we have extended our SAC(symmetry adapted cluster)-CI method to high-spin multiplicity.[21] The SAC-CI method[22] describes excited, ionized, and electron attached states using the functional space for such states generated by the SAC calculation[23] for the ground state. This method has been shown to be very accurate and useful.[24] We applied the method to the high-spin states of N_2, N_2^+, OH and m-PBM systems and confirmed that it is again accurate and efficient.[21] The remarkable advantage of the SAC-CI method is as follows. (1) It is applicable to a large number of excited states at the same time. (2) It is applicable to a various spin multiplicities in the same manner. (3) The effect of higher order excitations are included in the nonlinear unlinked terms. (4) If such effect is essential, it can also be included in the linked term.[25] However, the SAC-CI method critically depends on the validity of the SAC theory, which is the single reference cluster expansion theory. There should exist at least one such state for solving SAC method. For cases in which such state does not exist, we have proposed exponentially generated wave function (EG-WF) method[26] to which the MR(multi-reference)-SAC,[27] MEG(mixed exponentially generated),[28] and EGCI methods[29] belong.

The EGCI method has been designed to overcome the defect of the single-reference cluster expansion method, and nevertheless, to have desirable properties of the cluster expansion method.[26,29] The expansion operator in the EGCI method is generated along the exponential expansion and yet free variables are given for each

operator. Therefore, it is essentially one of the CI methods and therefore variational. However, it satisfies size-consistency and self-consistency to the order of truncations of the higher terms.[26] The EGCI method was extended to excited, ionized, electron attached states with the use of the excitator method,[29] which is common to the SAC-CI method.

In this paper, we apply the EGCI method to the high-spin states with quartet to septet multiplicities, and investigate its accuracy and efficiency. We apply the EGCI method to the ground and excited states of the quasi-degenerate high spin states of C_2, C_2^+, N_2, N_2^+, and m-phenylenebis(methylene) (m-PBM) molecules. The accuracy of the EGCI method is examined for the energy and spin density by comparing with the full-CI results calculated at the same time for these molecules.

II. EGCI METHOD FOR HIGH-SPIN MULTIPLICITY

In this series of papers,[26-29] we have introduced a new basic expansion operator defined by

$$\mathscr{EXP}\left(\sum_K a_K A_K^\dagger\right) = Q\left(a_0 + \sum_K a_K A_K^\dagger + \frac{1}{2}\sum_{(K,L)} a_{KL} A_K^\dagger A_L^\dagger + \ldots\right)$$

where the excitation operator $A_K^\dagger$ runs over all the space and spin symmetries and Q is a symmetry projector. Single and double excitation operators are usually adopted for the $A_K^\dagger$ operators. The constructions of the higher order excitation operators are made in the spirit of the cluster expansion theory: the higher order operators are generated as the products of lower-order operators as in the cluster expansion. In order to include all possible highly connected terms such as simultaneous double excitations, all independent spin and space functions are included for the product operators $\{A_K^\dagger A_L^\dagger\}$, and the redundant terms are deleted. The coefficients of the product operators a_{KL} are made free from those of the lower operators a_K, which is important for quasi-degenerate states.

The EGCI method normally starts from the totally symmetric singlet state and the wave function is defined with the $\mathscr{EXP}$ operator as[26,29]

$$\Psi_g^{EGCI} = \mathcal{EXP}\ (\sum_K a_K A_K^\dagger)\ |0\rangle$$

$$= Q\ (\ a_0 + \sum_K a_K A_K^\dagger + \frac{1}{2}\sum_{(K,L)} a_{KL} A_K^\dagger A_L^\dagger + \ldots\ )\ |0\rangle$$

where $|0\rangle$ is the Hartree-Fock determinant. The wave functions for the excited, ionized, and electron attached states are constructed by applying the excitation operator, $\mathfrak{R}$ as,

$$\Psi_e^{EGCI} = \mathfrak{R}\ \Psi_g^{EGCI}$$

The operator $\mathfrak{R}$, which is a kind of reaction operators, is called excitator in order to distinguish it from the more elemental excitation operators $A_K^\dagger$. This operator describes excitation, ionization, and electron attachment, and at the same time the reorganizations of orbitals and electron correlations. The excitator $\mathfrak{R}$ is expanded by a linear combination of the excitation operators $\{B_K^\dagger\}$ as

$$\mathfrak{R} = \sum_K b_K B_K^\dagger$$

and the resultant EGCI wave function of various spin multiplicity is expressed as

$$\Psi_e^{EGCI} = Q\ (\sum_K b_K B_K^\dagger + \frac{1}{2}\sum_{(K,L)} b_{KL} A_K^\dagger B_L^\dagger + \frac{1}{3!}\sum_{(K,L,M)} b_{KLM} A_K^\dagger A_L^\dagger B_M^\dagger + \ldots\ )\ |0\rangle$$

In the previous calculation for singlet, doublet and triplet states,[29] we included one- and two- electron operators for the $B_K^\dagger$ operators. For higher-spin multiplicity, higher order excitation operators are necessarily included in the $B_K^\dagger$ operators. In the present calculation, the $B_K^\dagger$ operators are taken to be identical with the operators defined as $R_K^\dagger$ operators in Table I of Ref. 21. For example, two- and three-electron operators, B(2) and B(3), are necessary for quartet and quintet states; namely symmetry adapted 2h1p, 3h2p and 2h2p, 3h3p operators are adopted for quartet and quintet, respectively. The SAC-CI calculations with these operators are referred to as SAC-CI(R-DT) in the present paper.

The physical basis of the excitator method is as follows. Electronic excitations usually involve only one or two electrons and the other electrons lie in the environments more or less similar to those of the ground state. Therefore, the

correlations in the excited states are more easily described by starting from those of the ground state than by starting from the beginning. In the EGCI method, we utilize the knowledge of the ground-state correlations through the operators $A_K^{\dagger}$.

In actual applications, we adopt the configuration selection method, especially for the higher order terms. The detailed algorithm of the configuration selection in the EGCI method was reported in the preceding paper.[26] We adopt the same configuration selection algorithm and use the set of the thresholds (λ_A, λ_{AA}, λ_{AAA}) in the following discussions and in the tables.

III. CALCULATIONAL DETAILS

The present method is applied to several high-spin states of C_2, C_2^+, N_2, N_2^+, and m-phenylenebis(methylene) (m-PBM) molecules. In the previous report,[29] we have applied the EGCI method to the singlet to triplet states of C_2, C_2^+, and C_2^-. The potential curves of the quartet states of C_2^+ and the quintet states of C_2 are calculated at appropriate 13 points. The hyperfine splitting constant (hfsc) is calculated for the $X^4\Sigma_g^+$ state of C_2^+ with the C-C distance of 1.41Å as in the previous theoretical studies.[1,2] For N_2 and N_2^+ we perform calculations at the internuclear distance of 2.0Å(1.82 r_e), because we are interested in the quasi-degenerate states of these molecules. The high-spin states of N_2 at the equilibrium geometry have successfully been calculated by the SAC-CI method.[21] The molecular structure of m-PBM and the numbering of the carbon atoms are depicted in Fig. 1. The molecular geometry is constructed from those of free benzene and methylene: the C-C and C-H lengths in benzene ring are set to 1.397Å and 1.084Å, respectively, and the C-C-H angle and the C-H length of the methylene group to 140° and 1.08Å, respectively.

The basis set for carbon is the [4s2p] set of Huzinaga Dunning[30] plus Rydberg s function with ζ_s=0.023 for the calculation of the potential curves of C_2 and C_2^+. The minimal STO-6G set is used for the calculation of the hfsc of C_2^+, because the complete full-CI calculations are difficult for the [4s2p] basis. The basis set for nitrogen is the [4s2p] set[30] augmented with the Rydberg s function of ζ_s=0.025. For the m-PBM molecule, the STO-6G set is used for both C and H atoms.

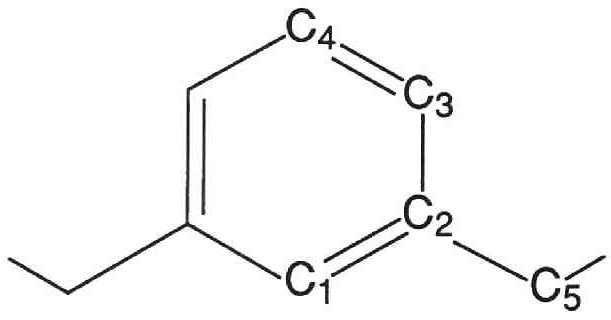

FIG. 1. Molecular structure of m-phenylenebis(methylene).

The EGCI calculations are performed with the thresholds (λ_A, λ_{AA}, λ_{AAA}) = (0.0, 0.04, 0.2). The EGCI program[31] is extended for high-spin multiplicity. The RHF MOs are calculated by the program HONDO7[32] and are used as the reference orbitals. The full-CI and SD-CI calculations are performed and compared with the present method. The active space is limited to be small in order to keep the size of the full-CI calculations to be practical. Ten MOs adopted for the active spaces of C_2 and N_2 system are $(2s\sigma_g)(2s\sigma_u)(p\pi_u)(p\sigma_g)$(Rydberg s, σ_g)(Rydberg s, σ_u)$(p\pi_g)(p\sigma_u)$, and four occupied and seven unoccupied MOs are used for m-PBM. Full-CI calculations of the hfsc and the spin density are performed by using the Slater-determinant-based algorithm of Knowles et al[33] coded by Momose.[34] Other full-CI calculations are carried out with the use of the program HONDO7.[32]

IV. RESULTS

A. C_2 and C_2^+ molecules

The electronic structures of C_2 and C_2^+ are very interesting. The valence shell of C_2 molecule is described as $(2s\sigma_g)^2(2s\sigma_u)^2(p\pi_u)^4(p\sigma_g)(p\pi_g)(p\sigma_u)$ in its ground state: the bonding $p\sigma$ MO is in the unoccupied region. This causes the existence of many quasi-degenerate states and the states of multiple excitation natures. Therefore, a number of high-spin states exist in a relatively low energy region. Actually, the ground state of C_2^+ is identified to be the quartet state $X^4\Sigma_g^+$.[1-8]

Here, we investigate the accuracy of the present EGCI method, applying to the high spin states of C_2 and C_2^+ and comparing the results with the full-CI ones. For

the low spin states of these molecules, we have already confirmed good performance of the EGCI method in the previous paper.[29] We note that the basis set and the active space used here are slightly different from those in the previous case. We calculate the quartet states of C_2^+ and the quintet states of C_2 at appropriate 13 geometries. The energies and the dimensions of the EGCI and full-CI calculations are compared in Tables I and II for the two representative distances, R=1.24253Å (equilibrium distance r_e of the ground state of C_2) and R=2.0Å, respectively. 'Excitation level' characterizes the main configuration by the number of electrons involved in the excitation from the closed-shell HF configuration. Many electronic states of C_2 and C_2^+ molecules are characterized by the multiple excitations with the excitation levels two, three, and four even at the equilibrium distance, as shown in Table I.

Low-lying 12 quartet states of C_2^+ are calculated. They dissociate to $C(^3P_g)$ + $C^+(^2P_u)$ in their atomic limit.[2] The excitation natures of these states obtained in the present calculation are the same as those of the previous MRD-CI calculation with the extended basis set.[2] Most of these states, except for the $1^4\Sigma_g^-$, $1^4\Delta_g$, and $1^4\Sigma_u^+$ states, change their excitation natures as the change in the C-C distance. A remarkable avoided crossing occurs between the potential curves of the $^4\Pi_g$ symmetry. $1^4\Pi_g$ state has the main electronic configuration, $(\sigma_g)^2(\sigma_u)^1(\pi_u)^3(\sigma_g)^1$ at $R=r_e$, while it is $(\sigma_g)^2(\sigma_u)^2(\pi_u)^2(\sigma_g)^1$ at R=2.0Å. The dominant configuration of the $2^4\Pi_g$ state is just reverse as seen from Tables I and II and further changes occur at larger distance. Though many quartet states shown in Tables I and II have multiple excitation nature, the present EGCI method reproduces the full-CI results in high accuracy. The errors of the EGCI method is always positive, since it is variational. The average discrepancy for the quartet states is 0.88 and 3.05 mhartree for $R=r_e$ and R=2.0Å, respectively. The EGCI dimension increases as the internuclear distance increases because of the quasi-degenerate character of the states. Since the higher order terms are included explicitly, the efficiency of the EGCI method is inferior to that of the SAC-CI method.[21] The calculational dimensions are 200 ~ 300 at $R=r_e$ and 380 ~ 430 at R=2.0Å in comparison with 1080 ~ 1220 of the full-CI method.

TABLE I. Full-CI and EGCI results for the quartet and quintet states of C_2 and C_2^+ at R=1.2425Å[a]

State	Excitation level	Main configuration[b]	EGCI[c]		Full-CI		Difference (mhartree)
			Size	Energy	Size	Energy	
Quartet states (Ion)[d]							
$1^4\Sigma_g^-$	2	0.92(22111)	239	-75.03590	1220	-75.03667	0.77
$1^4\Pi_g$	2	0.93(21121)	234	-75.03322	1160	-75.03408	0.86
$1^4\Sigma_u^-$	3	0.89(21112)	281	-74.94860	1220	-74.94914	0.54
$2^4\Pi_g$	2+4	0.86(2211001)+0.37(2011201)	234	-74.75926	1160	-74.76020	0.94
$1^4\Pi_u$	3	0.67(211111)+0.55(2120101)	296	-74.73055	1160	-74.73108	0.53
$1^4\Sigma_g^+$	2	0.67(211201)+0.67(2121001)	206	-74.71948	1080	-74.72086	1.38
$2^4\Pi_u$	3	0.55(211111)+0.48(2102101) -0.48(2120101)	296	-74.69038	1160	-74.69072	0.34
$1^4\Delta_g$	2	0.67(211201)-0.67(2121001)	206	-74.68319	1220	-74.68424	1.05
$1^4\Sigma_u^+$	3	0.57(221011)-0.57(2201101) +0.32(201211)+0.32(2021101)	252	-74.68101	1080	-74.68153	0.52
$1^4\Delta_u$	3	0.63(220111)+0.63(2210101)	252	-74.67774	1220	-74.67811	0.37
$2^4\Sigma_g^-$	2	0.67(212101)-0.67(2112001)	239	-74.64988	1220	-74.65103	1.15
$2^4\Sigma_u^-$	3	0.51(220111)-0.51(2210101) +0.37(21112)	281	-74.54956	1220	-74.55165	2.09
Average discrepancy							0.88
Quintet states[e]							
$1^5\Sigma_g^+$	2	0.66(2121101)+0.66(211211)	281	-75.31590	950	-75.31629	0.39
$1^5\Pi_g$	2	0.94(2211101)	216	-75.27614	1090	-75.27737	1.31
$1^5\Delta_g$	2	0.68(2121101)-0.68(211211)	281	-75.26653	950	-75.26677	0.24
$1^5\Pi_u$	3	0.91(211121)	280	-75.20033	1030	-75.20070	0.37
$1^5\Sigma_u^-$	2	0.89(221110001)	291	-75.12126	1090	-75.12278	1.52
$2^5\Sigma_g^+$	2+4	0.85(2211011)+0.40(2011211)	281	-75.02621	950	-75.02677	0.56
Average discrepancy							0.73

[a] Equilibrium distance of the ground state of the C_2 molecule.
[b] The MO ordering is $(\sigma_g)(\sigma_u)(p_x\pi_u)(p_y\pi_u)(p\sigma_g)(p_x\pi_g)(p_y\pi_g)(p\sigma_u)$(Rydberg s,$\sigma_g$)(Rydberg s$\sigma_u$).
[c] The threshold of the EGCI operator is $(\lambda_A, \lambda_{AA}, \lambda_{AAA})=(0, 0.04, 0.2)$.
[d] Quartet states which dissociate to $C(^3P_g) + C^+(^3P_u)$.
[e] Quintet states which dissociate to $C(^3P) + C(^3P)$.

TABLE II. Full-CI and EGCI results for the quartet and quintet states of C_2 and C_2^+ at R=2.0Å

State	Excitation level	Main configuration[a]	EGCI[b]		Full-CI		Difference (mhartree)
			Size	Energy	Size	Energy	
Quartet states (Ion)[c]							
$1^4\Sigma_g^-$	2	0.89(22111)	415	-75.04365	1220	-75.04605	2.40
$1^4\Delta_u$	3	0.67(220111)-0.67(2210101)	382	-74.99192	1220	-74.99285	0.93
$1^4\Sigma_u^+$	3	0.67(221011)+0.67(2201101)	382	-74.98966	1080	-74.99060	0.94
$1^4\Pi_g$	2	0.93(2211001)	406	-74.95419	1160	-74.95528	1.09
$1^4\Sigma_u^-$	3	0.52(220111)+0.52(2210101) -0.45(21112)	419	-74.91681	1220	-74.91981	3.00
$1^4\Pi_u$	3	0.85(2210011)-0.32(211111)	433	-74.87724	1160	-74.87855	1.31
$2^4\Sigma_g^-$	4	0.75(2200111)+0.31(210121) -0.31(2110201)	415	-74.86156	1220	-74.86778	6.22
$2^4\Pi_g$	2	0.75(21121)-0.31(2110102)	406	-74.84329	1160	-74.84950	6.21
$2^4\Sigma_u^-$	3	0.61(21112)+0.57(22110001)	419	-74.83424	1220	-74.83747	3.23
$2^4\Pi_u$	3	0.50(2120101)+0.39(12211) -0.35(211111)-0.33(211111)	433	-74.81097	1160	-74.81437	3.40
$1^4\Sigma_g^+$	4	0.47(211021)+0.47(2101201) +0.35(22100101)+0.35(22010011)	379	-74.78104	1080	-74.78535	4.31
$1^4\Delta_g$	4	0.52(211021)-0.52(2101201) +0.38(22100101)+0.38(22010011)	379	-74.78058	1220	-74.78418	3.60
Average discrepancy							3.05
Quintet states[d]							
$1^5\Pi_g$	2	0.93(2211101)	353	-75.40083	1090	-75.40298	2.15
$1^5\Sigma_g^+$	2	0.93(2211011)	412	-75.33548	950	-75.33837	2.89
$1^5\Pi_u$	3	0.86(2210111)-0.33(211121)	372	-75.32600	1030	-75.32664	0.64
$1^5\Sigma_u^-$	2	0.80(22111001)-0.40(221111)	361	-75.26128	1090	-75.26339	2.11
$2^5\Sigma_g^+$	2	0.54(2121101)-0.54(211211)	412	-75.25846	950	-75.26202	3.56
$1^5\Delta_g$	2	0.56(2121101)+0.56(211211)	412	-75.22117	950	-75.22188	0.71
Average discrepancy							2.01

[a] The MO ordering is $(\sigma_g)(\sigma_u)(p_x\pi_u)(p_y\pi_u)(p\sigma_g)(p_x\pi_g)(p_y\pi_g)(p\sigma_u)$(Rydberg s,$\sigma_g$)(Rydberg s,$\sigma_u$).
[b] The threshold of the EGCI operator is $(\lambda_A, \lambda_{AA}, \lambda_{AAA})$=(0, 0.04, 0.2).
[c] Quartet states which dissociate to $C(^3P_g) + C^+(^3P_u)$.
[d] Quintet states which dissociate to $C(^3P) + C(^3P)$.

Six quintet states of C_2, which dissociate to $C(^3P_g) + C(^3P_g)$ in the atomic limit, are examined in Tables I and II. The avoided crossing occurs between the first and second $^5\Sigma_g^+$ states: the dominant configuration of the $1^5\Sigma_g^+$ state is $(\sigma_g)^2(\sigma_u)^1(\pi_u)^3(\sigma_g)^1(\pi_g)^1$at R=$r_e$, while that is $(\sigma_g)^2(\sigma_u)^2(\pi_u)^2(\pi_g)^2$ at R=2.0Å. The $2^5\Sigma_g^+$ state has the complemental electronic configuration. The $1^5\Pi_u$ state also changes its electronic configuration from $(\sigma_g)^2(\sigma_u)^1(\pi_u)^2(\sigma_g)^2(\pi_g)^1$ at R=r_e to $(\sigma_g)^2(\sigma_u)^2(\pi_u)^1(\sigma_g)^1(\pi_g)^2$ at R=2.0Å. This state has three-electron excitation nature and is rather difficult to be described well. Again the results of the EGCI method is satisfactory for all the quintet states. The average discrepancy is 0.73 and 2.01 mhartree for R=r_e and R=2.0Å, respectively. The dimensions of the EGCI calculations are 200 ~ 300 at R=r_e and 350 ~ 400 at R=2.0Å, whereby those of the full-CI one are 950 ~ 1090.

The potential curves of the low-lying 12 quartet states of C_2^+ and 6 quintet states of C_2 are shown in Figs. 2 and 3, respectively. Though the active space and the basis set are small, the present calculation reproduces the overall behaviors of the potential curves reported in the previous studies.[2,8] The total energies of the EGCI method agree with the full-CI ones with the errors less than 10 mhartree in all the nuclear distances. Therefore, the potential curves calculated by the two methods almost overlap to each other.

The spectroscopic constants for the bound quartet and quintet states are calculated by the Dunham method.[35] The EGCI and full-CI results are compared in Table III. The term energy T_e of the quartet states of C_2^+ are calculated relative to the ground state $X^4\Sigma_g^+$. The EGCI calculation reproduces well the full-CI results for the T_e and r_e values. The errors lie within 0.03 eV for T_e and within 0.01 Å for r_e. The present T_e and r_e values are slightly larger than those due to Petrongolo et al.[2] The EGCI results are also encouraging for the vibrational constant ω_e: the average discrepancy of ω_e is 16.43 cm^{-1} for the quartet states and 15.2 cm^{-1} for the quintet states. The vibrational anharmonicity constant $\omega_e\chi_e$ sensitively reflects the shape of the potential curve. This value is also well reproduced by the EGCI method. The average discrepancies of $\omega_e\chi_e$ are 0.82 cm^{-1} and 2.16 cm^{-1} for the quartet and quintet states, respectively. The accuracy of the EGCI results is excellent even for the higher order terms, B_e, α_e: the errors are within 0.01 and 0.004 cm^{-1}, respectively. The shape of

TABLE III. Spectroscopic constants for the bound quartet and quintet states of C_2 and C_2^+.

State	Method	T_e (eV)	r_e (Å)	ω_e (Δ^a) (cm^{-1})	$\omega_e\chi_e$ (Δ^a) (cm^{-1})	B_e (cm^{-1})	α_e (cm^{-1})	r_{hump} (Å)
Quartet states (Ion)								
$1^4\Sigma_g^-$	EGCI	0.0	1.48	1168 (15)	18.25 (-0.94)	1.28	0.0219	
	Full-CI	0.0	1.48	1153	19.19	1.28	0.0231	
$1^4\Pi_g$	EGCI	1.51	1.29	1863 (-11)	21.96 (-1.95)	1.68	0.0042	
	Full-CI	1.50	1.30	1874	23.91	1.67	0.0043	
$1^4\Sigma_u^-$	EGCI	2.97	1.41	1406 (13)	16.99 (-0.53)	1.40	0.0184	
	Full-CI	2.97	1.42	1393	17.52	1.40	0.0190	
$1^4\Delta_u$	EGCI	2.67	2.14	522 (5)	4.77 (-0.11)	0.62	0.0074	
	Full-CI	2.66	2.14	527	4.88	0.62	0.0072	
$1^4\Sigma_u^+$	EGCI	2.72	2.13	572 (0)	9.49 (0.50)	0.62	0.0061	
	Full-CI	2.71	2.14	572	8.99	0.62	0.0058	
$2^4\Pi_g$	EGCI	5.10	1.60	1559 (37)	16.67 (-0.17)	1.10	0.0050	2.03
	Full-CI	5.08	1.60	1522	16.70	1.10	0.0055	2.03
$1^4\Sigma_g^+$	EGCI	7.97	1.55	1103 (34)	23.01 (-1.71)	1.17	0.0178	1.92
	Full-CI	7.94	1.55	1069	24.72	1.17	0.0197	1.91
Average discrepancy				(16.43)	(0.84)			
Quintet states								
$1^5\Pi_g$	EGCI	2.98	1.70	744 (24)	12.78 (5.41)	0.97	0.0203	
	Full-CI	2.99	1.71	720	7.37	0.96	0.0163	
$1^5\Sigma_g^+$	EGCI	4.39	1.45	1298 (0)	27.78 (0.66)	1.34	0.0220	1.89
	Full-CI	4.39	1.45	1298	27.12	1.33	0.0207	1.87
$1^5\Delta_g$	EGCI	6.12	1.42	1480 (13)	6.97 (0.41)	1.40	0.0038	1.92
	Full-CI	6.11	1.42	1467	6.56	1.40	0.0037	1.93
Average discrepancy				(15.20)	(2.16)			

[a] Values in parentheses show the deviations from the full-CI results (in cm^{-1}).

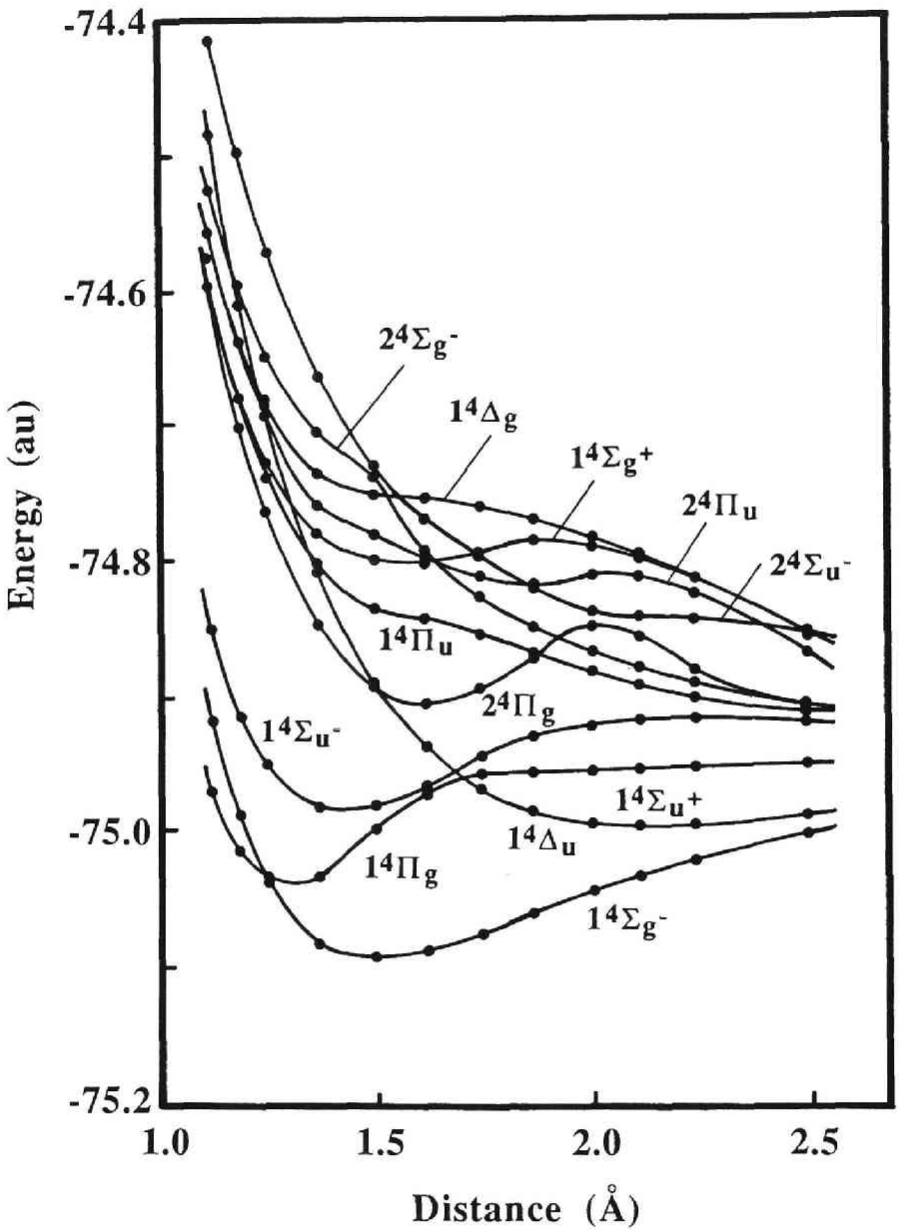

FIG. 2. Potential curves for the quartet states of C_2^+ molecule calculated by the full-CI and SAC-CI methods. Basis set is [4s2p] of Huzinaga-Dunning plus Rydberg s function with ζ=0.023 and the active space is limited to four occupied and six unoccupied MOs.

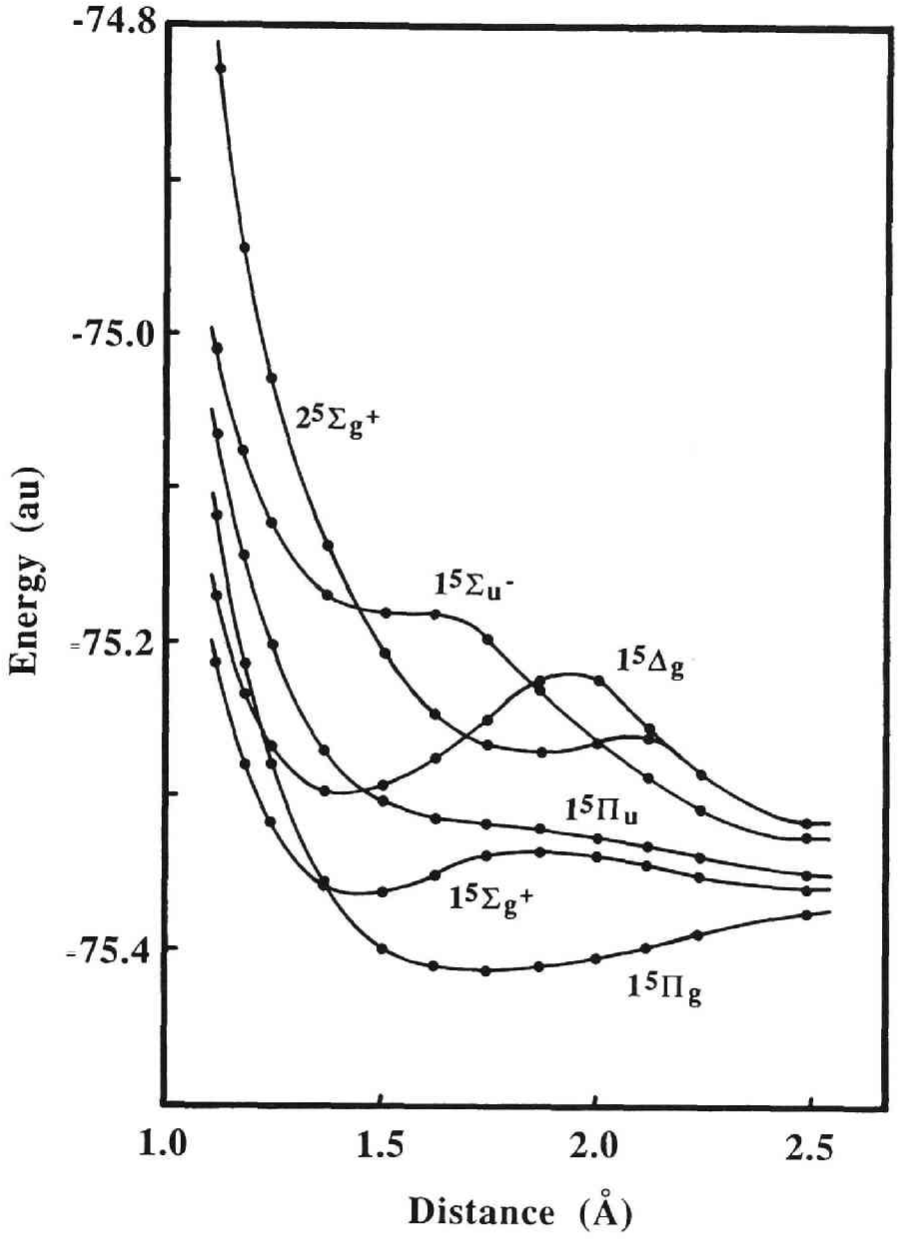

FIG. 3. Potential curves for the quintet states of C_2 molecule calculated by the full-CI and SAC-CI methods. Basis set is [4s2p] of Huzinaga-Dunning plus Rydberg *s* function with ζ=0.023 and the active space is limited to four occupied and six unoccupied MOs.

the repulsive potential curves is also well reproduced by the EGCI method as seen from Figs. 2 and 3.

The $2^4\Pi_g$ and $1^4\Sigma_g^+$ states of C_2^+ and the $1^5\Sigma_g^+$ and $1^5\Delta_g$ states of C_2 have characteristic humps in their potential curves. The r_{hump} in Table III gives the internuclear distance where the potential curve has the maximum in energy at the avoided crossing region. Again the EGCI method gives the excellent results for r_{hump} with the error of only ± 0.01 Å.

Thus, the EGCI method describes well the potential curves of the several quartet states of C_2^+ and the several quintet states of C_2. These results show that the EGCI method is useful for investigating the reaction dynamics involving high spin-multiplicity.

B. Hyperfine splitting constant of the $X^4\Sigma_g^-$ state of C_2^+

Next we investigate the accuracy of the high-spin EGCI wave function in terms of hyperfine splitting constants (hfsc). Since hfsc is a local property, proportional to the spin density at the nucleus, theoretical estimation sensitively depends on the quality of the wave function used. It is important to include adequately the electron correlation and spin correlation effects.[36,37] In particular, multiple excitation configurations are important for quantitative estimations of this property. The SAC-CI method, in which higher order terms are included in the unlinked terms, has been successfully applied to the calculations of the hfsc's of various radicals.[38-43] The EGCI method, which includes higher order terms more explicitly, would also be a reliable method for calculating the hfsc's.

The ground state of the C_2^+ molecule is $X^4\Sigma_g^-$ and it has some multiple excitation nature and therefore would give a good example for the present examination. Since inner core polarization is quite important for theoretical estimation of hfsc's, CI calculations should include all the core and valence orbitals in the active space. Because of this requirement, full-CI calculations using the extended basis are impossible, and therefore, we use the minimal STO-6G basis for the present calculation. The total energy and the hfsc of the $X^4\Sigma_g^-$ state calculated by the EGCI, full-CI, and SD-CI methods are summarized in Table IV. The full-CI method gives the hfsc of 56.37 (G) in comparison with the observed value, 34.5 (G).[7] The SD-CI

TABLE IV. Total energy and hyperfine splitting constant (hfsc) for the $X^4\Sigma_g^-$ state of C_2^+ calculated by the EGCI, Full-CI, and SD-CI method with the use of the STO-6G basis.

Method	Dimension	Total energy		Hfsc[b]		
		(au)	Δ^a(mhartree)	(G)	Δ^a(G)	Δ^a(%)
full-CI[c]	3176	-75.07686	-	56.37	-	
EGCI	223	-75.07573	1.13	56.73	0.36	0.6
SD-CI[d]	97	-74.98276	94.10	84.65	28.28	50.2

[a] Deviation from the full-CI results.
[b] Experimental hfsc is 34.5 (G).
[c] Reference calculation is performed using the slater-determinant-based full-CI algorithm.
[d] With 2h-2p and 3h-3p configurations from closed-shell HF.

method gives the hfsc of 84.65 (G); the deviation is as large as 28.28 (G), which corresponds to 50.2 % of the exact value. This indicates the importance of multiple excitations. On the other hand, the EGCI method reproduces the full-CI result quantitatively with the error of only 0.35 (G) (0.6% of the exact value). The dimension of the EGCI calculation is 223, while that of the full CI is 3176.

The EGCI method for high spin multiplicity thus reproduces the full-CI results not only for the total energy but also for the hfsc. Though the examinations are only for small systems, the EGCI method, which includes the effect of multiple excitations, would give an accurate and useful method for calculating the energy and the hfsc of high-spin states.

C. N_2 and N_2^+ molecules

N_2 molecule has three higher occupied and three lower unoccupied valence MO's, and therefore, N_2 and N_2^+ molecules have a number of various high-spin states; high-spin states up to septet states exists for N_2 and up to sextet states for N_2^+. Some of the high-spin states play an important role in the predissociation and recombination processes. However, most of these states have multiple-excitation nature at large internuclear distances, and therefore, quantitative descriptions of these states are difficult. Previously, the SAC-CI method is applied to these molecules at R=1.09768Å, which is the equilibrium distance of N_2 in the ground state, and shown to be quite accurate for the states from singlet to septet multiplicities.[21] Here, we apply the EGCI method to the quartet to septet states of N_2 and N_2^+ at the elongated internuclear distance, R=2.0Å. The results are summarized in Table V.

Ten quartet states of N_2 and eleven quintet states of N_2^+ are calculated. These quartet states dissociate to $N(^4S^0) + N^+(^3P)$ and $N(^4S^0) + N^+(^1D)$, and these quintet states to $N(^4S^0) + N(^4S^0)$, $N(^4S^0) + N(^2D^0)$, and $N(^4S^0) + N(^2P^0)$ in their atomic limits. At R=1.098Å, most of these states are described by two electron excitations from the closed-shell configuration, so that the SAC-CI (R-DT) method gave an excellent result.[21] However, at 2.0Å, three- and four-electron excitations become important, as seen from Table V, and therefore, multiple excitations are essentially important for the descriptions of these states. However, as seen from Table V, the EGCI method gives very accurate descriptions for all the states. The average discrepancies in the total energy are 3.49 and 0.70 mhartree for the quartet and quintet states, respectively. The dimensions of the EGCI calculations are about one-sixth of those of the full CI for the quartet states and one-fifth for the quintet states.

Four sextet states of N_2^+ are examined and they dissociate to $N(^4S^0) + N^+(^3P)$ in the atomic limit. The dominant configurations of the $1^6\Pi_g$ and $1^6\Sigma_u^+$ states are described by the four-electron excitation operators, so that they are difficult to be described by the previous SAC-CI(R-TQ) method: we have to use SAC-CI(R-general) method.[21] The errors of the present EGCI method for these sextet states are within 1.24 mhartree and the average error is only 0.65 mhartree.

Finally, only one septet state $1^7\Sigma_g^+$ is calculated. Since the excitation level increases as the spin multiplicity increases, the number of independent spin functions

TABLE V. Full-CI and EGCI results for the quartet, quintet, sixtet, and septet states of N_2 and N_2^+ at R=2.0Å.

State	Excitation level	Main configuration[a]	EGCI[b]		Full-CI		Difference (mhartree)
			Size	Energy	Size	Energy	
Quartet states (Ion)[c]							
$1^4\Sigma_u^+$	2+4	0.57(222110001-22121001) +0.36(221010012-220110021)	384	-108.22715	2416	-108.23246	5.31
$1^4\Pi_g$	2	0.88(221120001)	417	-108.22359	2480	-108.22606	2.47
$1^4\Pi_u$	3	0.84(221020011)	368	-108.17541	2480	-108.17858	3.17
$1^4\Delta_u$	2+4	0.60(222110001+22121001) -0.31(221010012+220110021)	381	-108.16424	2524	-108.16826	4.23
$1^4\Sigma_g^+$	3	0.90(221110011)	378	-108.15390	2524	-108.15702	3.12
$1^4\Delta_g$	2	(0.69+0.55+0.39)(221110011)	378	-108.14628	2416	-108.14911	2.83
$1^4\Sigma_u^-$	2	0.53(22211001+221210001) -0.44(2211201)	381	-108.14476	2524	-108.14767	2.91
$2^4\Pi_g$	2+4	0.76(2212101)-0.38(221010102)	417	-108.12077	2480	-108.12470	3.93
$1^4\Sigma_g^-$	3	0.47(22111002+221110002) -0.46(222010011+220210011)	390	-108.11626	2524	-108.11961	3.35
$2^4\Pi_u$	3	0.54(222010101)+0.48(22111011) -0.44(22111011)	368	-108.09026	2480	-108.09383	3.57
Average discrepancy							3.49
Quintet states[d]							
$1^5\Sigma_g^+$	2	0.80(221120011)	306	-108.72949	1540	-108.73043	0.94
$1^5\Pi_u$	2+4	0.87(221210011)+0.35(221100112)	289	-108.64625	1540	-108.64718	1.15
$2^5\Sigma_g^+$	2+4	0.48(222110101-22121011-221120011) -0.33(221010112+220110121)	306	-108.64091	1540	-108.64162	0.71
$1^5\Pi_g$	3	0.78(221110021)-0.49(222100111)	273	-108.60619	1540	-108.60670	0.51
$1^5\Delta_g$	2+4	0.56(222110101+22121011) +0.37(221010112-220110121)	306	-108.60038	1540	-108.60094	0.56
$2^5\Pi_u$	2+4	0.84(22112011)-0.34(221010211)	289	-108.59603	1540	-108.59701	0.98
$1^5\Delta_u$	3	0.48(222010111-220210111) +0.47(221110102-221110102)	283	-108.58659	1515	-108.58706	0.47
$1^5\Sigma_u^+$	3	(0.60-0.58+0.34)(221110111)	283	-108.58108	1515	-108.58154	0.46
$1^5\Sigma_g^-$	2	0.56(22211011+221210101) +0.35(221010121+220110112)	308	-108.57115	1540	-108.57181	0.66
$2^5\Pi_g$	3	0.76(220120111)-0.45(221110201)	273	-108.55644	1540	-108.55719	0.75
$1^5\Sigma_u^-$	3	0.47(222010111+220210111) -0.46(221110102+221110102)	297	-108.55552	1580	-108.55605	0.53
Average discrepancy							0.70
Sixtet states (Ion)[e]							
$1^6\Sigma_g^+$	3	0.97(221110011)	190	-108.23046	629	-108.23066	0.20
$1^6\Pi_u$	3	0.92(22111011)-0.33(2211100101)	180	-108.15496	615	-108.15515	0.19
$1^6\Pi_g$	4	0.91(220110111)-0.32(2201100111)	198	-108.09662	615	-108.09757	0.95
$1^6\Sigma_u^+$	4	0.79(221100111)+0.45(211120011)	201	-108.05795	629	-108.05919	1.24
Average discrepancy							0.65
Septet state[f]							
$1^7\Sigma_u^+$	3	0.95(221110111)+0.31(2211100111)	120	-108.68711	287	-108.68728	0.17

[a] The MO ordering is $(\sigma_g)(\sigma_u)(p_x\pi_u)(p_y\pi_u)(p\sigma_g)$(Rydberg s,$\sigma_g$)(Rydberg s,$\sigma_u$)$(p_x\pi_g^*)(p_y\pi_g^*)(p\sigma_u^*)$.

[b] The threshold of the EGCI operator is $(\lambda_A, \lambda_{AA}, \lambda_{AAA})$=(0, 0.04, 0.2).

[c] Quartet states which dissociate to $N(^4S^0) + N^+(^3P)$ and $N(^4S^0) + N^+(^1D)$.

[d] Quintet states which dissociate to $N(^4S^0) + N(^4S^0)$, $N(^4S^0) + N(^2D^0)$, and $N(^4S^0) + N(^2P^0)$.

[e] Sixtet states which dissociate to $N(^4S^0) + N^+(^3P)$.

[f] Septet state which dissociates to $N(^4S^0) + N(^4S^0)$.

and therefore the dimension of the EGCI calculation increases relative to that of the full-CI method. The discrepancy is 0.17 mhartree.

We thus conclude that the EGCI method describes well the quasi-degenerate states and the states of multiple excitation natures in the high-spin multiplet states of the N_2 and N_2^+ molecules.

D. m-Phenylenebis(methylene) (m-PBM)

Here, we investigate the ground and excited states of m-phenylenebis(methylene) (m-PBM), which is the smallest unit of a series of the organic high-spin molecules.[14-20] The quintet ground state of this molecule was examined by the SAC-CI method in the previous paper.[21] Here, we consider the ground state 1^5A_1 and the low-lying two excited states, 1^3B_2 and 1^1A_1 states. The results of the EGCI, full-CI and SD-CI methods are summarized in Tables VI.

The relative stability of these three states is calculated as $1^5A_1 < 1^3B_2 < 1^1A_1$, which is consistent with the calculations of Teki et al[17] using the Heizenberg Hamiltonian, though the space symmetries of these states were not given in their report. Though the energy separations of these three states are overestimated in comparison with the experimental evidence, the ordering of these states is correctly reproduced both by the SD-CI and EGCI methods. However, the absolute values of the total energies of the SD-CI method deviate by 48, 72, and 68 mhartree from those of the full CI for the 1^5A_1, 1^3B_2, and 1^1A_1 states, respectively. Since the two excited states, 1^3B_2 and 1^1A_1, have two-electron excitation nature as seen from the main configurations, multiple excitation operators are necessary for quantitative descriptions of these states. The EGCI method includes such multiple excitation operators, so that the errors in the total energy are small, ~ 6 mhartree: these three states having different spin-multiplicity are quantitatively described in a good balance by the EGCI method. The calculational dimensions of the EGCI method are less than one-tenth of those of the full CI. These results indicate that the excitation operators in the EGCI method are selected appropriately and efficiently for all the spin-multiplicities. We note that in the previous SAC-CI(R-DT) method,[21] the ground 1^5A_1 state is described with the error of 6.73 mhartree.

TABLE VI. EGCI, Full-CI, and SD-CI results for the 1^5A_1, 1^3B_2, and 1^1A_1 states of m-phenylenebis(methylene).

State	Main configuration[a]	SD-CI[b]				EGCI				Full-CI			Exptl.
		Size	Energy (au)	Δ[c]	Excitation energy (cm^{-1})	Size	Energy (au)	Δ[c]	Excitation energy (cm^{-1})	Size	Energy(au)	Excitation energy(cm^{-1})	Excitation energy(cm^{-1})
1^5A_1	0.68(221111) +0.41(2211101) -0.38(22110101) -0.23(22110011)	354	-305.47948	47.81	-	400[d]	-305.52094	6.35	-	5462	-305.52729		
1^3B_2	0.39(222011) -0.39(220211) -0.25(22112) +0.23(2220101) -0.23(2220101)	135	-305.44637	72.36	7270	1012[e]	-305.51280	5.93	1790	12730	-305.51873	1880	> 300[f]
1^1A_1	0.38(221111) +0.28(22021001-22201001) +0.26(22022-22202) +0.25(2220011) +0.25(222002-220202)	120	-305.44423	68.37	7740	754[e]	-305.50744	5.16	2960	8300	-305.51260	3220	

[a] The MO ordering is (core)$(a_2)(b_1)(a_1)(b_2)(a_2)(b_1)(b_1)(a_2)(b_1)(a_1)(a_1)$.
[b] With 2h-2p and 3h-3p configurations from closed-shell HF.
[c] Deviation from the full-CI result (in mhartree).
[d] EGCI calculation using the threshould of $(\lambda_A, \lambda_{AA}, \lambda_{AAA})=(10^{-5}, 0.1, 10.0)$.
[e] EGCI calculation using the threshould of $(\lambda_A, \lambda_{AA}, \lambda_{AAA})=(0, 0.04, 0.2)$.
[f] Reference 16,17: ENDOR experiment

E. Spin density distribution in m-PBM

Spin density distribution is one of the most important and characteristic properties of ferromagnetic molecules. We investigate the spin density distributions in the ground 1^5A_1 state and the first excited 1^3B_2 state of m-PBM. The hfsc's are experimentally determined and the comparison of the hfsc's is a good examination of the quality of the wave function. However, the estimation of the hfsc's without including inner core polarizations is meaningless, and for including them the present system requires the active space of 46 MO's even if the minimal set is adopted, so that the full-CI calculation is impossible for this system. We therefore compare the spin density distributions on the valence pπ and pn orbitals of each carbon atom of m-PBM calculated from the wavefunctions obtained in the previous section by the EGCI, full-CI, and SD-CI method. The results for the 1^5A_1 and 1^3B_2 states are summarized in Table VII. Total spin densities are normalized to 2S. The numbering of the carbon atoms is shown in Fig. 1.

In the 1^5A_1 state, the unpaired π-electrons are distributed alternately in accordance with the ENDOR experiment[16] and this feature was also obtained from the Heizenberg Hamiltonian.[17] The SD-CI method also reproduces this feature, but, it underestimates the amplitude of the π-spin densities by 0.015 ~ 0.037 in comparison with the full-CI results: the errors are 3 ~ 28% of the exact values and they are attributed to the lack of the multiple excitation configurations. On the other hand, the errors of the EGCI method for the π and n-spin densities are only $1.33 \sim 6.26 \times 10^{-3}$ (1 ~ 3% of the exact values).

The effect of the multiple excitations is more remarkable for the spin densities of the 1^3B_2 state than those for the 1^5A_1 state. The π-spin densities of 1^3B_2 state also change their signs alternately, though the amplitudes are rather small. The SD-CI calculation gives positive π-spin densities for all the carbon sites. On the other hand, the EGCI calculation, which includes up-to-six-electron excitation operators, reproduces this alternate nature of the π-spin densities. Again the errors of the EGCI method are in the order of 10^{-3}, which correspond to 2 ~ 6 % of the exact values.

We thus conclude that the EGCI method is accurate not only for the energetics but also for spin density distributions.

TABLE VII. Spin density distribution on each carbon of m-phenylenebis(methylene) for the 1^5A_1 and 1^3B_2 states calculated by the EGCI, Full-CI, and SD-CI methods.

atom: x	SD-CI			EGCI			Full-CI
	$<x\|\rho^{\alpha-\beta}\|x>^a$	$\Delta^b X 10^3$	$\Delta^b(\%)$	$<x\|\rho^{\alpha-\beta}\|x>^a$	$\Delta^b X 10^3$	$\Delta^b(\%)$	$<x\|\rho^{\alpha-\beta}\|x>^a$
1^5A_1 state							
C1: pπ	0.28720	-23.79	(7.6)	0.31622	+5.23	(1.7)	0.31099
C2: pπ	-0.12073	+32.97	(21.5)	-0.14843	+5.27	(3.4)	-0.15370
C3: pπ	0.26277	-14.96	(5.4)	0.27542	-2.31	(0.8)	0.27773
C4: pπ	-0.09570	+36.55	(27.6)	-0.13092	+1.33	(1.0)	-0.13225
C5: pπ	0.79115	-23.29	(2.9)	0.80818	-6.26	(0.8)	0.81444
C5: pn	0.70256	+1.28	(0.2)	0.70351	+2.23	(0.3)	0.70128
1^3B_2 state							
C1: pπ	0.07256	-140.07	(65.8)	0.20270	-9.93	(4.7)	0.21263
C2: pπ	0.00156	+102.62	(101.5)	-0.09516	+5.90	(5.8)	-0.10106
C3: pπ	0.05455	-133.52	(71.0)	0.18185	-6.22	(3.3)	0.18807
C4: pπ	0.00023	+88.63	(100.3)	-0.08362	+4.78	(5.4)	-0.08840
C5: pπ	0.47618	-36.65	(7.1)	0.51482	+1.99	(3.9)	0.51283
C5: pn	0.32097	+72.17	(29.0)	0.25330	+4.50	(1.8)	0.24880

[a] Total spin density is normarized to 2S, the number of unpaired α spins.
[b] Deviation from the full-CI results.

V. SUMMARY

The EGCI method is extended to high-spin multiplicity and test calculations are performed for quartet, quintet, sextet, and septet states. This method, in which excited, ionized, and electron attached states are calculated using the information on the correlated wave function of the ground state, is applicable to quasi-degenerate states of various spin multiplicities and various numbers of excitation processes. The examinations of the EGCI method are performed for several high-spin states of C_2, C_2^+, N_2, N_2^+, and m-PBM, especially for the states whose main configurations are described by multiple excitation operators. The EGCI method reproduces well the full-CI results for the potential curves and the spectroscopic constants of the quartet states of C_2^+ and the quintet states of C_2. The quasi-degenerate high-spin states of N_2 and N_2^+ at R=2.0Å and the various spin-multiplet states of m-PBM are also described well by the EGCI method.

The accuracy of the EGCI method is also investigated in terms of the hfsc's and the spin density distributions. The results of the EGCI method show good agreements with those of the full CI. For the hfsc of the $X^4\Sigma_g^-$ state of C_2^+, the deviation from the full-CI value is only 0.6% of the exact value. The $p\pi$- and pn-spin densities are examined for the 1^5A_1 and 1^3B_2 states of m-PBM. The errors of the EGCI method is 0.8 ~ 3.4 % and 1.8 ~ 5.8 % of the exact values for the 1^5A_1 and 1^3B_2 states, respectively.

In conclusion, the EGCI method is confirmed to be accurate and useful not only for investigating the energetics appearing in the studies dynamics and reactions, but also for studying the spin density distributions of various spin multiplet states.

ACKNOWLEDGMENTS

The authors wish to thank Dr. T. Momose for kindly letting us use his Slater-determinant-based full-CI program. The full-CI calculations have been carried out with the HITAC M-680H and S-820 computer at the Institute for Molecular Science. This study has partially been supported by the Grant-in-Aid for Scientific Research from the Japanese Ministry of Education, Science, and Culture, and by CIBA-GEIGY Foundation (Japan) for the Promotion of Science.

REFERENCES

[1] G. Verhaegen, J. Chem. Phys. **49** 4696 (1968).

[2] C. Petrongolo, P. J. Bruna, S. D. Peyerimhoff, and R. J. Buenker, J. Chem. Phys. **74** 4594 (1981).

[3] P. Rosmus, H. J. Werner, E. A. Reinsch, and M. Larsson, J. Electron. Spectrosc. **41** 289 (1986).

[4] G. Hirsch and R. J. Buenker, J. Chem. Phys. **87** 6004 (1987).

[5] M. Rosslein, M. Wyttenbach, and J. P. Maier, J. Chem. Phys. **87** 6770 (1987); D. Forney, H, Althaus, and J. P. Maier, J. Phys. Chem. (in press).

[6] M. Rasanen, J. Y. Liu, T. P. Dzugan, and V. E. Bondybey, Chem. Phys. Lett. **142** 308 (1987).

[7] L. B. Knight, Jr., S. T. Cobranchi and E. Earl, J. Chem. Phys. **88** 7348 (1988).

[8] S. N. Beck, E. A. McCullough Jr., and D. Feller, Chem. Phys. Lett. **175** 629 (1990).

[8] K. Kirby and B. Liu, J. Chem. Phys. **70** 893 (1979).

[9] F. R. Gilmore, J. Quant. Spectrosc. Radiat. Transfer **5** 369 (1965).

[10] M. Krauss and D. B. Neumann, Mol. Phys. **32** 101 (1976).

[11] H. H. Michels and F. E. Harris, Chem. Phys. Lett. **3** 441 (1969).

[12] I. Easson and M. H. L. Pryce, Can. J. Phys. **51** 518 (1973).

[13] K. R. German, J. Chem. Phys. **63** 5252 (1975).

[14] K. Itoh, Chem. Phys. Lett. **1** 235 (1967).

[15] K. Itoh, in *Magnetic Molecular Materials*, edited by D. Gatteschi *et al.* (Kluwer Acad. Publ. Netherlands, 1991).

[16] Y. Teki, T. Takui, K. Itoh, H. Iwamura, and K. Kobayasi, J. Am. Chem. Soc. **108** 2147 (1986).

[17] Y. Teki, T. Takui, M. Kitano, and K. Itoh, Chem. Phys. Lett. **142** 181 (1987).

[18] I. Fujita,Y. Teki, T. Takui, T. Kinoshita, K. Ito, F. Miko, Y. Sawaki, H. Iwamura, A. Izuoka, and T. Sugawara, J. Am. Chem. Soc. **112** 4074 (1990).

[19] T. Sugawara, H. Tukada, A. Izuoka, and H. Iwamura, J. Am. Chem. Soc. **108** 4272 (1986).

[20] A. Izuoka, S. Murata, T. Sugawara and H. Iwamura, J. Am. Chem. Soc. **109** 2631 (1987).

[21] H. Nakatsuji and M. Ehara, J. Chem. Phys. **98** 7179 (1993).

[22] H. Nakatsuji, Chem. Phys. Lett. **59** 362 (1978); **67** 329, 334 (1979).

[23] H. Nakatsuji and K. Hirao, J. Chem. Phys. **68** 2053 (1978).

[24] H. Nakatsuji, Acta Chim. Hungarica **129** 719 (1992).

[25] H. Nakatsuji, Chem. Phys. Lett. **177** 331 (1991).

[26] H. Nakatsuji, J. Chem. Phys. **83** 5743 (1985).

[27] H. Nakatsuji, J. Chem. Phys. **83** 713 (1985).

[28] H. Nakatsuji, J. Chem. Phys. **95** 4296 (1991).

[29] H. Nakatsuji, J. Chem. Phys. **94** 6716 (1991).

[30] S. Huzinaga, J. Chem. Phys. **42** 1293 (1965).
T. H. Dunning Jr., J. Chem. Phys. **53** 2823 (1970).

[31] H. Nakatsuji, Program system for the exponentially generated wave functions for ground, excited, ionized, and electron attached states (to be published).

[32] M. Dupuis, J. D. Watts, H. O. Viller, and G. J. B. Hurst,
Program System HONDO7, Program Library No. 544,
Computer Center of the Institute for Molecular Science, (1989).

[33] P. J. Knowles and N. C. Handy, Chem. Phys. Lett. **111** 315 (1984).

[34] T. Momose, Slater-determinant-based full-CI program based on Knowles algorithm.

[35] J. L. Dunham, Phys. Rev. **41** 713, 721 (1932).

[36] H. Nakatsuji, H. Kato, and T. Yonezawa, J. Chem. Phys. **51** 3175 (1969);
H. Nakatsuji, J. Chem. Phys. **59** 2586 (1973).

[37] H. Nakatsuji and K. Hirao, J. Chem. Phys. **68** 4279 (1978).

[38] H. Nakatsuji, K. Ohta, and T. Yonezawa, J. Phys. Chem. **87** 3068 (1983).

[39] T. Momose, T. Shida, and H. Nakatsuji, J. Chem. Phys. **89** 4185 (1988).

[40] H. Nakatsuji and M. Izawa, J. Chem. Phys. **91** 6205 (1989).

[41] T. Momose, M. Yamaguchi, and T. Shida, J. Chem. Phys. **93** 7284 (1990).

[42] L. B. Knight, Jr., B. W. Gregory, D. W. Hill, C. A. Arrington, T. Momose, and T. Shida, J. Chem. Phys. **94** 67 (1991).

[43] H. Nakatsuji and M. Izawa, J. Chem. Phys. **97** 435 (1992).

PART II

Theoretical Studies on the Excited and Ionized States of Titanium Tetraharides

Chapter 4

Theoretical study on the excited and ionized states of titanium tetrachloride

ABSTRACT

The excitation and ionization spectra of $TiCl_4$ have been studied theoretically by the symmetry adapted cluster(SAC)/SAC-CI and multi-reference CI (MRD-CI) methods. The calculated spectra show good agreement with the observed spectra. The present results indicate several new assignments for the excitation spectrum. The peaks below 8.0 eV are assigned to valence excitations and those at 9.35 eV and 10.04 eV are assigned to Rydberg type excitations within chlorine ligands. The ordering of the ionized states in the outer valence region is $(1t_1)^{-1} < (3t_2)^{-1} < (1e)^{-1} < (2t_2)^{-1} < (2a_1)^{-1}$, which supports the result of earlier Green's function calculations.

I. INTRODUCTION

Titanium tetrachloride is both a fundamental molecule and typical of the tetrahedral compounds of transition metals. Furthermore, it is important in both organic and inorganic chemistry as a Lewis acid. For example, $TiCl_4$ plays an important role in polymerization of alkenes by Ziegler-Natta catalysis.

A number of experimental studies have been reported to investigate the electronic structure of this important molecule. Details of the electronic excitation spectrum have been observed over a wide energy range up to the VUV region.[1-5] A schematic diagram of the spectrum is shown in Figure 1; there are five main bands in the region from 4 to 10 eV, of which the three at highest energy are the strongest.

The UV photo-ionization spectrum of $TiCl_4$ has also been investigated intensively; the He(I) and He(II) photoelectron spectra observed in the gas phase[6-9] are complex because there are five peaks in the narrow energy range (11.76 13.96 eV), thus leading to a range of possible assignments for this region; a schematic diagram of this spectrum is shown in Figure 2. A summary of assignments by elementary MO considerations, together with He(I), He(II) intensity changes, and considerations of photo-ionization cross-sections under synchrotron irradiation[10] support the early UV photoelectron spectral assignments.[6-9]

The X-ray photoelectron spectra of $TiCl_4$ and related molecules show well-defined satellites on the Ti($^2P_{3/2}$) line at 4.0 and 9.4 eV above the main line.[11] However, interpretation of these shake-up states, in terms of the VUV data, has been controversial[12,13] owing to the intensity ratio of the two bands.

Several theoretical studies have focussed upon these spectroscopic results; thus the VUV spectrum has been partially assigned by using both semiempirical methods,[2,5,14-17] SCF-Xα methods[18-20] and small scale CI calculations.[21] However, there are no ab initio calculations which include a detailed analysis of electron correlations.

Assignment of the UV photoelectron spectrum by means of theoretical methods, using semi-empirical or Xα calculations, is summarized in the study on the Green's function method;[22] this gave the ionization ordering :

$(1t_1)^{-1} < (3t_2)^{-1} < (1e)^{-1}$, $(2t_2)^{-1} < (2a_1)^{-1}$

This order is the same for the lowest three IPs as that obtained by open-shell INDO-SCF calculations.[23]

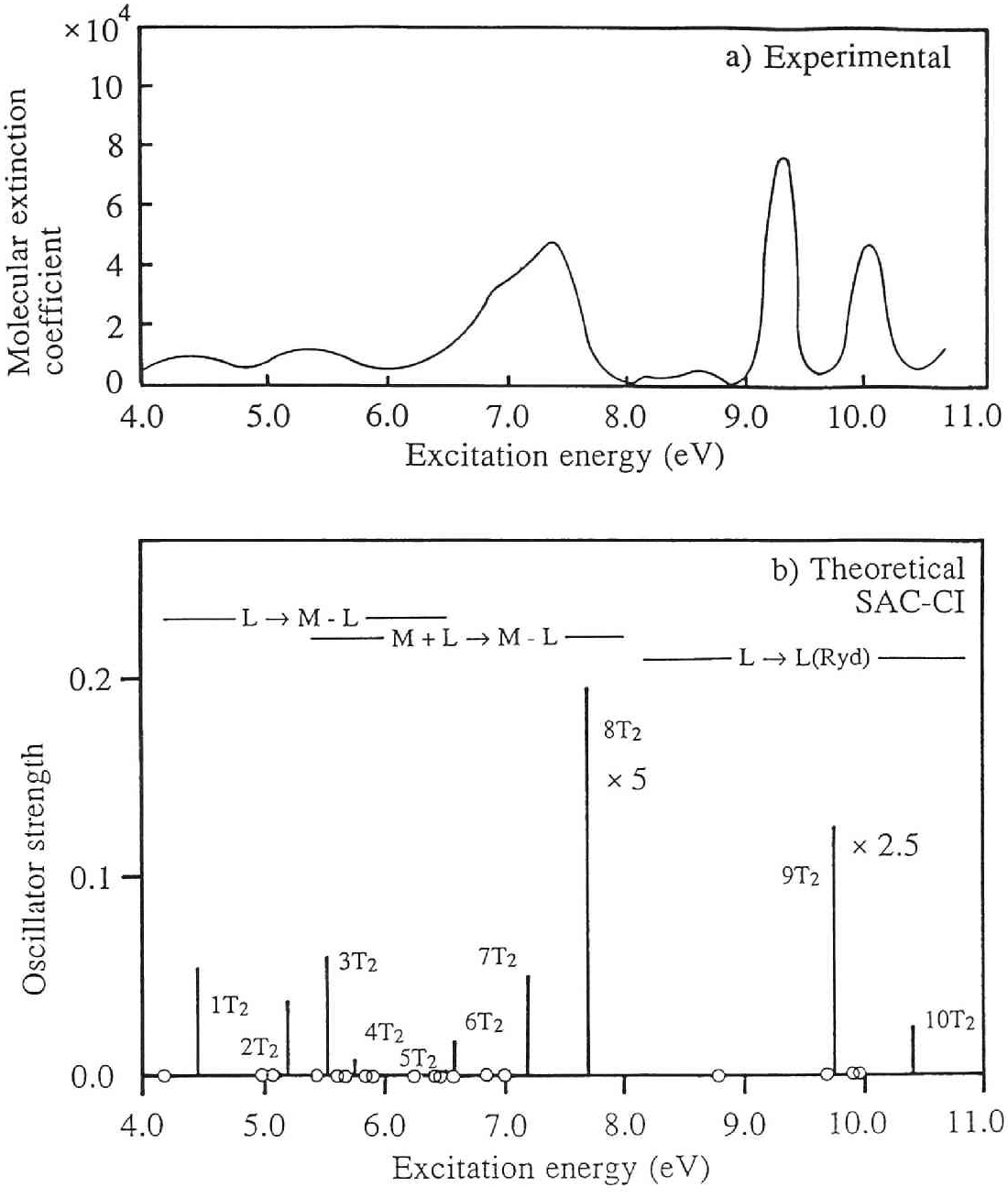

FIG. 1. (a) Experimental (b) SAC-CI theoretical excitation spectra of $TiCl_4$. For the $8T_2$ and $9T_2$ states the intensities given for the SAC-CI spectrum are 1/5 and 2/5 of the calculated ones.

In this paper, we re-investigate the excited and ionized states of $TiCl_4$, in order to put the theoretical aspect on a more rigorous level. We use the SAC (Symmetry Adapted Cluster expansion)[24]/SAC-CI method[25] which has been applied to a number of molecules including transition metal complexes.[26-28] This method has been shown to be useful for investigating spectroscopies of excited and ionized states of molecules and given many reliable new assignments for the experimental spectra. In addition, a parallel investigation using multi-reference CI has been performed; we have previously found that this method is capable of giving a good interpretation of the VUV spectra of aromatic compounds.[29,30] The present paper presents the consolidated results of the two approaches.

II. COMPUTATIONAL DETAILS

The structure of $TiCl_4$ is tetrahedral with Ti-Cl bond length of 2.17 Å[31]. Since we did not include structural relaxation effects in the present study, we focus upon vertical excitations of the $TiCl_4$ molecule. In all the calculations (including both the SAC-CI and MRD-CI ones below), the computations were performed in the C_{2V} subset of T_D; under these circumstances the MO identities are

$t_1(a_2 + b_1 + b_2)$, $t_2(a_1 + b_1 + b_2)$, $e(a_1 + a_2)$, and $a_1(a_1)$

with the inverse relationships shown in Table IV below. The B_1 and B_2 states are degenerate under these circumstances; there are no a_2 (T_D) MOs for $TiCl_4$ with the present basis sets. The T_D symmetry of $TiCl_4$ leads to the following open shell direct products of MOs in the low-lying excited states:

$t_1 * t_2 = T_1 + T_2 + A_2 + E$

$t_2 * t_2 = T_1 + T_2 + A_1 + E$

$t_1 * e = T_1 + T_2$

$t_2 * e = T_1 + T_2$

$t_2 * a_2 = T_1$

$t_1 * a_2 = T_2$

$e * e = A_1 + A_2 + E$

We tested two types of basis sets in these parallel studies, the effective core potentials of Hay and Wadt[32] and the all-electron GTO basis of Huzinaga,[33] but with various expansions and appended Rydberg functions, as described below.

A. Examination of basis sets

Initially in the SAC-CI study, we calculated the atomic excitation spectra of Ti^{3+}, Cl atom and Cl anion, and determined the final set to best reproduce the excitation energies of $TiCl_4$. Since the $TiCl_4$ bonds are polarized Ti^{+}-Cl^{-}, and some of the excitations were expected to approximate to ligand excitations, we examined the effect of diffuse functions on Cl that would produce an anion type basis. Table I shows the excitation energies of Ti^{3+} and the Cl atom together with the experimental values[34]. There exist large discrepancies between the theoretical results with the ECP and the experimental values; about 5.5 eV for the 4p state of Ti^{3+}. With the all-electron basis set of Huzinaga on the other hand, we can reproduce the experimental values within 0.20 eV. Furthermore, extensive tests of this ECP by both the SAC-CI and MRD-CI procedures failed to produce an acceptable envelope for the VUV excitation spectrum of $TiCl_4$. Table II shows $3p \rightarrow 4s$, 4p excitation energies of the Cl anion calculated with and without the anion s, p basis ($\zeta_s=\zeta_p=0.049$).[37] The effect is as large as 0.49 eV for some states and important for obtaining the correct ordering of the 4s and 4p states.

In the initial phase of the MRD-CI calculations, the ECP[33] was performed with a Ti [3s2p3d] and Cl [2s2p] valence shell, and an active space of 55 MOs and 24 electrons. Not only was the 8-10 eV region poorly interpreted, but the lowest excitations were also difficult to assign to the experimental envelope. Increase of the valence shell basis to Ti [3s4p3d1f] and Cl [2s2p1d] and a similar active space led to little improvement. Further, there were technical problems of extrapolation in the MRD-CI calculations owing to coupling of the roots into groups with similar composition, but with wide energy ranges.[36]

In view of the problems with fitting the experimental VUV envelope for $TiCl_4$, we decided to abandon the ECP, and further tests of the all-electron bases were undertaken. We finally selected the following three sets for the molecular calculations. Some features are summarized in Table III.

TABLE I. Excitation energies of Ti^{3+} ion and Cl atom calculated by the SAC-CI method (in eV).

		Basis set	
State	Exptl.[a]	ECP[b]	All electron[c]
Ti^{3+} ion			
4s	9.97	10.61	10.18
4p	15.86, 15.96	21.44	15.64
4d	24.40, 24.41	25.15	24.55
5s	26.33	26.91	27.03
5p	28.59, 28.63	33.19	28.58
Cl atom[d]			
(3p→ 4s)			
^2P	9.20, 9.28	9.30	9.43
^2D	10.43, 10.43	10.82	10.86
(3p→ 4p)			
^2S	10.56	10.37	10.61
^2P	10.56, 10.65	10.56	10.74
^2P	11.69, 11.71	12.00	12.14
^2F	11.79, 11.80	12.19	12.24

[a]Reference 35
[b]Basis sets in reference 33 are used.
[c]Basis sets in reference 34 are used.
[d]SAC-CI (R-general) method [Reference 35] is used.

TABLE II. Excitation energies of Cl anion with and without the anion basis calculated by the SAC-CI method (in eV).

		Anion basis[a]				
		Without		With		Effect of anion basis
State	Degeneracy	Singlet	Triplet	Singlet	Triplet	
(3p→ 4s)	3	4.62	4.43	4.16	4.08	-0.46
(3p→ 4p)	5	4.55	4.49	4.39	4.36	-0.16
	3	4.61	4.60	4.44	4.43	-0.17
	1	5.02	4.27	4.53	4.22	-0.49

[a]Anion bases with the exponents of $\zeta_s=\zeta_p=0.049$ are included or not included to the all electron [4s3p] set plus Rydberg basis with the exponents of $\zeta_s=0.025$, $\zeta_p=0.020$.

TABLE III. Basis set, active space, and SCF and correlation energies of the ground state for $TiCl_4$.

	Basis set		SCF		Correlated			
	Ti	Cl	Dimension	Energy (au)	Method	Active space (occ x vac)	Energy	Correlation energy
Set I	[6s4p3d]	[4s3p] +2s2p (diffuse)	120	-2685.87048	SAC/SAC-CI	58 MO's (12 x 46)	-2685.98434	-0.11386
Set II	[6s4p3d]	[4s3p]	88	-2685.86284	SAC/SAC-CI	58 MO's (16 x 42)	-2686.06560	-0.20276
Set III	[10s8p3d] +1s1p (Ryd)	[7s4p] +1d (pol)	156	-2686.68406	MRD-CI	52 MO's (12 x 40)	-2686.88429	-0.21023

Set I :

This set was designed, based on the calculations shown in Tables I and II, for studying singlet and triplet states by the SAC-CI method. For the Ti atom, Huzinaga's (14s8p5d)/[6s2p3d] set[33] augmented with two p-type functions with $\zeta_p = 0.15, 0.073$ to represent the 4p-orbitals was utilized. For the Cl atoms, Huzinaga's (11s8p)/[4s3p] set[33] enlarged with Rydberg s, p-functions of $\zeta_s = 0.025$, $\zeta_p = 0.02$ and anion s, p functions with the exponents of $\zeta_s = \zeta_p = 0.049$[37] seemed appropriate. As shown in Table II, the anion basis is important for describing 3s→ 4s, 4p excitations of the Cl anion. Thus the final set for the $TiCl_4$ molecule consisted of 120 functions. For the SAC-CI study the 12 highest occupied orbitals and 46 lowest virtual orbitals were selected for the active space.

Set II :

This set was used for the ionized states (SAC-CI only). The Rydberg functions and the anion basis on the Cl atom were removed from the basis set of Set I. The total number of basis functions was 88. The active space was composed of the 16 highest occupied orbitals and 42 lowest unoccupied orbitals.

In all the SAC-CI calculations, the Hartree-Fock SCF MO's of the ground state were obtained by use of the HONDO7[38] program, and were utilized as the reference set in the subsequent SAC/SAC-CI calculations performed with the SAC85 program.[39]

Set III :

The MRD-CI study used an all-electron triple zeta valence set[40a] on both Ti and Cl, augmented by Ti [1s1p] of Rydberg type (ζ_s 0.0314, ζ_p 0.016)[40b] and Cl [1d] polarization function. This led to 156 basis functions; the CI subset consisted of 52 MOs and 24 electrons with up to 69 main reference functions (69M20R in the usual[41a,b] MRD-CI terminology). The diagonalization dimensions were around 13,000 varying with irreducible representation, with a total selected configuration space of 400,000. The SCF calculations preceding the MRD-CI study were performed with the GAMESS suite of programs.[42]

B. Details of the SAC-CI Calculation

Electron correlation in the ground state was computed by the SAC theory[24] and those in the excited and ionzied states by the SAC-CI theory.[25] We included all single

excitations and selected double excitations in the linked terms. The contributions of triple and quadruple excitations are considered in the unlinked terms. To reduce the size of the matrices involved, we performed configuration selection as reported previously.[44] For the singlet and triplet states, the thresholds λ_g and λ_e were set to $2*10^{-5}$ and $4*10^{-5}$ a.u., respectively (Set I). Configuration selection was performed for the lowest 20, 17, and 18 SE(single excitation)-CI solutions for the $^1A_1$, $^1A_2$, and $^1B_1$ states, respectively, and lowest 10 solutions for each symmetry of the triplet states. For the ionized states, λ_g and λ_e were set to $3*10^{-5}$ and $1*10^{-5}$ a.u. (Set II). The resultant dimensions of the present calculations are shown in Table IV.

III. THE $TiCl_4$ GROUND STATE

The HF configuration of the ground state of $TiCl_4$ and the orbital character in each of the all-electron calculations are shown in Table V. We adopted the valence shell numbering of previous work[22] for easy comparison throughout the present paper. The lowest occupied valence MO's, $1a_1$ and $1t_2$ are composed of the inner valence 3s orbitals of the Cl ligands: four 3s AO's split into non-degenerate a_1 and three-fold degenerate t_2 MO's, whose orbital energies are very close. The next three occupied MO's $2a_1$, $2t_2$, and 1e are bonding MO's between Ti and Cl atoms. The Ti 4s orbital is used in the $2a_1$ MO and the Ti d orbital is used in the $2t_2$ and 1e MOs. The highest two occupied MO's, $3t_2$ and $1t_1$, are non-bonding lone-pair orbitals localized on the ligands. We note that the orbital energies of the occupied orbitals $2a_1$, $2t_2$, 1e, and $3t_2$ are very close to each other. We will see later that this causes the complexity of the main configurations of the valence excitations and the different assignments in the ionization spectrum.

The lowest unoccupied MOs 2e and $4t_2$ are anti-bonding between Ti and Cl: they have negative orbital energy. The next group of unoccupied orbitals are mainly composed of the Rydberg type 4s and 4p orbitals of the Cl ligands, but $6t_2$ is of mixed character of Ti 4p and Cl 4p orbitals. These orbitals shown in Table V were the only group of MOs found to be important for describing the primary nature of the excited states.

The energy for the ground states of $TiCl_4$ is summarized in Table III. The correlation energy is the difference between the SAC or MRD-CI energy and the SCF

TABLE IV. Dimensions of the SAC/SAC-CI calculations for $TiCl_4$

State symmetry		
Td	C_{2v}	Dimension
Basis Set I		
Ground $^1A_1$	$^1A_1$	1326
Excited states		
$^1T_2$, ^1E, $^1A_1$	$^1A_1$	6139
$^1T_1$, ^1E, $^1A_2$	$^1A_2$	6645
$^1T_1$, $^1T_2$	$^1B_1$	5927
$^3T_2$, ^3E, $^3A_1$	$^3A_1$	5309
$^3T_1$, ^3E, $^3A_2$	$^3A_2$	5918
$^3T_1$, $^3T_2$	$^3B_1$	5874
Basis Set II		
Ground $^1A_1$	$^1A_1$	2780
Ionized states		
$^2T_2$, ^2E, $^2A_1$	$^2A_1$	2083
$^2T_1$, ^2E, $^2A_2$	$^2A_2$	1001
$^2T_1$, $^2T_2$	$^2B_1$	1777

TABLE V. Orbital energy and orbital nature of $TiCl_4$

MO	Orbital energy (au)[a]	Orbital nature[b]	
Valence occupied MO			
$(1a_1)^2$	-1.13453	L(s)	: non-bonding
$(1t_2)^6$	-1.11758	L(s)	: non-bonding
$(2a_1)^2$	-0.56970	M(s)-L(pσ)	: weakly antibonding
$(2t_2)^6$	-0.55865	M(dσ)+L(pσ)	: σ-bonding
$(1e)^4$	-0.54428	M(dπ)+L(pπ)	: π-bonding
$(3t_2)^6$	-0.52994	L(pπ)	: non-bonding, lone pair
$(1t_1)^6$	-0.48081	L(pπ)	: non-bonding, lone pair
Low-lying unoccupied MO			
(2e)	-0.02170	M(dπ)-L(pπ)	: π-antibonding
$(4t_2)$	-0.01165	M(d)-L(pσ,pπ)	: σ, π-antibonding
$(3a_1)$	0.02534	L(s*)	: Rydberg
$(5t_2)$	0.03377	L(p*)	: Rydberg
$(6t_2)$	0.05571	M(p*)-L(p*)	: antibonding
(3e)	0.05814	L(p*)	: Rydberg

[a]Set I result

[b]M(i), L(j) denote valence i and j-type orbitals on Ti and Cl atoms, respectively, and the asterisk indicates the Rydberg orbitals. Plus and minus signs show bonding and antibonding characters, respectively.

energy. The SCF energy indicates the quality of the valence basis set: Set III is by far the best among the basis sets used. The correlation energy of the SAC calculation for Set II is larger than that for Set I because the former involves the correlations of the 3s electrons of Cl. The MRD-CI correlation energy is larger than the SAC correlation energy of Set I because it involves angular correlations of Cl represented by the polarization functions.

Table VI shows a population analysis for $TiCl_4$ with different basis sets. We see that atomic populations are very subject to basis set. For example, when we take off the Cl anion bases from Set I, the Ti charge changes from -0.2328 to +0.5199: a large change occurs on the Ti s and d AO populations. A well-known difficulty of the Mulliken population analysis occurs when the basis set includes very diffuse bases. When the bases do not include the anion basis on Cl, the Ti gross charge is positive(+0.5 ~ +1.0) and Cl is negative(-0.13 ~ -0.26), though the charge is still very much basis-set dependent. For further examples, basis sets (Ti/Cl) 149 (7s6p4d/7s4p1d), 156 (Basis III) (11s9p3d/7s4p1d) and 178 (11s9p4d/8s5p1d) give charges on Ti of (+)1.437, 1.027 and 0.661, respectively.

The effect of f-functions (ζ_f = 1.550 , and hence of valence character) was insufficient to justify further investigation (the total f-population was 0.006). Since $TiCl_4$ is somewhat volatile (bp 137deg, mp -23deg), a significant amount of covalence must pertain. The ^{35}Cl NQR frequency for $TiCl_4$ is very low,[45,46] and this has led to suggestions of considerable π-bonding,[46] also supported by comparison of the lone-pair Cl IPs with related compounds.[47]

IV. EXCITED STATES

A. The overall position

The excitation energies, oscillator strengths and second moments of the singlet excited states are summarized in Table VII, both for SAC-CI and MRD-CI calculations, while the excitation energies of the low-lying triplet states are given in Table VIII for SAC-CI calculations alone. The MRD-CI results are generally similar to the SAC-CI results, with a standard deviation of corresponding states in a linear regression of 0.349 eV. The discrepancy is smaller at the high energy end of the spectrum than the lower end. This makes it possible to consider only one of the two

TABLE VI. Mulliken population analysis for the ground state of $TiCl_4$.

Basis set	Mulliken population									
	Ti					Cl				
	s	p	d[a]	Total	Charge	s	p	d	Total	Charge
Set I without Cl anion basis	5.9244	12.8314	2.7243	21.4801	+.5199	5.9464	11.1836	-	17.1300	-.1300
Set I (with Cl anion basis)	7.1365	12.9394	2.1569	22.2328	-.2328	5.8856	11.0562	-	16.9418	+.0582
Set II	5.7948	12.8309	2.8235	21.4492	+.5508	5.9486	11.1891	-	17.1377	-.1377
Set III	6.3782	12.7210	1.8739	20.9731	+1.0269	5.9441	11.2931	0.0196	17.2568	-.2568
ECP	0.6777	0.5513	1.6684	2.8974	+1.1026	1.9801	5.2956	-	7.2757	-.2757

[a]Population in dr^2 is also included in d-AO.

Table VII. Excitation energies, oscillator strengths and second moments of singlet excited states for $TiCl_4$.

State	Main configurations[a]	SAC-CI Excitation energy	SAC-CI Oscillator strength	SAC-CI Second moment	Expt. BBT[b]	Expt. IR[c]	MRD-CI Excitation energy	MRD-CI Oscillator strength
Ground state		0.0		433			0.0	
Region I								
$1T_1$	$0.89(1t_1 \rightarrow 2e)$	4.19	forbidden	433	(4.00)		4.97	0.0
$1T_2$	$0.85(1t_1 \rightarrow 2e)$	4.42	$5.60*10^{-2}$	433	4.43	4.41	5.08	$5.10*10^{-2}$
1E	$0.85(1t_1 \rightarrow 4t_2)$	4.99	forbidden	433			6.24	0.0
$2T_1$	$0.67(1t_1 \rightarrow 4t_2), 0.23(3t_2 \rightarrow 2e)$	4.98	forbidden	434			6.02	0.0
$1A_2$	$0.78(1t_1 \rightarrow 4t_2), 0.14(1e \rightarrow 2e)$	5.05	forbidden	433			5.47	0.0
$2T_2$	$0.83(1t_1 \rightarrow 4t_2)$	5.22	$3.72*10^{-2}$	433	5.38	5.31	6.69	$4.10*10^{-2}$
$3T_1$	$0.48(2t_2 \rightarrow 2e), 0.26(3t_2 \rightarrow 2e), 0.13(1t_1 \rightarrow 4t_2)$	5.44	forbidden	434			6.32	0.0
$3T_2$	$0.80(3t_2 \rightarrow 2e)$	5.53	$5.97*10^{-2}$	433	5.38	5.31	6.93	$4.20*10^{-2}$
$4T_1$	$0.40(3t_2 \rightarrow 2e), 0.37(2t_2 \rightarrow 2e)$	5.61	forbidden	434			5.94	0.0
2E	$0.70(1e \rightarrow 2e), 0.09(3t_2 \rightarrow 4t_2)$	5.70	forbidden	433			6.89	0.0
$4T_2$	$0.83(2t_2 \rightarrow 2e)$	5.74	$7.63*10^{-3}$	433	5.38	5.31	6.95	$7.40*10^{-3}$
$2A_2$	$0.77(1e \rightarrow 2e), 0.14(1t_1 \rightarrow 4t_2)$	5.83	forbidden	433			6.61	0.0
$1A_1$	$0.63(1e \rightarrow 2e), 0.28(2t_2 \rightarrow 4t_2)$	5.92	forbidden	433			7.14	0.0
$5T_1$	$0.77(3t_2 \rightarrow 4t_2), 0.10(1e \rightarrow 4t_2)$	6.26	forbidden	434			7.07	0.0
3E	$0.81(2a_1 \rightarrow 2e), 0.06(2t_2 \rightarrow 4t_2)$	6.27	forbidden	434			7.22	0.0
4E	$0.77(3t_2 \rightarrow 4t_2), 0.12(1e \rightarrow 2e)$	6.40	forbidden	433			6.94	0.0
$2A_1$	$0.79(3t_2 \rightarrow 4t_2)$	6.45	forbidden	433			7.99	0.0
$5T_2$	$0.61(3t_2 \rightarrow 4t_2), 0.14(2t_2 \rightarrow 4t_2), 0.11(1e \rightarrow 4t_2)$	6.52	$6.14*10^{-4}$	433			7.76	$3.40*10^{-3}$
$6T_1$	$0.77(1e \rightarrow 4t_2), 0.11(3t_2 \rightarrow 4t_2)$	6.60	forbidden	434			7.54	0.0
$6T_2$	$0.55(1e \rightarrow 4t_2), 0.22(3t_2 \rightarrow 4t_2), 0.10(2t_2 \rightarrow 4t_2)$	6.61	$1.73*10^{-2}$	433			7.85	$4.00*10^{-4}$
$7T_1$	$0.83(2t_2 \rightarrow 4t_2), 0.05(2t_2 \rightarrow 2e)$	6.84	forbidden	433			7.99	0.0
5E	$0.81(2t_2 \rightarrow 4t_2), 0.09(2a_1 \rightarrow 2e)$	7.00	forbidden	434			8.07	0.0
$7T_2$	$0.38(2t_2 \rightarrow 4t_2), 0.34(2a_1 \rightarrow 4t_2), 0.14(1e \rightarrow 4t_2)$	7.20	$4.86*10^{-2}$	433	7.07	6.85	8.18	$1.70*10^{-1}$
$3A_1$							8.52	0.0
$8T_2$	$0.52(2a_1 \rightarrow 4t_2), 0.15(2t_2 \rightarrow 4t_2), 0.09(1e \rightarrow 4t_2)$	7.72	0.982	433	7.39	7.33	8.79	0.591
Region II								
$8T_1$	$0.65(1t_1 \rightarrow 3a_1), 0.19(1t_1 \rightarrow 4a_1)$	8.81	forbidden	448	(8.18, 8.68)	(8.39, 8.89)	8.67	0.0
6E	$0.70(1t_1 \rightarrow 5t_2), 0.08(1e \rightarrow 3a_1), 0.05(1t_1 \rightarrow 7t_2)$	9.75	forbidden	456			9.71	0.0
$9T_2$	$0.62(1t_1 \rightarrow 5t_2), 0.17(3t_2 \rightarrow 3a_1)$	9.79	$2.86*10^{-1}$	453	9.35	9.29	9.84	0.276
$9T_1$	$0.68(1t_1 \rightarrow 5t_2), 0.18(1t_1 \rightarrow 6t_2)$	9.92	forbidden	456			10.04	0.0
$3A_2$	$0.71(1t_1 \rightarrow 5t_2), 0.14(1t_1 \rightarrow 6t_2)$	9.95	forbidden	455			9.89	0.0
$10T_2$	$0.25(1t_1 \rightarrow 3e), 0.24(1t_1 \rightarrow 6t_2), 0.23(3t_2 \rightarrow 3a_1), 0.08(1t_1 \rightarrow 5t_2)$	10.43	$2.39*10^{-2}$	455	10.04	9.99	10.23	$7.10*10^{-2}$

[a]Configurations and square values of the coefficients are listed for those whose square values are larger than 0.04 (SAC-CI results).

[b]Reference 2

[c]Reference 4

TABLE VIII. SAC-CI excitation energies for the low-lying triplet states of $TiCl_4$.

State	Main configurations[a]	Excitation energy	Exptl.[b]
1^3T_2	$0.85(1t_1 \rightarrow 2e)$	4.12	(4.00)
1^3T_1	$0.88(1t_1 \rightarrow 2e)$	4.19	4.43
2^3T_2	$0.64(1t_1 \rightarrow 4t_2)$, $0.23(3t_2 \rightarrow 2e)$	4.95	
1^3E	$0.80(1t_1 \rightarrow 4t_2)$, $0.10(1e \rightarrow 2e)$	4.95	
2^3T_1	$0.60(1t_1 \rightarrow 4t_2)$, $0.28(3t_2 \rightarrow 2e)$	4.96	
1^3A_1	$0.72(1e \rightarrow 2e)$, $0.05(3t_2 \rightarrow 4t_2)$	5.12	
1^3A_2	$0.76(1t_2 \rightarrow 4t_2)$, $0.16(1e \rightarrow 2e)$	5.12	
3^3T_2	$0.57(3t_2 \rightarrow 2e)$, $0.22(1t_1 \rightarrow 4t_2)$, $0.07(1e \rightarrow 4t_2)$	5.32	
3^3T_1	$0.72(2t_2 \rightarrow 2e)$, $0.05(3t_2 \rightarrow 2e)$, $0.04(1t_1 \rightarrow 4t_2)$	5.36	5.38
4^3T_2	$0.82(2t_2 \rightarrow 2e)$	5.48	

[a]Configurations and square values of the coefficients are listed for those whose square values are larger than 0.04 (SAC-CI results).

[b]Reference 2

sets of data in the following discussion; we consider the SAC-CI results from this point, except where indicated. The SAC-CI theoretical spectrum and the experimental (gas phase) absorption spectrum[2] are compared in Figure 1; dipole forbidden transitions are indicated by circles.

We may divide the excitation spectrum into two regions; that from 4 eV (30,000 cm^{-1}) to 8 eV (70,000 cm^{-1}) (Region I) corresponds to valence excitations, while the range from there up to 10.5 eV (90,000 cm^{-1}) (Region II) involves Rydberg excitations. Region I is further characterized by two kinds of excitations; (a) charge transfer excitation from L(p) non-bonding MO's to M(d)-L(p) anti-bonding MO's, and (b) the transition from M-L bonding MO's to M-L antibonding MO's. These two types of excitations (a,b) are analogous to those of regions A and B in the study of RuO_4 and OsO_4,[28b] where they were well separated, though they are not for $TiCl_4$. This difference arises from the separation of the ionized states of $(L)^{-1}$ and $(M+L)^{-1}$; this is large for RuO_4 and OsO_4, whereas $TiCl_4$ has several ionized states in a very narrow energy range (11.76 - 13.96 eV).[6-9] The M-L bond in $TiCl_4$ is not as strong as that in RuO_4 and OsO_4, since the TiCl bonds are effectively single, whereas the RuO and OsO bonds are partial double bonds.

In outline, as one can see in Table VII, the lower end of Region I has charge transfer character and the higher end has M-L bonding to antibonding transition character; the intermediate region ($3T_1$ to $6T_1$) has "mixed character". In this sense, we cannot divide Region I and need to treat the two types of excitations together as a valence region. Region II is characterized mainly as the excitation from L(p) non-bonding MO on Cl to L(s*, p*) Rydberg MO on Cl, that is, Rydberg excitation within ligands.

B. Assignment of the Region I Spectrum

Region I of the absorption spectrum in Figure 1 shows 4 prominent bands at 4.43, 5.38, 7.07, and 7.39 eV.[2] The observed bands have no vibrational structure, which indicates that there are considerable dynamic and static Jahn-Teller effects. In T_d symmetry, only the optical transitions to T_2 states are dipole allowed. In this region, a number of dipole forbidden states of T_1, E, A_1, and A_2 symmetry were found as

shown in Table VII. Since these states are located close to dipole allowed transitions, they are able to gain intensity through vibronic coupling.

An unresolved absorption band is observed at 4.0 eV on the shoulder of the first band.[2] This shoulder was interpreted as an electronic dipole forbidden transition and assigned to the $1t_1 \rightarrow 3a_1$ transition by CNDO calculations.[2] In our calculations, the dipole forbidden transition to the $1T_1$ state ($1t_1 \rightarrow 2e$) is calculated at 4.19 eV; another possible assignment for this weak shoulder is a transition to a triplet state. We found several low-lying triplet states in the low energy region, with ten triplet states calculated below 5.50 eV (Table VIII); thus, there are two candidates for this shoulder, the 1^3T_2 ($1t_1 \rightarrow 2e$) and 1^3T_1($1t_1 \rightarrow 2e$) states which are calculated to lie at 4.12 eV and 4.19 eV, respectively. In conclusion, we cannot specify the origin of this weak shoulder; either, it is a $1T_1$ state which borrows its intensity from the transition to the $1T_2$ state, or it is a spin-forbidden triplet state, that is 1^3T_2 and 1^3T_1. Further spectroscopic measurements in this region are warranted.

The first main band has its maximum at 4.43 eV; this is attributed to the $1T_2$ state ($1t_1 \rightarrow 2e$), calculated at 4.42 eV, and is a transition from chlorine lone-pair MO to the Ti($d\pi$)-Cl($p\pi$) anti-bonding MO, ie, a charge transfer transition from the ligand to the metal. The second observed band has its maximum at 5.38 eV. Three dipole allowed transitions are calculated in this energy region; they are the $2T_2$ state ($1t_1 \rightarrow 4t_2$) at 5.22 eV, the $3T_2$ state ($3t_2 \rightarrow 2e$) at 5.53 eV, and the $4T_2$ state ($2t_2 \rightarrow 4t_2$) at 5.74 eV. These three states are assigned to the second band. The $2T_2$ and $3T_2$ states are charge transfer excitation in type, while the $4T_2$ state is the transition from the Ti-Cl bonding to the Ti-Cl anti-bonding MO's. Consequently, this band has "mixed character" as described above. The intensities of the first two transitions are stronger than that of the third one as seen from Figure 1.

The band centered at about 7.4 eV has a low energy shoulder at 7.07 eV; the latter is assigned to the $7T_2$ state calculated at 7.20 eV. This state consists of a linear combination of three main configurations; they are $2t_2 \rightarrow 4t_2$, $2a_1 \rightarrow 4t_2$, and $1e \rightarrow 4t_2$; thus configuration interaction is very important for the precise description of this state. Two other dipole allowed transitions are calculated in the 6.5 - 6.7 eV region, namely the $5T_2$ state which has a small oscillator strength, and the $6T_2$ state which has a more considerable one. These are attributed to the tail in the lower energy region of

the peak at 7.07 eV. Since these transitions are from the Ti-Cl bonding MO to the antibonding MO, the geometries of the excited states would be very much relaxed.

The strong maximum band at 7.39 eV is attributed to the $8T_2$ state, which also has the same excitation nature as both the $7T_2$ and $6T_2$ states. The experimental spectrum shows a very large molecular extinction coefficient for this band; this is in agreement with the SAC-CI and MRD-CI calculations, where we calculate a very intense band (F 0.982). A broad nature of the peak may be attributed to the geometrical relaxation on the excited state.

Robin assigned these two peaks (7.07, 7.39 eV) to Jahn-Teller distortion originating from the same electronic transition; he suggested the assignment $2t_2 \rightarrow 4t_2$ ($7T_2$). However, he overlooked a possibility of a large oscillator strength of the $2a_1 \rightarrow 4t_2$ transition ($8T_2$ state). Actually, this transition has the largest oscillator strength as shown in Table VII. Therefore, we assign these two peaks to the different electronic transitions; transitions to $7T_2$ and $8T_2$ states.

The previous theoretical studies on the excitation spectrum of $TiCl_4$ either relied upon one-electron energy differences[2,14,15] or were small scale CI calculations, in which only 192 singly excited configurations were considered;[21] the latter also concentrated upon the T_2 states with the exception of the lowest T_1 state. These early CI calculations inevitably gave considerable errors in excitation energy relative to experiment (often 2-3 eV), but the general order of upper and lower states follows the present work. The SCF-Xα transition state calculations of Tossell[12a] show a number of similarities to the present work, but comparison is not immediately obvious, since the overall state symmetries were not given. The 1e to 2e and $4t_2$ states are calculated low by about 2 eV in that study and he assigned the shoulder of the third band to the transition $1e \rightarrow 2e$. However, this excitation is dipole forbidden. Another SCF-Xα calculation also gave slightly different assignments.[18] The difference between our results and these SCF-Xα results seems to exist in the ordering of the $2a_1$ and $2t_2$ orbitals.

The shake-up states observed in the x-ray photo-electron spectrum agree for the 4.0 eV excitation accompanying the 2p ionization as $1T_2$, $1t_1$ to 2e.[13] The higher excitations computed by Veal et al[13] at 5.0 and 10.4 eV do not correspond closely to the present results for the same processes; the present results suggest that $2a_1$ to $4t_2$

excitation is more likely at 7.4 eV; with further excitations L to L* above 9 eV, as discussed below.

C. Region II Spectral Assignments

We see from Table VII that the electronic component of the second moments of the states in Region I lie in the range 433-434 au, essentially the same as the ground state value of 433 au. This is another reason why the excited states in Region I are assigned as valence states. On the other hand, most of the states in Region II have larger second moments of about 455 au suggesting a Rydberg set of transitions.

The dipole forbidden transition to the $8T_1$ state is calculated at 8.81 eV and its second moment is estimated 448 au. This transition may correspond to the weak absorption band at 8.68 eV in the experimental spectrum. We were unable to compute a singlet excited T_2 state which is assignable to the weak absorption at 8.18 eV. This weak absorption may also be due to a triplet state.

The strong two peaks observed at 9.35 and 10.04 eV are assigned to the $9T_2$ and the $10T_2$ states calculated at 9.79 and 10.43 eV, respectively. Previous workers have offered alternative assignments; thus Tossell assigned these bands to the transition from Cl(3p) to the Ti(4s,4p)-Cl(3p) anti-bonding MO by SCF-Xα-SW calculations,[12a] while Robin suggested the assignment to the Rydberg excitation within the Cl atoms (3p$\rightarrow$ 4p) from the similarity of the term values to that transition in the CCl_4 and related molecules.[5] Thus he concluded that the first peak at 9.35 eV originates from the $1t_1$ MO and the second peak at 10.04 eV is from the $3t_2$ MO.

Our result supports Robin's assignment.[5] The first peak is calculated at 9.79 eV and its main configuration is $1t_1\rightarrow 5t_2$: the transition from the Cl lone pair 3p orbital to the Rydberg 4p orbital of Cl. We see a small admixture of the $3t_2\rightarrow 3a_1$ transition which is a 3p$\rightarrow$ 4s Rydberg transition within chlorine. The $10T_2$ state is also a pure Rydberg excitation within the Cl ligands and is described by the linear combination of the excitations $1t_1\rightarrow 3e$, $1t_1\rightarrow 6t_2$, and $3t_2\rightarrow 3a_1$. A difference from the $9T_2$ state is a mixing of the outer p orbital of the Ti atom in the $6t_2$ orbital. Thus, the orbital basis must contain Rydberg type and anion bases for description of these states quantitatively.

In conclusion, the SAC-CI and MRD-CI calculations give essentially consistent assignments of the spectrum, supporting the validity of the present assignments. The average discrepancy between theoretical and experimental values for the excitation spectrum is 0.22 eV for the SAC-CI case.

V. IONIZED STATES AND ASSIGNMENT OF THE PHOTOELECTRON SPECTRUM

Ionization potentials and intensities for $TiCl_4$ calculated by the SAC-CI method are compared with experimental values and the results of the Green's function approach in Table IX. Theoretical and experimental ionization spectra for the outer valence region are shown in Figure 2. For the inner valence region, only the theoretical spectrum is shown, since no experimental data have been reported. Theoretical intensities are calculated with the use of the monopole approximation.[49]

As noted in the introduction, differing assignments for the outer valence region[7] have been proposed, although there is common agreement over the identity of the first peaks;[22] if we use the notation of Egdell *et al*,[7] the first two bands A and B are assigned to $(1t_1)^{-1}$ and $(3t_2)^{-1}$ respectively. Bancroft *et al* measured He I and He II photoelectron spectra[9] and proposed the ordering $(1e)^{-1} < (2a_1)^{-1} < (2t_2)^{-1}$ for the bands C, D, and E from the proportion of d-character in each orbital. A recent MS Xα study also gave the same ordering.[50] On the other hand, analysis by synchrotron radiation[10] and theoretical investigation by the Green's function method[22] gives the order $(1e)^{-1} < (2t_2)^{-1} < (2a_1)^{-1}$. The present results support the latter assignment. Overlapping bands (C+D) correspond to $((1e)^{-1} + (2t_2)^{-1})$, which are calculated at 13.25 eV and 13.52 eV; band E is attributed to $(2a_1)^{-1}$. These five states are located in the low energy region and away from shake up states. Therefore, monopole intensities for these states are relatively large. The average discrepancies between theory and experimental values for the outer valence ionization is 0.19 eV.

Next we examine the fine structures in the bands A and B. There exist weak shoulders in these bands and the splitting between the main peak and the shoulder is observed as 0.145 eV for band A and 0.196 eV for band B. Bancroft *et al* estimated[9] the vibrational broadening only for the a_1 mode and gave the vibrational progressions for each band. We estimated the spin-orbit effect for the $(1t_1)^{-1}$ state in the way

TABLE IX. Ionization potentials of $TiCl_4$.

State		Expt. LSW[a]	Expt. BPT[b]	SAC-CI Koopmans	SAC-CI I.P. (Δ[c])	Intensity[d]	2ph-TDA[e]
Outer valence ionization[f]							
A 1^2T_1	$(1t_1)^{-1}$	11.80	11.69	13.09	11.38 (-.42)	0.88	11.70
B 1^2T_2	$(3t_2)^{-1}$	12.79	12.67	14.44	12.69 (-.10)	0.88	12.98
C 1^2E	$(1e)^{-1}$	13.29	13.17	14.83	13.25 (-.04)	0.87	13.44
D 2^2T_2	$(2t_2)^{-1}$	13.54	13.46	15.21	13.52 (-.02)	0.86	13.69
E 1^2A_1	$(2a_1)^{-1}$	13.98	13.91	15.49	13.61 (-.37)	0.87	13.91
Inner valence ionization[g]							
^2E					18.14[h]		
$^2A_1$					18.20[h]		
$^2T_2$					18.24[h]		
$^2T_2$	0.007(2)[i]			30.43	25.19	0.010	
	0.025(6)				25.35	0.029	
	0.013(2)				25.78	0.017	
	0.117(2), 0.033(4)				25.96	0.150	
	0.009(2)				26.52	0.018	
	0.024(4), 0.009(2)				26.63	0.035	
	0.018(6)				26.87	0.018	
	0.283(2)				27.25	0.284	
	0.005(2)				27.29	0.005	
	0.184(2)				27.52	0.184	
	0.026(2)				27.77	0.026	
	0.021(2)				27.87	0.022	
	0.029(2)				28.27	0.030	
	0.043(2)				29.00	0.044	
	0.064(2)				29.08	0.064	
$^2A_1$	0.101(1), 0.012(3)			30.90	26.20	0.113	
	0.048(3)				26.86	0.049	
	0.104(1)				27.37	0.104	
	0.341(1)				27.78	0.342	
	0.010(1)				27.83	0.010	
	0.038(1)				28.30	0.039	
	0.037(1)				28.61	0.038	
	0.026(1)				29.08	0.027	
	0.141(1)				29.15	0.142	
	0.008(1)				29.34	0.008	
^2E	0.009(5)				25.37	0.009	
	0.018(5)				25.93	0.018	
	0.021(5)				26.22	0.020	
	0.011(5)				26.79	0.011	

[a]Reference 10
[b]Reference 9
[c]Deviation from experimental value
[d]Only the states whose intensity is larger than 0.005 are tablated.
[e]Reference 22
[f]Figure 2-b
[g]Figure 2-c
[h]Many satellite peaks with very small monopole intensities (< 0.001) are calculated in the energy region 18-25 eV. We give only the first three peaks in the table.
[i]Contribution of one-electron process. (1): $(1a_1)^{-1}$, (2): $(1t_2)^{-1}$, (3): $(2a_1)^{-1}$, (4): $(2t_2)^{-1}$, (5): $(1e)^{-1}$, (6): $(3t_2)^{-1}$

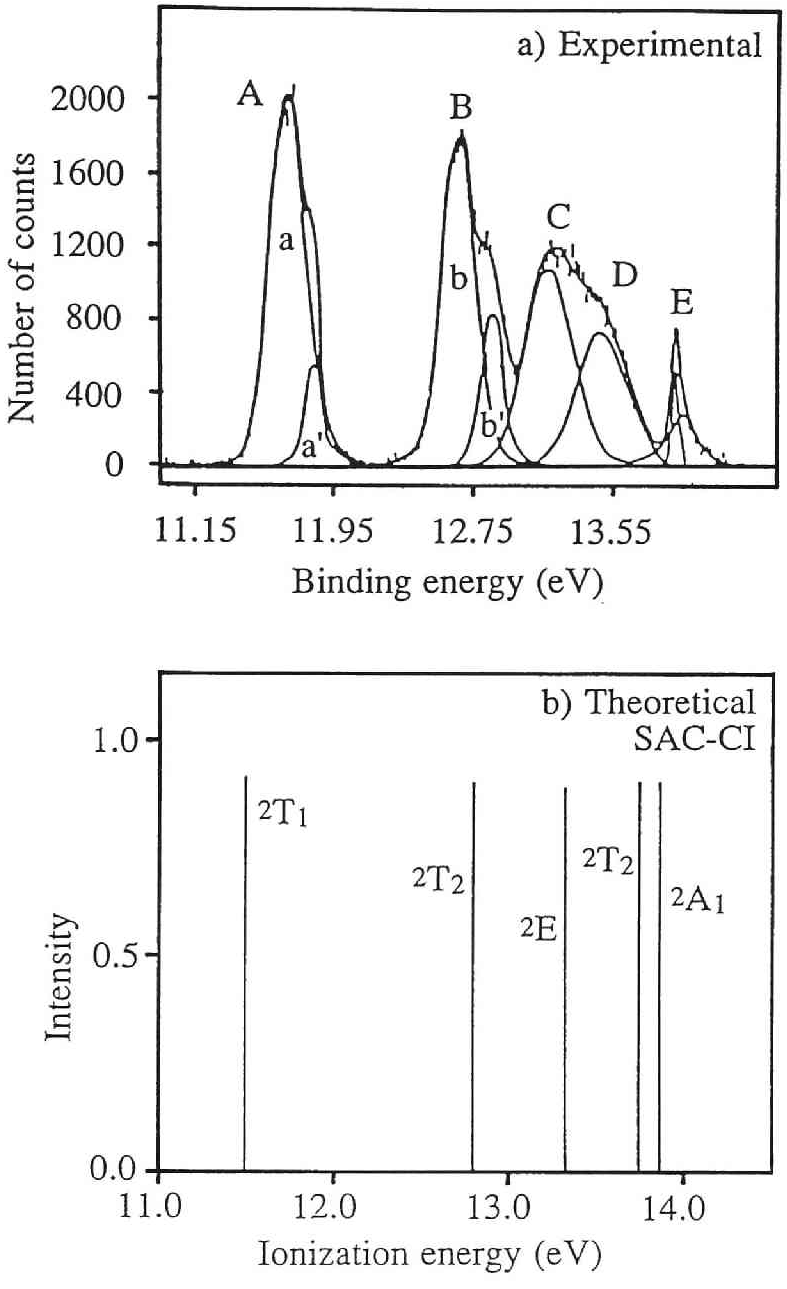

FIG. 2. (a) Experimental spectrum, (b) SAC-CI theoretical outer-valence ionization spectrum, and (c) SAC-CI theoretical inner-valence ionization spectrum for $TiCl_4$. (1): $(1a_1)^{-1}$, (2): $(1t_2)^{-1}$, (3): $(2a_1)^{-1}$, (4): $(2t_2)^{-1}$, (5): $(1e)^{-1}$, (6): $(3t_2)^{-1}$

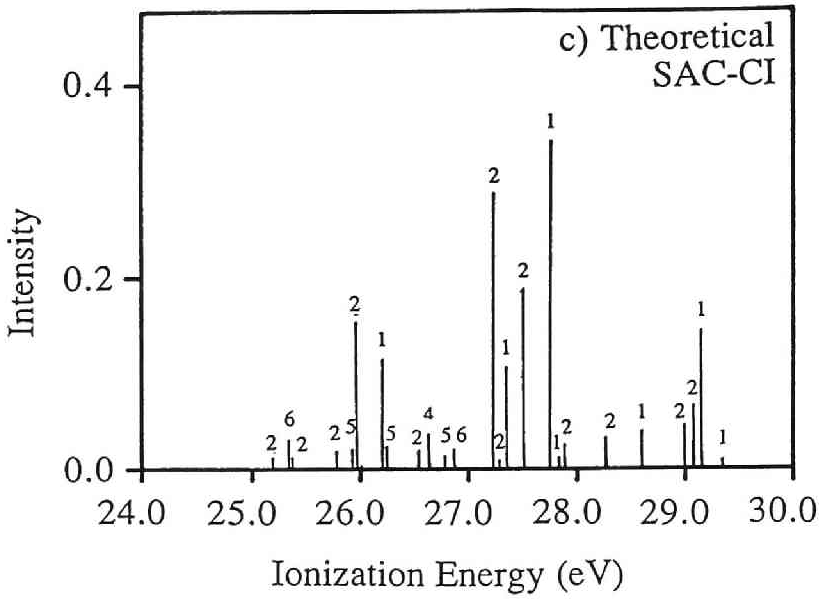

FIG. 2. (a) Experimental spectrum, (b) SAC-CI theoretical outer-valence ionization spectrum, and (c) SAC-CI theoretical inner-valence ionization spectrum for $TiCl_4$. (1): $(1a_1)^{-1}$, (2): $(1t_2)^{-1}$, (3): $(2a_1)^{-1}$, (4): $(2t_2)^{-1}$, (5): $(1e)^{-1}$, (6): $(3t_2)^{-1}$

reported previously[51] and obtained the splitting as 0.058 eV, which is only one third of the observed splitting. The vibrational frequencies[52] of the nomal modes were also not enough to explain the experimental splitting (ν_1 = 0.0482, ν_2 = 0.0141, ν_3 = 0.0617, and ν_4 = 0.0169 eV). Therefore, we attribute these shoulders to the combination of the spin-orbit interaction, vibronic coupling, and Jahn-Teller effect, as Bancroft *et al* considered.[9]

Lastly, we investigate the inner valence region; a large number of shake-up states were calculated with onset at 18.3 eV. They are largely separated from the Koopmans' type ionization (one-electron) processes. Furthermore, the satellite peaks in the low energy region are calculated to have very weak intensities (less than 0.001). Therefore, we show in Fig. 2c the calculated satellite peaks in the region greater than 25 eV. Ionizations from $1a_1$ and $1t_2$ show a breakdown of the Koopmans' picture. Shake-up states with symmetry $^2T_2$ and $^2A_1$ mix with these one-electron processes in the range 25.0 - 30.0 eV. They have considerable intensity through final state correlation. These features were also obtained by the Green's function approach.[22] It was reported that the halogen 3s subshells have a low cross-section under u.v. excitation,[8] so there is no experimental information for this energy region.

VI. CONCLUSION

We have applied the SAC-CI and the MRD-CI methods to the calculation of the excited and ionized states of $TiCl_4$. We have successfully reproduced the whole energy region of the experimental spectra. We give several new assignments and a detailed picture for the excitation spectrum of $TiCl_4$. The spectrum is divided into two regions; Region I, 4 eV - 8 eV and Region II 8 eV - 10.5 eV. Region I involves valence excitations and Region II Rydberg excitations within Cl ligands. Since the occupied valence MO's lie in a narrow energy range, the excitation nature in Region I is very complex for this molecule, and there are considerable configuration mixings in the states. In Region I, the lower excitations are from the Cl lone-pair MO to the (metal d - ligand p) antibonding MO and thus they are electron transfer excitations from ligand to metal. The higher excitations in Region I are from M-L bonding MO to M-L antibonding MO, so that large geometrical relaxation is expected after the transitions. The excitations in the medium energy range (around 6.5 eV) are therefore mixtures of both types of excitations. In addition to the dipole-allowed transitions, a large number of dipole-forbidden states were calculated. It was also found that many triplet states exist in the low energy region. These states may be responsible for weak features in the VUV spectrum. The strong peaks observed at 9.35 eV and 10.04 eV of Region II are assigned to Rydberg type excitations, $3p \rightarrow 4p$ within the Cl ligands in accordance with the earlier Robin's assignment. For the peak at 9.35 eV, a small

admixture of the Cl 3p→ 4s Rydberg transition is found and for the peak at 10.04 eV, a mixing of the titanium outer 4p orbital is calculated.

For the ionized spectrum, our present calculations confirm the assignments of Egdell and Orchard[8] from experimental observations, and the theoretical study of von Niessen.[22] The ordering of the ionized states in the outer valence region is calculated as $(1t_1)^{-1} < (3t_2)^{-1} < (1e)^{-1} < (2t_2)^{-1} < (2a_1)^{-1}$. Many shake-up states were calculated in the inner valence region. Though these two-electron processes start from 18.3 eV, the observable states whose intensities are larger than 0.005 only appear above 25.0 eV. Further experimental study of this region is required.

ACKNOWLEGMENTS

The SAC-CI calculations were performed on the FACOM M780 computer at the Data Processing Center of Kyoto University and the HITAC M-680H and S-820 computer at the Institute for Molecular Science. The MRD-CI study was performed on the Rutherford-Appleton Laboratory Cray XMP-48. This study has been supported by a Grant-in-Aid for Scientific Research from the Japanese Ministry of Education, Science and Culture; by the Kurata Foundation; and by the UK Science and Engineering Research Council. The authors wish to thank British Council, Japan Society for the Promotion of Science, and the Royal Society for supporting scholar exchange programs for promoting this collaboration.

REFERENCES

[1] D. S. Alderdice, J. Molecular Spectrosc. **15**, 509 (1965).

[2] C. A. Becker, C. J. Ballhausen, and I. Trabjerg, Theoret. Chim. Acta **13**, 355 (1969).

[3] C. Dijkgraaf and J. P. G. Rousseau, Spectrochim. Acta **A25**, 1831 (1969).

[4] A. A. Iverson and B. R. Russell, Spectrochim. Acta **A29**, 715 (1973).

[5] M. B. Robin, *Higher Excited States of Polyatomic Molecules* (Academic, Press New York, 1975), Vol. 3, p. 383.

[6] J. C. Green, M. L. H. Green, P. J. Joachim, A. F. Orchard and D. W. Turner, Phil. Trans. Roy. Soc. Lond. **A268**, 111 (1970).

[7] R. G. Egdell, A. F. Orchard, D. R. Lloyd and N. V. Richardson, J. Electron Spectrosc. and Relat. Phenom. **12**, 415 (1977).

[8] R. G. Egdell and A. F. Orchard, J. Chem. Soc. Faraday Trans. 2 **74**, 485 (1978).

[9] G. M. Bancroft, E. Pellach, and J. S. Tse, Inorg. Chem. **21**, 2950 (1982).

[10] M. Lubcke, B. F. Sonntag, H. E. Wetel, *Conference Proceedings, International Conference on X-ray and Inner-Shell Processes in Atoms, Molecules, and Solids*, edited by A. Meisel, (Karl-Marx-Universitat; Leipzig, 1984), Abstracts Part I, p. 281.

[11] B. Wallbank, J. S. H. Q. Perera, D. C. Frost and C. A. McDowell, J. Chem. Phys. **69**, 5405 (1978).

[12] (a) J. A. Tossell, Chem. Phys. Lett. **65**, 371 (1979);
(b) A. Gupta and J. A. Tossell, J. Electron Spectrosc. Rel. Phenom. **26**, 223 (1982);
(c) J. S. Tse, Chem. Phys. Lett. **373**, 15 (1981).

[13] B. W. Veal, K. Lee and D. E. Ellis, Phys. Rev. **A37**, 1839 (1988).

[14] C. A. L. Becker and J. P. Dahl, Theor. Chim. Acta **14**, 26 (1969).

[15] T. Parameswaran and D. E. Ellis, J. Chem. Phys. **58**, 2088 (1973).

[16] S. S. L. Surana and A. Muller, Chem. Phys. Lett. **67**, 527 (1979).

[17] A. Golebiewski and M. Witko, Acta Phys. Pol. **A51**, 629 (1977).

[18] A. E. Foti, V. H. Smith, Jr., and M. A. Whitehead, Mol. Phys. **45**, 385 (1982).

[19] A. Golebiewski and M. Witko, Acta Phys. Pol. **A57**, 585 (1980).

[20] S. A. Titov, Teor. Espk. Khim. **20**, 709 (1984).

[21] I. H. Hillier and J. Kendrick, Inorg. Chem. **15**, 520 (1976).

[22] W. von Niessen, Inorg. Chem. **26**, 567 (1987).

[23] D. R. Traux, J. A. Geer and T. Ziegler, J. Chem. Phys. **59**, 6662 (19123).

[24] H. Nakatsuji and K. Hirao, J. Chem. Phys. **68**, 2053 (1978).

[25] H. Nakatsuji, Chem. Phys. Lett. **59**, 362 (1978); **67**, 329, 334 (1979).

[26] H. Nakatsuji, Reports in Molecular theory, (in press).

[27] (a) H. Nakatsuji, J. Chem. Phys. **80**, 3703 (1984);
(b) H. Nakatsuji, O. Kitao and T. Yonezawa, *ibid.* **83**, 723 (1985);
(c) H. Nakatsuji and O. Kitao, *ibid.* **87**, 1169 (1987);
(d) O. Kitao and H. Nakatsuji, Chem. Phys. Lett. **143**, 528 (1988).

[28] (a) H. Nakatsuji and S. Saito, J. Chem. Phys. **93**, 1865 (1990);
(b) H. Nakatsuji and S. Saito, Intern. J. Quantum Chem. **39**, 93 (1991);
(c) H. Nakatsuji, M. Sugimoto, and S. Saito, Inorg. Chem. **29**, 3095 (1990).

[29] M. H. Palmer, I. C. Walker, M. F. Guest and A. Hopkirk, Chem. Phys. **147**, 19 (1990).

[30] I. C. Walker and M. H. Palmer, Chem. Phys. **153** 169 (1991).

[31] Y. Morino, U. Uehara, J. Chem. Phys. **45**, 4543 (1966).

[32] P. J. Hay and W. R. Wadt, J. Chem. Phys. **82**, 299 (1985).

[33] S. Huzinaga, J. Andzelm, M. Klobukowski, E. Radzio-Andzelm, Y. Sakai and H. Tatewaki, *Gaussian basis sets for molecular calculations* (Elsevier, Amsterdam, 1984).

[34] C. E. Moore, U. S. Natl. Bur. Stand. Circ. No 467, Vol. I (1949).

[35] H. Nakatsuji, Chem. Phys. Letters **177**, 331 (1991).

[36] It was clear that one of the problems of MRD-CI was coupling of roots, often in groups of four, and that these were well separated in energy; extrapolation based upon only some members of the group led to perturbed energies, relative to those obtained when all members of the group were present. Hence it became imperative to expand the number of roots simultaneously determined in MRD-CI from 10 to 20. This caused extensive modification of the code, with major array expansions. A further problem with the MRD-CI method here, is the balancing of the reference set to obtain accurately degenerate roots for E and T states. In general, even with up to 70 main reference functions, it was not possible to obtain degenerate roots closer than about 0.1 eV, although this was sometimes reduced to 0.02eV; the problem arises from the differing numbers of a_1 and a_2 MOs from b_1 and b_2, and is thus not capable of being exactly solved. In general this did not lead to problems of assignment; the result from the larger diagonalisation is quoted in these circumstances. However, there are no such problems in SAC-CI and the degeneracy was kept to within 0.02 eV.

[37] T. H. Dunning, Jr. and P. J. Hay, in *Methods of Electronic Structure Theory*, edited by H. F. Schaefer III (Plenum, New York, 1977).

[38] M. Dupuis, J. D. Watts, H. O. Viller, and G. J. B. Hurst, Program System HONDO7, Program Library No. 544, Computer Center of the Institute for Molecular Science, (1989).

[39] H. Nakatsuji, Program system for the SAC and SAC-CI calculations for ground, excited, ionized and electron-attached states of molecules, Program Library No. 146 (Y4/SAC), Data Processing Center of Kyoto University, 1985; H. Nakatsuji, Program Library SAC85 (No. 1396), Computer Center of the Institute for Molecular Science, Okazaki, 1986.

[40] (a) A. J. H. Watchers, J. Chem. Phys. **52**, 1033 (1970);
(b) D. M. Hood, R. M. Pitzer, and H. F. Schaefer III, *ibid.* **71**, 705 (1979).

[41] (a) R. J. Buenker. in *Proc. of the Workshop on Quantum Chemistry and Molecular Physics, Wollongong, Australia*, 1980; edited by P. G. Burton
(Wollongong Univ. Press, Wollongong, 1980);

(b) R. J. Buenker and R. A. Phillips, J. Molec. Struct. (THEOCHEM) **123**, 291 (1985).

[42] M. Dupuis, D. Spangler and J. J. Wendoloski, NRCC Software Catalog,Vol. 1, GAMESS, Program QC01 (1980); M. F. Guest and P. Sherwood, GAMESS User's Guide and Reference Manual, SERC Daresbury Laboratory (1991).

[43] H. Nakatsuji, Theor. Chem. Acta. **71**, 201 (1987).

[44] H. Nakatsuji, Chem. Phys. **75**, 425 (1983).

[45] H. G. Dehmelt, J. Chem. Phys. **21**, 380 (1953).

[46] R. P. Hamlen and W. S. Koski, J. Chem. Phys. **25**, 360 (1956).

[47] E. A. C. Lucken, *Nuclear Quadrupole Coupling Constants* (Academic Press, London, 1969), Chap. 13, p. 308.

[48] W. L. Jolly, Chem. Phys. Lett. **100**, 546 (1983).

[49] R. L. Martin and D. A. Shirley, J. Chem. Phys. **64**, 3685 (1976).

[50] V. Subramanian, M. Vijayakumar, and T. Ramasami, Chem. Phys. Lett. **182**, 232 (1991).

[51] (a) H. Nakatsuji, Y. Matsuzaki, and T. Yonezawa, J. Chem. Phys. **88**, 5759 (1988);
(b) C. A. Masmanidis, H. H. Jaffe, and R. L. Ellis, J. Phys. Chem. **79**, 2052 (1975);
(c)S. Kato, R.L. Jaffe, A. Komornicki, and K. Morokuma, J. Chem. Phys. **78**, 4567 (1983).

[52] T. Shimanouchi, J. Phys. Chem. Data **6**, 993 (1977).

Chapter 5

Theoretical study on the excited and ionized states of $TiBr_4$ and TiI_4

ABSTRACT

The excitation and ionization spectra of TiX_4 (X=Br, I) are studied theoretically by the SAC(symmetry adapted cluster)/SAC-CI method. The valence excited states of these molecules are investigated systematically and compared with the previous study on $TiCl_4$. The experimental spectra are well reproduced by the SAC-CI calculation with including spin-orbit interaction of the ligand p-AO and Ti d-AO. Nine A_1, ten A_2, twenty E, thirty T_1 and T_2 states are calculated for the excited states, and the oscillator strengths are distributed among the transitions to thirty T_2 states, which cause the excitation spectra very complicated, especially for TiI_4 molecule. The ordering of the ionized states in the outer valence region is $(1t_1)^{-1} < (3t_2)^{-1} < (1e)^{-1} < (2t_2)^{-1} < (2a_1)^{-1}$, which is the same as that of $TiCl_4$. The spin-orbit splittings in the $^2T_2$ states of $TiBr_4$ and TiI_4 are estimated to be smaller than those of the previous studies, and we propose a new assignment for the experimental PE spectra.

I. INTRODUCTION

Titanium tetrahalides[1-6] are representative molecules of the transition metal complexes in tetrahedral coordination. Their electronic structure[1-6] and stereochemistry[7] were studied extensively by various experimental and theoretical techniques. However, there still remain some uncertainties even in the assignments of the electronic spectra of these molecules.[1-6]

In the preceding paper,[5] we have investigated the excited and ionized states of $TiCl_4$ molecule. We reproduced its excitation spectrum just below the ionization threshold and proposed detailed assignments and pictures of the excited states. We also could reproduce the ionization spectrum both in outer and inner valence regions. It is worthwhile to investigate the changes in the electronic structure caused by a systematic substitution of the ligands. Theoretical description of the electronic structures of TiX_4 (X=Br, I) is more difficult than that of $TiCl_4$ in the following two points. (1) There are five electronic valence shells in a very narrow energy region. (2) Spin-orbit effect of the ligands is large.

Experimental excitation spectrum of $TiBr_4$ in vapor phase and that of TiI_4 in cyclohexane solution were reported.[2] These spectra are observed only for the region of the valence excitations and not for that of the Rydberg excitations. As the ligands become soft, the peaks in the experimental spectra shift toward lower energy and the spectra show more complicated structures. These trends are supposed to be caused by the lower ionization potentials and larger spin-orbit interaction of the ligands. However, there are no theoretical works which explain quantitatively these features of the spectra.

Ionization spectra of these species are systematically studied experimentally by the gas phase photoelectron spectroscopy.[3,4] Experimental spectra are assigned with the aids of the extend Hückel MO calculations. The difference in the cross section between He(I) and He(II) excitations also gives significant information about the orbital nature.[3] However, more reliable theoretical treatments including electron correlations are necessary for the systematic assignment of the spectra of these molecules.

In this paper, we theoretically investigate the excited and ionized states of TiX_4 (X=Br, I) using the SAC (symmetry adapted cluster expansion)[8] and SAC-CI[9] theories. The SAC/SAC-CI method describes electron correlations effectively and it

has been confirmed that this method is accurate and useful for studying spectroscopies of various excited and ionized systems[5,10-13]: the experimental spectra are well reproduced and reliable new assignments are proposed.

We also study the spin-orbit effect of the ligands using the contracted CI scheme and therefore, precise descriptions of both singlet and triplet excited states are very important. The SAC-CI method, which is applicable to various spin multiplicity,[14] is suitable for the present purpose.

II. COMPUTATIONAL DETAILS

The geometries of TiX_4 (X=Br, I) are fixed to regular tetrahedron with the experimental bond lengths of 2.339 and 2.546 Å for $TiBr_4$ and TiI_4, respectively[7a] Geometrical relaxation effects are not considered in the present study: we calculate only vertical excitations and ionizations of these molecules.

For Ti atom, we use the same Gaussian basis set as in the previous study;[5] (14s8p5d)/[6s2p3d] set[15] augmented with two p type functions of ζ_p= 0.15, 0.073 are employed. The relativistic effective core potential (RECP) and the (3s3p)/[2s2p] sets[16] are used for bromine and iodine atoms. Since we need the spectra only in the valence region, neither Rydberg type functions nor anion type functions are added on the ligands. The final basis sets for TiX_4 (X=Br, I) molecules consist of 68 CGTO's.

Electron correlations in the ground state is taken into account by the SAC theory[8] and those in the excited states by the SAC-CI theory.[9] Details of the SAC/SAC-CI calculations were reported elsewhere.[17] Twelve higher occupied orbitals and 46 lower unoccupied orbitals are used for the active space in the calculations of singlet and triplet states (active space I). For the ionized states, the active space is enlarged for the occupied space as 16 higher occupied orbitals (active space II), since we need the spectral information of the inner valence region. We adopt all the singly excited configurations and selected doubly excited ones for the linked terms. The contributions of the triple and quadruple excitations are taken into account by the unlinked terms. The calculations are done in the C_{2v} subset of the T_d point group. Table I gives the correspondence of the irreducible representations of C_{2v} and T_d.

TABLE I. Dimensions of the SAC/SAC-CI calculations for $TiBr_4$ and TiI_4

State symmetry		Dimension	
Td	C_{2v}	$TiBr_4$	TiI_4
Ground state $^1A_1$	$^1A_1$	1749	1495
Singlet excited states			
$^1T_2$, ^1E, $^1A_1$	$^1A_1$	5383	4634
$^1T_1$, ^1E, $^1A_2$	$^1A_2$	4377	4555
$^1T_1$, $^1T_2$	$^1B_1$	5402	4715
Triplet excited states			
$^3T_2$, ^3E, $^3A_1$	$^3A_1$	7189	7828
$^3T_1$, ^3E, $^3A_2$	$^3A_2$	7138	7779
$^3T_1$, $^3T_2$	$^3B_1$	7464	8108
Ground state $^1A_1$	$^1A_1$	2109	1835
Ionized states			
$^2T_2$, ^2E, $^2A_1$	$^2A_1$	1760	1714
$^2T_1$, ^2E, $^2A_2$	$^2A_2$	841	825
$^2T_1$, $^2T_2$	$^2B_1$	1531	1464

Configuration selection is performed in the perturbative way[17] in order to reduce the size of the calculations. For singlet and triplet states, the thresholds λ_g and λ_e were set to $3*10^{-5}$ and $4*10^{-5}$ au, respectively. Reference configurations are selected from the lower 16, 14, and 15 SE-CI solutions for the A_1, A_2, and B_1 symmetries, respectively. For the ionized states, λ_g and λ_e were set to $3*10^{-5}$ and $1*10^{-5}$ au. The resultant dimensions of the present calculations are summarized in Table I. As the reference orbitals, we use the HFSCF MO's of the ground state for all the calculations. They are calculated by the program GAMESS.[18] The SAC/SAC-CI calculations are carried out by SAC85 program.[19]

The effect of spin-orbit interaction is considered for the excited and ionized states. The method has been reported previously[20] and some accounts are given in Appendix A.

III. GROUND STATE

The HF configuration of the ground state of TiX_4 (X=Br, I) and its orbital characters are as follows. The numbering of the orbitals is due to the experimental works for the ionized states.[3,4]

Valence occupied MO's

$(1a_1)^2$	L(s)	: non-bonding
$(1t_2)^6$	L(s)	: non-bonding
$(2a_1)^2$	Ti(s)-L(pσ)	: weakly antibonding
$(2t_2)^6$	Ti(dσ)+L(pσ)	: σ-bonding
$(1e)^4$	Ti(dπ)+L(pπ)	: π-bonding
$(3t_2)^6$	L(pπ)	: non-bonding
$(1t_1)^6$	L(pπ)	: non-bonding

Low-lying unoccupied MO's

(2e)	Ti(dπ)-L(pπ)	: π-antibonding
$(4t_2)$	Ti(d)-L(pσ,pπ)	: σ, π-antibonding

where Ti(x), L(y) denote titanium valence x orbital and ligand(Cl or Br) y orbital, respectively. Plus and minus signs indicate bonding and antibonding combinations, respectively. The directions of σ and π are due to those defined by Ballhausen et al.[21] The lowest four orbitals, $1a_1$ and $1t_2$, represent s lone pair orbitals of four ligands.

The next $2a_1$ orbital has a weak anti-bonding character. $2t_2$ and 1e MO's are characterized as the bonding MO's between Ti and halogens. The highest six occupied MO's $3t_2$ and $1t_1$ are non-bonding π-orbitals of the ligands. Valence occupied MOs from $2a_1$ to $1t_1$ are dominated by the ligand p-AO's. The lowest virtual orbitals 2e and $4t_2$ are the anti-bonding MO's between Ti and the ligands and are dominated by the d AO's of Ti.

The HF energies are calculated to be -900.10665 and -892.99143 au for $TiBr_4$ and TiI_4, respectively. The correlation energy of the ground state for $TiBr_4$ is calculated to be -0.16852 au with the active space I, while -0.18719 au with the active space II. Inclusion of $(1a_1)$ and $(1t_2)$ MO's into active space improve the ground state energy by 0.01867 au for $TiBr_4$. Similarly, the correlation energy for the ground state of TiI_4 is -0.16437 au with the active space I, and -0.18003 au with the active space II.

The atomic net charges on ligands are -0.052 ($TiBr_4$) and +0.039 (TiI_4) in the HF level using the Mulliken population analysis. Comparative data[5] for $TiCl_4$ is -0.138 for the atomic net charge on chlorine. The ionicity of the M-L bond reduces as the ligand becomes soft, as expected. We note that the Mulliken population itself is strongly basis-set dependent. The electronic parts of second moments are 240 au and 291 au for $TiBr_4$ and TiI_4, respectively, which indicate the sizes of these molecules.

IV. EXCITED STATES

All the excited states calculated in this paper are valence excitations which are characterized as excitations from either the L lone-pair MO or the M-L bonding MO to the M-L anti-bonding MO. Rydberg excitations are expected to lie above 7.4 eV for $TiBr_4$ from the consideration on the term value,[1] so that the observed excitation spectrum[2] is explained within the valence excitations: this corresponds to Region I in the study of $TiCl_4$.[5] For $TiBr_4$ and TiI_4, we study only the valence excitations and Rydberg excitations are not examined here.

The valence excited states are characterized by the products of the symmetry designations of the twelve occupied MOs and the five lowest virtual MOs. For example, the excitation $2t_2 \rightarrow 4t_2$ generates the A_1, E, T_1 and T_2 states. In this way, the singly excited configurations within the 12X5 space give three A_1, two A_2, five E,

seven T_1 and eight T_2 states. The present calculation deals with all of these states except for the 3^1A_1 state, since it lies in higher energy regions.[5,22] Among these excited states, only the transitions to the T_2 states are optically dipole allowed in the Td point group, and eight such $^1T_2$ states exist in the present system, though only four prominent peaks are detected in the region of the valence excitation of $TiCl_4$.

Assignments of the excitation spectra for $TiBr_4$ and TiI_4 are very complicated because of dense states in valence region and strong spin-orbit interaction, and therefore, several possibilities are shown in some points. They are systematically performed in comparison with $TiCl_4$ [5] and also in consistent with the ionization potentials of TiX_4 species. Detailed explanations of these assignments are shown in section IV.E.

A. Excited states of $TiBr_4$ without including spin-orbit interaction

The excitation energies, oscillator strengths of the singlet excited states of $TiBr_4$ are summarized in Table II. Theoretically calculated spectrum is compared in Figure 1 with the experimental absorption spectrum observed in gas phase.[2] Dipole forbidden transitions are indicated by circles in the theoretical spectra. The excitation energies and the natures of the triplet excited states are given in Table III.

The excitation spectrum of $TiBr_4$ is very similar to that of $TiCl_4$. The observed spectrum consists of three bands. The third band has an asymmetric shape, which indicates that this band is composed of more-than-two peaks. These peaks are different by 0.8 - 1.1 eV toward lower energy side from those of $TiCl_4$. This monotonic shift of the excitation energy is explained by the change in the ionization potential (IP). Furthermore, there exists a close parallelism between the change in IP caused by the substitution of the ligand and that for the corresponding halogen atoms. This is because the valence MO's are dominated by the ligand p-AO's. Green et al[4] also noted this tendency for the IP's of the carbon-tetrahalides. Details will be explained in section VI.E.

Inclusion of the spin-orbit interaction is important for a detailed analysis of the excitation spectrum. However, overall structures of the spectrum are understood without including the spin-orbit interaction in the case of $TiBr_4$, as seen in Figure 1. Therefore, we first present our results without including the spin-orbit interaction.

TABLE II. Excitation energy and oscillator strength for the singlet excited state of $TiBr_4$ calculated by the SAC-CI method without including spin-orbit interaction (in eV).

State	Dominant configurations	Excitation character	Excitation energy SAC-CI (Δ^a)	Exptl.[b]	Oscillator strength
1^1T_1	$0.89(1t_1 \rightarrow 2e)$	L → M-L	3.20	3.47	forbidden
1^1T_2	$0.85(1t_1 \rightarrow 2e)$	L → M-L	3.43 (-.23)	3.66	$5.69*10^{-2}$
1^1E	$0.89(1t_1 \rightarrow 4t_2)$	L → M-L	3.74		forbidden
2^1T_1	$0.80(1t_1 \rightarrow 4t_2)$, $0.08(3t_2 \rightarrow 2e)$	L → M-L	3.79		forbidden
1^1A_2	$0.85(1t_1 \rightarrow 4t_2)$, $0.04(1e \rightarrow 2e)$	L → M-L, M+L → M-L	3.84		forbidden
2^1T_2	$0.84(1t_1 \rightarrow 4t_2)$	L → M-L	3.96		$6.23*10^{-2}$
3^1T_1	$0.52(3t_2 \rightarrow 2e)$, $0.29(2t_2 \rightarrow 2e)$, $0.04(1t_1 \rightarrow 4t_2)$	L → M-L, M+L → M-L	4.32		forbidden
3^1T_2	$0.72(3t_2 \rightarrow 2e)$, $0.09(2t_2 \rightarrow 4t_2)$, $0.08(2t_2 \rightarrow 2e)$	L → M-L, M+L → M-L	4.53 (+.09)	4.44, 4.59	$6.15*10^{-2}$
2^1E	$0.65(1e \rightarrow 2e)$, $0.14(3t_2 \rightarrow 4t_2)$	M+L → M-L, L → M-L	4.60		forbidden
4^1T_1	$0.51(2t_2 \rightarrow 2e)$, $0.24(3t_2 \rightarrow 2e)$, $0.05(2t_2 \rightarrow 4t_2)$	M+L → M-L, L → M-L	4.67		forbidden
2^1A_2	$0.85(1e \rightarrow 2e)$	M+L → M-L	4.73		forbidden
4^1T_2	$0.67(2t_2 \rightarrow 2e)$, $0.11(3t_2 \rightarrow 4t_2)$, $0.09(3t_2 \rightarrow 2e)$	M+L → M-L, L → M-L	4.75		$7.99*10^{-3}$
1^1A_1	$0.67(1e \rightarrow 2e)$, $0.25(2t_2 \rightarrow 4t_2)$	M+L → M-L	4.81		forbidden
5^1T_1	$0.70(3t_2 \rightarrow 4t_2)$, $0.09(1e \rightarrow 4t_2)$, $0.05(3t_2 \rightarrow 2e)$	L → M-L, M+L → M-L	4.99		forbidden
3E	$0.69(3t_2 \rightarrow 4t_2)$, $0.21(1e \rightarrow 2e)$,	L → M-L, M+L → M-L	5.17		forbidden
5^1T_2	$0.50(3t_2 \rightarrow 4t_2)$, $0.17(1e \rightarrow 4t_2)$, $0.13(2t_2 \rightarrow 2e)$, $0.09(2t_2 \rightarrow 4t_2)$	L → M-L, M+L → M-L	5.21		$5.86*10^{-3}$
2^1A_1	$0.76(3t_2 \rightarrow 4t_2)$, $0.13(2t_2 \rightarrow 4t_2)$	L → M-L, M+L → M-L	5.24		forbidden
6^1T_1	$0.76(1e \rightarrow 4t_2)$, $0.11(3t_2 \rightarrow 4t_2)$	M+L → M-L, L → M-L	5.26		forbidden
6^1T_2	$0.54(1e \rightarrow 4t_2)$, $0.26(3t_2 \rightarrow 4t_2)$, $0.05(3t_2 \rightarrow 2e)$	M+L → M-L, L → M-L	5.34		$5.93*10^{-2}$
4^1E	$0.49(2a_1 \rightarrow 2e)$, $0.41(2t_2 \rightarrow 4t_2)$	M+L → M-L	5.46		forbidden
7^1T_1	$0.81(2t_2 \rightarrow 4t_2)$, $0.06(2t_2 \rightarrow 2e)$	M+L → M-L	5.56		forbidden
5^1E	$0.48(2t_2 \rightarrow 4t_2)$, $0.43(2a_1 \rightarrow 2e)$	M+L → M-L	5.82		forbidden
7^1T_2	$0.49(2t_2 \rightarrow 4t_2)$, $0.20(2a_1 \rightarrow 4t_2)$, $0.14(1e \rightarrow 4t_2)$, $0.05(2t_2 \rightarrow 2e)$	M+L → M-L	5.99 (-.02)	6.01	0.183
8^1T_2	$0.69(2a_1 \rightarrow 4t_2)$, $0.10(2t_2 \rightarrow 4t_2)$	M+L → M-L	6.66 (+.15)	6.51	1.040
average descrepancies			0.12		

[a] Deviations from the experimental values.
[b] Reference 2

TABLE III. Excitation energy for the triplet excitated state of $TiBr_4$ calculated by the SAC-CI method without including spin-orbit interaction (in eV).

State	Dominant configurations	Excitation character	Excitation energy
1^3T_2	$0.81(1t_1 \rightarrow 2e)$, $0.09(1t_1 \rightarrow 4t_2)$	L → M-L	3.10
1^3T_1	$0.86(1t_1 \rightarrow 2e)$	L → M-L	3.18
1^3E	$0.87(1t_1 \rightarrow 4t_2)$	L → M-L	3.67
2^3T_2	$0.66(1t_1 \rightarrow 4t_2)$, $0.08(1t_1 \rightarrow 2e)$, $0.07(3t_2 \rightarrow 2e)$	L → M-L	3.70
2^3T_1	$0.74(1t_1 \rightarrow 4t_2)$, $0.14(3t_2 \rightarrow 2e)$	L → M-L	3.75
1^3A_2	$0.84(1t_1 \rightarrow 4t_2)$, $0.05(1e \rightarrow 2e)$	L → M-L, M+L → M-L	3.85
1^3A_1	$0.58(1e \rightarrow 2e)$, $0.24(3t_2 \rightarrow 4t_2)$	M+L → M-L, L → M-L	3.93
3^3T_2	$0.65(3t_2 \rightarrow 2e)$, $0.12(2t_2 \rightarrow 2e)$, $0.10(1e \rightarrow 4t_2)$	L → M-L, M+L → M-L	4.20
3^3T_1	$0.44(2t_2 \rightarrow 2e)$, $0.34(3t_2 \rightarrow 2e)$, $0.10(1t_1 \rightarrow 4t_2)$	M+L → M-L, L → M-L	4.23
2^3E	$0.68(1e \rightarrow 2e)$, $0.13(3t_2 \rightarrow 4t_2)$	M+L → M-L, L → M-L	4.39
4^3T_2	$0.69(2t_2 \rightarrow 2e)$, $0.11(3t_2 \rightarrow 2e)$, $0.09(2t_2 \rightarrow 4t_2)$	M+L → M-L, L → M-L	4.51
4^3T_1	$0.36(3t_2 \rightarrow 2e)$, $0.35(2t_2 \rightarrow 2e)$, $0.10(2t_2 \rightarrow 4t_2)$	L → M-L, M+L → M-L	4.59
1^3A_1	$0.64(2t_2 \rightarrow 4t_2)$, $0.24(1e \rightarrow 2e)$	M+L → M-L	4.72
2^3A_2	$0.84(1e \rightarrow 2e)$	M+L → M-L	4.73
5^3T_2	$0.62(3t_2 \rightarrow 4t_2)$, $0.19(2t_2 \rightarrow 4t_2)$, $0.04(2t_2 \rightarrow 2e)$	L → M-L, M+L → M-L	4.85
3^3E	$0.34(2t_2 \rightarrow 4t_2)$, $0.30(3t_2 \rightarrow 4t_2)$, $0.16(2a_1 \rightarrow 2e)$, $0.12(1e \rightarrow 2e)$	M+L → M-L, L → M-L	4.87
5^3T_1	$0.56(3t_2 \rightarrow 4t_2)$, $0.21(1e \rightarrow 4t_2)$, $0.09(3t_2 \rightarrow 2e)$	L → M-L, M+L → M-L	4.91
6^3T_2	$0.60(2t_2 \rightarrow 4t_2)$, $0.21(3t_2 \rightarrow 4t_2)$	M+L → M-L, L → M-L	5.12
2^3A_1	$0.64(3t_2 \rightarrow 4t_2)$, $0.14(2t_2 \rightarrow 4t_2)$, $0.11(1e \rightarrow 2e)$	L → M-L, M+L → M-L	5.14
4^3E	$0.41(3t_2 \rightarrow 4t_2)$, $0.25(2a_1 \rightarrow 2e)$, $0.14(2t_2 \rightarrow 4t_2)$, $0.04(1e \rightarrow 2e)$	M+L → M-L, L → M-L	5.20
6^3T_1	$0.65(1e \rightarrow 4t_2)$, $0.25(3t_2 \rightarrow 4t_2)$	M+L → M-L, L → M-L	5.20
7^3T_2	$0.77(1e \rightarrow 4t_2)$, $0.08(3t_2 \rightarrow 2e)$	M+L → M-L, L → M-L	5.26
7^3T_1	$0.79(2t_2 \rightarrow 4t_2)$, $0.08(2t_2 \rightarrow 2e)$	M+L → M-L	5.53
5^3E	$0.51(2a_1 \rightarrow 2e)$, $0.39(2t_2 \rightarrow 4t_2)$	M+L → M-L	5.70
8^3T_2	$0.86(2a_1 \rightarrow 4t_2)$	M+L → M-L	6.11

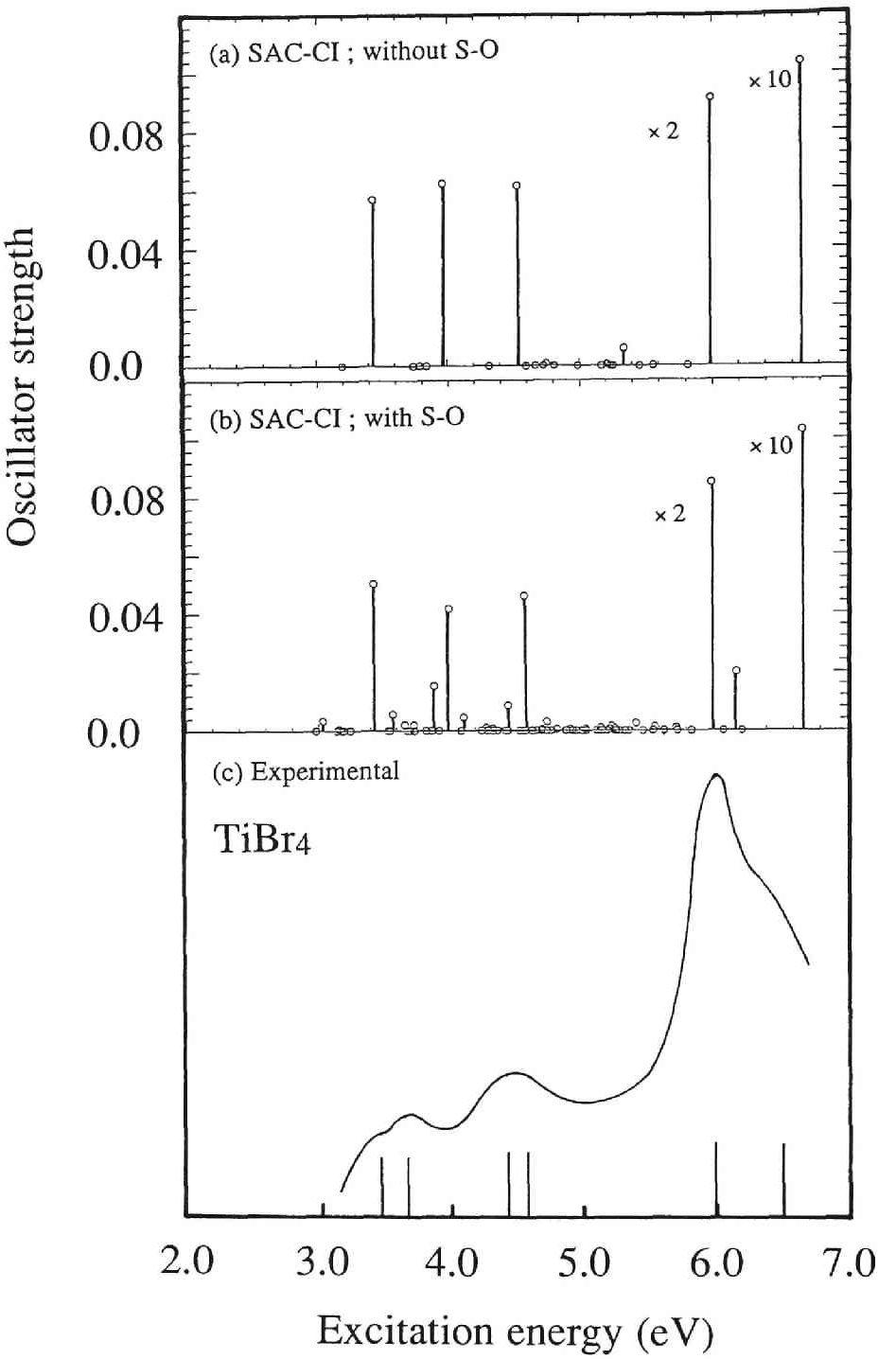

FIG. 1. Theoretical excitation spectrum of $TiBr_4$ (a) without including spin-orbit interaction, (b) with including spin-orbit interaction, and (c) experimental excitation spectrum.[2]

Among the dipole allowed $^1T_2$ states, five states have relatively large oscillator strengths. Two kinds of assignments are possible for the first and second bands. One assignment is possible in accordance with the excitation spectrum of $TiCl_4$: 1^1T_2 state is assigned to the first band, 2^1T_2 and 3^1T_2 states to the second band, and 7^1T_2 and 8^1T_2 states to the third band. The other possibility of the first and second band is due to the calculated oscillator strength and shapes of the spectrum: 2^1T_2 state, which has larger oscillator strength than that of $TiCl_4$, is assigned to the first band with 1^1T_2 state to the shoulder of the first band, 3^1T_2 state to the second band. In both of the assignments, all the observed peaks are assigned to the dipole allowed $^1T_2$ states. The difference, Δ, between the calculated excitation energy and the observed peak maximum is shown in Table II in the parentheses and is smaller than 0.30 eV. The average discrepancy between theory and experiment for the excitation energy is 0.12 eV.

The lower energy side of the spectrum is characterized as L $\rightarrow$ M-L, while the higher energy side as M+L$\rightarrow$ M-L. Many dipole forbidden states also exist in the valence region. Dipole forbidden 1^1T_1 state ($1t_1\rightarrow$ 2e) is calculated at the lowest energy, 3.20 eV, of the singlet excited states. This trend is similar to other transition metal complexes.[11-13] Furthermore, all the $^1T_1$ states are calculated to be more stable than the corresponding $^1T_2$ states by 0.08 ~ 0.43 eV. The electronic parts of the second moments of all the singlet excited states lie within 240-242 au and are almost the same as that of the ground state: all of these states are valence excited states.

We next examine triplet excited states of $TiBr_4$. Triplet T_2 states are found to be more stable by 0.22 ~ 0.73 eV than the corresponding singlet T_2 states. The singlet and triplet separations for the T_2 symmetry are relatively large compared to those for the other symmetries; those for T_1, E, and A_2 symmetries are -0.02 ~ -0.09, -0.07 ~ 0.30, and +0.01 ~ 0.00 eV, respectively. All the $^3T_2$ states are calculated to be more stable than the corresponding $^3T_1$ states by 0.08 ~ 0.27 eV, which is a reverse relationship to that observed for the symmetry of the singlet states. Triplet excited states do not necessarily have the same excitation natures as the corresponding singlet excited states. For example, 6^1T_2 state is characterized as $1e\rightarrow 4t_2$, $3t_2\rightarrow 4t_2$, $3t_2\rightarrow$ 2e, while 6^3T_2 state is as $2t_2\rightarrow 4t_2$, $3t_2\rightarrow 4t_2$.

B. Spin-orbit interaction in the Td symmetry

In the Td point group, triplet spin transforms in the same way as the basis of the t_1 symmetry. Therefore, triplet states split as follows by the inclusion of the spin-orbit interaction:

$$^3A_1 \rightarrow T_1$$
$$^3A_2 \rightarrow T_2$$
$$^3E \rightarrow T_1, T_2$$
$$^3T_1 \rightarrow A_1, E, T_1, T_2$$
$$^3T_2 \rightarrow A_2, E, T_1, T_2$$

where the irreducible representations[5] on the right-hand side denote the symmetry of the spin functions. Dipole allowed T_2 states are generated from the $^3A_2$, ^3E, $^3T_1$ and $^3T_2$ states and have certain oscillator strength through the interaction with the $^1T_2$ states. In the present calculation, the spin-orbit interactions between all the valence excited states except for the 3^1A_1 state are considered. Therefore, nine A_1, ten A_2, twenty E, thirty T_1 and T_2 states are calculated. The excited states in the next higher energy region are supposed to be Rydberg excitations, as shown in the previous study,[5] so that the inclusion of these states into the spin-orbit interactions will have only a small influence on the present results. Method of calculating the spin-orbit interaction is summarized in Appendix A.

It is useful to get the approximate spin-orbit splittings by estimating the spin-orbit interaction stepwisely. For example, $^3T_1$ state split into A_1, three hold T_1, and five hold (T_2+E) level under first order perturbation. The splitting between A_2 and (T_2+E) level of the lowest excited states is calculated as 0.10 and 0.20 eV for $TiBr_4$ and TiI_4, respectively.

C. Excited states of $TiBr_4$ with including spin-orbit interaction

We discuss here the effect of spin-orbit interaction on the excitation spectrum of $TiBr_4$. There are many triplet states in the lower energy region of the spectrum as summarized in Table III. Therefore, the oscillator strengths of the $^1T_2$ states are distributed to several states through the spin-orbit interaction. Figure 1b) shows the results with including the spin-orbit interaction on the results of the SAC/SAC-CI calculations. Table IV gives the weight of the singlet and triplet components for the

TABLE IV. Excitation energy and oscillator strength for the excitated state of $TiBr_4$ calculated by the SAC-CI method with including spin-orbit correction (in eV).

State[a]	Dominant configurations[b]	Excitation energy		Oscillator strength
		SAC-CI (Δ[c])	Expt.[d]	
$1T_2$	$0.53(1^3T_1)$, $0.40(1^3T_2)$, $0.06(1^1T_2)$	3.04		$3.40*10^{-3}$
$2T_2$	$0.55(1^3T_2)$, $0.40(1^3T_1)$, $0.003(1^1T_2)$	3.16	3.47	$6.04*10^{-4}$
$2T_1$	$0.29(1^3T_1)$, $0.29(1^3T_2)$, $0.28(1^1T_1)$	3.20		forbidden
$3T_1$	$0.50(1^1T_1)$, $0.47(1^3T_1)$	3.25		forbidden
$3T_2$	$0.88(1^1T_2)$	3.43 (-0.23)	3.66	$5.03*10^{-2}$
$4T_2$	$0.66(2^3T_2)$, $0.10(1^3E)$, $0.10(1^3A_2)$ $0.04(2^1T_2)$	3.57		$5.65*10^{-3}$
$7T_2$	$0.67(1^3A_2)$, $0.22(2^1T_2)$	3.89		$1.53*10^{-2}$
$8T_2$	$0.66(2^1T_2)$, $0.20(2^3T_2)$, $0.10(1^3A_2)$	4.00		$4.16*10^{-2}$
$12T_2$	$0.60(4^3T_2)$, $0.14(3^1T_2)$, $0.10(2^3A_2)$	4.45 (+0.01)	4.44	$8.57*10^{-3}$
$13T_2$	$0.75(3^1T_2)$, $0.15(4^3T_2)$	4.58 (-0.01)	4.59	$4.59*10^{-2}$
$28T_2$	$0.92(7^1T_2)$	5.99 (-0.02)	6.01	0.170
$29T_2$	$0.92(8^3T_2)$, $0.06(7^1T_2)$	6.18		$2.00*10^{-2}$
$30T_2$	$0.99(8^1T_2)$	6.67 (+0.18)	6.51	1.029
average descrepancy		0.09		

[a] Excited states whose oscillator strength is larger than 0.005. $1T_2$, $2T_2$, $2T_1$ and $3T_1$ states are listed for the assignments of shoulder ar 3.47 eV.

[b] Dominant configurations and square values of the coefficients are listed for those square values are larger than 0.1. At least, components of singlet T_2 states are listed for triplet dominant states.

[c] Deviation from experimental values

[d] Reference 2

T_2 states which have relatively large oscillator strengths. Some lower T_1 states are also shown. As noted in the previous section, two assignments are possible for the first and second bands. Here, we follow the first possibility in the following discussions. Another assignments are performed by comparing the states with and without including spin-orbit interaction shown in Tables II and IV, respectively.

The first band whose main peak is observed at 3.66 eV is assigned to the transition to the $3T_2$ state calculated at 3.43 eV. This state corresponds to 1^1T_2 state ($1t_1 \rightarrow 2e$) and is characterized as a charge transfer state from ligand to metal. The shoulder is observed at 3.47 eV, which is located in the lower energy side of the main peak by 0.19 eV. This shoulder is assumed to be a spin-forbidden and/or a dipole forbidden state. The candidates for the spin-fobidden states are 1^3T_2 and 1^3T_1. The $1T_2$ and $2T_2$ states are derived from these states, as shown in Table IV, at 3.04 and 3.16 eV, respectively, though these states have very small oscillator strengths of $3.40*10^{-3}$ and $6.04*10^{-4}$, respectively. On the other hand, dipole-forbidden states are calculated around 3.20 eV originated from 1^1T_1 and 1^3T_1 states. Candidates of this shoulder are the $2T_1$(3.20 eV) and $3T_1$(3.25 eV) states. The forbidden nature of these states may be relaxed to some extent through the static and/or dynamic Jahn-Teller distortion. Since we did not examine the induced intensities for these dipole forbidden states, it is difficult to specify here the dominant origin of the shoulder.

The second band in the experimental spectrum consists of the two peaks at 4.44 and 4.59 eV.[2] The present results of the $7T_2$(3.89 eV), $8T_2$(4.00 eV), $12T_2$(4.45 eV), and $13T_2$(4.58 eV) states are attributed to the second band. $7T_2$ and $8T_2$ states originate from 1^3A_2 and 2^1T_2 states whose main configuration is $1t_1 \rightarrow 4t_2$. $12T_2$ and $13T_2$ states are generated through the interaction of 3^1T_2 and 4^3T_2 states whose dominant configurations are $3t_2 \rightarrow 2e$, $2t_2 \rightarrow 4t_2$, and $2t_2 \rightarrow 2e$. Oscillator strengths of the transitions for $14T_2$ to $27T_2$ states are calculated to be small, since these states correspond to 4^1T_2 to 6^1T_2 states whose intensities are very small (Table II).

The third band has two peaks and the lower one has a larger intensity in the experimental spectrum. We assign these peaks from the energetic point of view. The lower peak observed at 6.01 eV is assigned to $28T_2$ state(5.99 eV) and the higher one at 6.51 eV is to $30T_2$ state(6.67 eV). $28T_2$ and $30T_2$ states, which have large oscillator strength, originate from 7^1T_2 and 8^1T_2, respectively. The 7^1T_2 state is

expressed by a linear combination of the four configurations, $2t_2 \rightarrow 4t_2$, $2a_1 \rightarrow 4t_2$, $1e \rightarrow 4t_2$, and $2t_2 \rightarrow 2e$, which indicates the configuration interaction is indispensable in order to describe this state. The present calculation shows that the 8^1T_2 state has larger oscillator strength than the 7^1T_2 state.

D. Excited states of TiI_4

Table V gives the calculated excitation energies and oscillator strengths for the singlet excited states of TiI_4. Results for triplet excited states are also given in Talbe VI. Theoretical spectra with and without including the spin-orbit interaction and the experimental absorption spectrum are compared in Figure 2. Table VII summarizes the dipole allowed T_2 states having certain oscillator strengths obtained after including the spin-orbit interaction.

The spin-orbit interaction is very important for the excited states of TiI_4, as shown in Figure 2, reflecting large spin-orbit coupling constant of the iodine atom. Strong mixing between singlet and triplet states occurs especially in the lower energy region. Oscillator strengths are considerably distributed to these T_2 states as seen from Table VII. So far, absorption bands are regarded as to be composed by several peaks, however, this picture does not hold good for TiI_4. Due to the strong spin-orbit interaction, large numbers of allowed transitions occur and cooperatively contribute to each bands. Therefore, we discuss the excitation spectrum of this molecule using the results shown in Table VII.

The first band whose maximum is observed at 2.43 eV is assigned as being due to the $3T_2$ and $4T_2$ states calculated at 2.65 and 2.73 eV, respectively. These states originate from 1^1T_2 state ($1t_1 \rightarrow 4t_2$). $1T_2$ and $2T_2$ states are calculated in the lower energy side of these states and are mainly derived from 1^3T_1 and 1^3T_2 states, respectively. These states have relatively large oscillator strengths ($7.57*10^{-3}$, $6.41*10^{-3}$) through the interaction with the 1^1T_2 state, though there are no experimental evidence for these states. Split peaks are observed at 3.10 and 3.45 eV and we assign these peaks to $7T_2$ and $9T_2$ states calculated at 3.05 and 3.31 eV, respectively. These states originate from 2^1T_2 state ($3t_2 \rightarrow 4t_2$) and have 1^3A_2 and 2^3T_2 components. The third band observed at 4.28 eV is due to $14T_2$ state calculated at 3.91 eV, which corresponds to 3^1T_2 state. 3^1T_2 state is destabilized by 0.15 eV

TABLE V. Excitation energy and oscillator strength for the singlet excitated state of TiI_4 calculated by the SAC-CI method without including the spin-orbit interaction (in eV).

			SAC-CI (Δ^a)	
State	Dominant configurations	Excitation character	Excitation energy	Oscillator strength
1^1T_1	$0.89(1t_1 \rightarrow 2e)$	L → M-L	2.53	forbidden
1^1T_2	$0.85(1t_1 \rightarrow 2e)$	L → M-L	2.73	$5.39*10^{-2}$
1^1E	$0.89(1t_1 \rightarrow 4t_2)$	L → M-L	2.94	forbidden
2^1T_1	$0.84(1t_1 \rightarrow 4t_2)$, $0.05(3t_2 \rightarrow 2e)$	L → M-L	2.98	forbidden
1^1A_2	$0.87(1t_1 \rightarrow 4t_2)$	L → M-L	3.02	forbidden
2^1T_2	$0.83(1t_1 \rightarrow 4t_2)$	L → M-L	3.16	$8.69*10^{-2}$
3^1T_1	$0.58(3t_2 \rightarrow 2e)$, $0.26(2t_2 \rightarrow 2e)$,	L → M-L, M+L → M-L	3.53	forbidden
3^1T_2	$0.62(3t_2 \rightarrow 2e)$, $0.16(2t_2 \rightarrow 2e)$, $0.12(2t_2 \rightarrow 4t_2)$	L → M-L, M+L → M-L	3.76	$5.61*10^{-2}$
2^1E	$0.60(1e \rightarrow 2e)$, $0.27(3t_2 \rightarrow 4t_2)$	M+L → M-L, L → M-L	3.83	forbidden
2^1A_2	$0.87(1e \rightarrow 2e)$	M+L → M-L	3.97	forbidden
4^1T_1	$0.37(3t_2 \rightarrow 4t_2)$, $0.26(2t_2 \rightarrow 2e)$, $0.09(3t_2 \rightarrow 2e)$, $0.10(2t_2 \rightarrow 4t_2)$	L → M-L, M+L → M-L	4.00	forbidden
1^1A_1	$0.71(1e \rightarrow 2e)$, $0.18(2t_2 \rightarrow 4t_2)$	M+L → M-L	4.03	forbidden
4^1T_2	$0.39(2t_2 \rightarrow 2e)$, $0.29(3t_2 \rightarrow 4t_2)$, $0.19(3t_2 \rightarrow 2e)$	M+L → M-L, L → M-L	4.06	$1.19*10^{-2}$
5^1T_1	$0.35(3t_2 \rightarrow 4t_2)$, $0.30(2t_2 \rightarrow 2e)$, $0.11(3t_2 \rightarrow 2e)$, $0.09(1e \rightarrow 4t_2)$	L → M-L, M+L → M-L	4.20	forbidden
3^1E	$0.62(3t_2 \rightarrow 4t_2)$, $0.28(1e \rightarrow 2e)$	L → M-L, M+L → M-L	4.35	forbidden
5^1T_2	$0.36(1e \rightarrow 4t_2)$, $0.25(2t_2 \rightarrow 2e)$, $0.20(3t_2 \rightarrow 4t_2)$, $0.09(2t_2 \rightarrow 4t_2)$	M+L → M-L, L → M-L	4.38	$2.27*10^{-3}$
6^1T_1	$0.74(1e \rightarrow 4t_2)$, $0.16(3t_2 \rightarrow 4t_2)$	M+L → M-L, L → M-L	4.39	forbidden
2^1A_1	$0.66(3t_2 \rightarrow 4t_2)$, $0.26(2t_2 \rightarrow 4t_2)$	L → M-L, M+L → M-L	4.49	forbidden
6^1T_2	$0.38(3t_2 \rightarrow 4t_2)$, $0.37(1e \rightarrow 4t_2)$ $0.08(2t_2 \rightarrow 2e)$, $0.04(3t_2 \rightarrow 2e)$	L → M-L, M+L → M-L	4.51	$1.83*10^{-3}$
7^1T_1	$0.79(2t_2 \rightarrow 4t_2)$, $0.07(2t_2 \rightarrow 2e)$	M+L → M-L	4.75	forbidden
4^1E	$0.78(2t_2 \rightarrow 4t_2)$, $0.11(2a_1 \rightarrow 2e)$	M+L → M-L	4.80	forbidden
7^1T_2	$0.59(2t_2 \rightarrow 4t_2)$, $0.13(1e \rightarrow 4t_2)$, $0.08(2a_1 \rightarrow 4t_2)$	M+L → M-L	5.16	0.377
5^1E	$0.80(2a_1 \rightarrow 2e)$, $0.07(2t_2 \rightarrow 4t_2)$	M+L → M-L	5.21	forbidden
8^1T_2	$0.81(2a_1 \rightarrow 4t_2)$	M+L → M-L	5.95	0.893

[a] Reference 2

TABLE VI. Excitation energy for the triplet excitated state of TiI_4 calculated by the SAC-CI method without including spin-orbit interaction (in eV).

State	Dominant configurations	Excitation character	Excitation energy
1^3T_2	$0.78(1t_1 \rightarrow 2e)$, $0.12(1t_1 \rightarrow 4t_2)$	L → M-L	2.43
1^3T_1	$0.84(1t_1 \rightarrow 2e)$	L → M-L	2.51
1^3E	$0.88(1t_1 \rightarrow 4t_2)$	L → M-L	2.86
2^3T_2	$0.75(1t_1 \rightarrow 4t_2)$, $0.11(1t_1 \rightarrow 2e)$	L → M-L	2.91
2^3T_1	$0.76(1t_1 \rightarrow 4t_2)$, $0.09(3t_2 \rightarrow 2e)$ $0.06(1t_1 \rightarrow 2e)$	L → M-L	2.96
1^3A_2	$0.87(1t_1 \rightarrow 4t_2)$	L → M-L	3.04
1^3A_1	$0.46(1e \rightarrow 2e)$, $0.34(3t_2 \rightarrow 4t_2)$, $0.13(2t_2 \rightarrow 4t_2)$	M+L → M-L, L → M-L	3.15
3^3T_1	$0.43(3t_2 \rightarrow 2e)$, $0.38(2t_2 \rightarrow 2e)$	L → M-L, M+L → M-L	3.42
3^3T_2	$0.62(3t_2 \rightarrow 2e)$, $0.17(2t_2 \rightarrow 2e)$, $0.10(1e \rightarrow 4t_2)$	M+L → M-L, L → M-L	3.43
2^3E	$0.60(1e \rightarrow 2e)$, $0.28(3t_2 \rightarrow 4t_2)$	M+L → M-L, L → M-L	3.63
4^3T_2	$0.40(2t_2 \rightarrow 2e)$, $0.20(2t_2 \rightarrow 4t_2)$, $0.16(3t_2 \rightarrow 4t_2)$, $0.12(3t_2 \rightarrow 2e)$	M+L → M-L, L → M-L	3.82
2^3A_1	$0.45(2t_2 \rightarrow 4t_2)$, $0.38(1e \rightarrow 2e)$	M+L → M-L	3.88
4^3T_1	$0.34(3t_2 \rightarrow 4t_2)$, $0.21(2t_2 \rightarrow 2e)$, $0.17(3t_2 \rightarrow 2e)$, $0.12(2t_2 \rightarrow 4t_2)$	L → M-L, M+L → M-L	3.89
2^3A_2	$0.86(1e \rightarrow 2e)$	M+L → M-L	3.96
5^3T_2	$0.48(3t_2 \rightarrow 4t_2)$, $0.06(1e \rightarrow 4t_2)$, $0.27(2t_2 \rightarrow 2e)$	L → M-L, M+L → M-L	3.98
3^3E	$0.36(3t_2 \rightarrow 4t_2)$, $0.25(2t_2 \rightarrow 4t_2)$, $0.24(1e \rightarrow 2e)$, $0.05(2a_1 \rightarrow 2e)$	L → M-L, M+L → M-L	4.02
5^3T_1	$0.26(3t_2 \rightarrow 4t_2)$, $0.21(1e \rightarrow 4t_2)$, $0.21(3t_2 \rightarrow 2e)$, $0.19(2t_2 \rightarrow 2e)$	L → M-L, M+L → M-L	4.12
6^3T_1	$0.61(1e \rightarrow 4t_2)$, $0.28(3t_2 \rightarrow 4t_2)$	M+L → M-L, L → M-L	4.34
6^3T_2	$0.44(1e \rightarrow 4t_2)$, $0.30(2t_2 \rightarrow 4t_2)$, $0.08(3t_2 \rightarrow 2e)$	M+L → M-L, L → M-L	4.36
3^3A_1	$0.50(3t_2 \rightarrow 4t_2)$, $0.34(2t_2 \rightarrow 4t_2)$	L → M-L, M+L → M-L	4.38
7^3T_2	$0.39(2t_2 \rightarrow 4t_2)$, $0.31(1e \rightarrow 4t_2)$ $0.21(3t_2 \rightarrow 4t_2)$, $0.04(3t_2 \rightarrow 2e)$	M+L → M-L, L → M-L	4.39
4^3E	$0.46(2t_2 \rightarrow 4t_2)$, $0.27(3t_2 \rightarrow 4t_2)$ $0.14(2a_1 \rightarrow 2e)$	M+L → M-L	4.51
7^3T_1	$0.77(2t_2 \rightarrow 4t_2)$, $0.12(2t_2 \rightarrow 2e)$	M+L → M-L, L → M-L	4.70
5^3E	$0.72(2a_1 \rightarrow 2e)$, $0.12(2t_2 \rightarrow 4t_2)$	M+L → M-L	5.10
8^3T_2	$0.94(2a_1 \rightarrow 4t_2)$	M+L → M-L	5.48

TABLE VII. Excitation energy and oscillator strength for the excited state of TiI_4 calculated by the SAC-CI method with including spin-orbit correction (in eV).

State[a]	Dominant configurations[b]	Excitation energy		Oscillator strength
		SAC-CI (Δ[c])	Expt.[d]	
$1T_2$	$0.60(1^3T_1)$, $0.24(1^3T_2)$, $0.14(1^1T_2)$	2.22		$7.57*10^{-3}$
$2T_2$	$0.42(1^3T_2)$, $0.14(1^3T_1)$, $0.11(1^3A_2)$ $0.10(2^3T_2)$, $0.04(2^1T_2)$	2.38		$6.41*10^{-3}$
$3T_2$	$0.29(2^3T_2)$, $0.21(1^1T_2)$, $0.20(1^3T_1)$ $0.11(1^3T_2)$, $0.10(1^3A_2)$	2.65	2.43	$1.45*10^{-2}$
$4T_2$	$0.50(1^1T_2)$, $0.16(1^3T_1)$, $0.15(2^3T_2)$	2.73 (+0.30)		$3.05*10^{-2}$
$6T_2$	$0.74(2^3T_1)$, $0.04(2^1T_2)$, $0.03(3^1T_2)$	2.89		$7.59*10^{-3}$
$7T_2$	$0.45(2^1T_2)$, $0.43(1^3A_2)$	3.05 (-0.05)	3.10	$4.10*10^{-2}$
$8T_2$	$0.33(3^3T_1)$, $0.29(3^3T_2)$, $0.12(3^1T_2)$	3.20		$9.17*10^{-3}$
$9T_2$	$0.29(2^1T_2)$, $0.28(2^3T_2)$, $0.21(1^3A_2)$	3.31 (-0.14)	3.45	$2.72*10^{-2}$
$10T_2$	$0.42(2^3E)$, $0.12(4^3T_2)$, $0.12(4^3T_1)$ $0.07(4^1T_2)$	3.46		$5.01*10^{-3}$
$12T_2$	$0.41(4^3T_2)$, $0.26(2^3A_2)$ $0.08(4^1T_2)$	3.70		$5.12*10^{-3}$
$13T_2$	$0.30(3^3E)$, $0.24(5^3T_2)$, $0.15(2^3E)$ $0.06(3^1T_2)$	3.75		$6.13*10^{-3}$
$14T_2$	$0.69(3^1T_2)$	3.91 (-0.37)	4.28	$3.87*10^{-2}$
$15T_2$	$0.24(2^3A_2)$, $0.18(4^3T_2)$, $0.17(6^3T_2)$ $0.11(2^3E)$, $0.06(4^1T_2)$	3.94		$5.22*10^{-3}$
$27T_2$	$0.67(5^3E)$, $0.28(7^1T_2)$	5.13	4.96	$1.06*10^{-1}$
$28T_2$	$0.66(7^1T_2)$, $0.27(5^3E)$	5.21 (+0.25)		$2.52*10^{-1}$
$29T_2$	$0.87(8^3T_2)$, $0.09(8^1T_2)$	5.59		$9.05*10^{-2}$
$30T_2$	$0.90(8^1T_2)$	6.01		$8.06*10^{-1}$
average descrepancy		0.22		

[a] Excited states whose oscillator strength is larger than 0.005.

[b] Dominant configurations and square values of the coefficients are listed for those square values are larger than 0.1. At least, components of singlet T_2 states are listed for triplet dominant states.

[c] Deviation from experimental values

[d] Reference 2

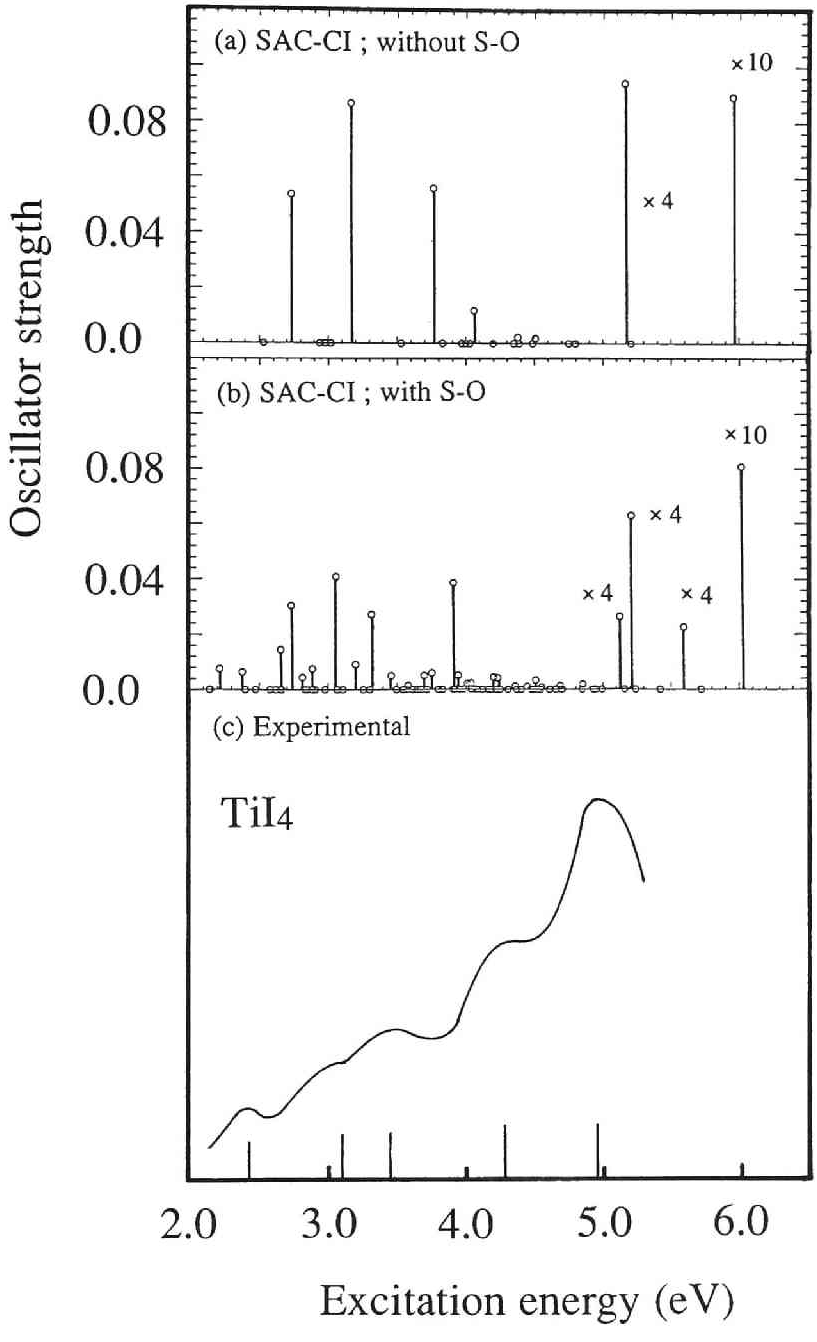

FIG. 2. Theoretical excitation spectrum of TiI_4 (a) without including spin-orbit interaction, (b) with including spin-orbit interaction, and (c) experimental excitation spectrum.[2]

through the second order perturbation of spin-orbit interaction, which improve the calculated values. $27T_2$ and $28T_2$ states calculated at 5.13 and 5.21 eV are attributed to the forth band whose peak maximum is observed at 4.96 eV. These states are generated by the interaction of 7^1T_2 and 5^3E states. $30T_2$ state with large oscillator strength ($8.06*10^{-1}$) is calculated at 6.01 eV. Experimental spectrum has no information around this energy region.

All observed peaks are assigned to T_2 states whose oscillator strengths are larger than 10^{-2}. However, there exist a number of T_2 states which have certain oscillator strengths around these states. These T_2 states cooperatively contribute to the absorption bands. In this way, the excitation spectrum of TiI_4 should be assigned with including the spin-orbit interaction. The average discrepancy between theory and experimental values is 0.22 eV

E. Comparison of the excited states of TiX_4

Figure 3 show the energy diagram for TiX_4 system (X= Cl, Br, I) based on the present and previous assignments. Ionization potentials of Ti^+ and halogen atoms are also given. We show simple and useful picture of the valence excitations of these molecules using the experimental values.[2,4,5] For $TiBr_4$ and TiI_4, all states are considered without spin-orbit interaction by using the average of corresponding states.

The term values of (2e) and ($4t_2$) are almost same for all the TiX_4 species, since 2e and $4t_2$ MO's are composed mainly by Ti d-AO. Therefore, the shift of excitation energy accompanied by the substitution of the ligands is explained by the difference of the IP's of TiX_4 species, which is parallel to that of the IP's of the ligand halogens as seen in fig. 3. According to the present assignments, term values of (2e) and ($4t_2$) for $TiCl_4$ are estimated as 7.4 and 6.5 eV, if we use the experimental values. The (2e)-($4t_2$) splitting is estimated as 0.9 eV, which is only a half of that estimated by Robin.[1] He noted splitting value is about twice larger than that is normally seen in tetrahedral species and therefore, our assignments would to be reliable. Another suggestion from the present analysis is about the excitation spectra of TiI_4, in which the peak for $8T_2$ state is not observed. Admitting our assignments of first and second peak, $7T_2$ and $8T_2$ should be located 4.8 and 5.4 eV above the ground state. Therefore, the experimental spectrum has the possibility of missing $8T_2$ state.

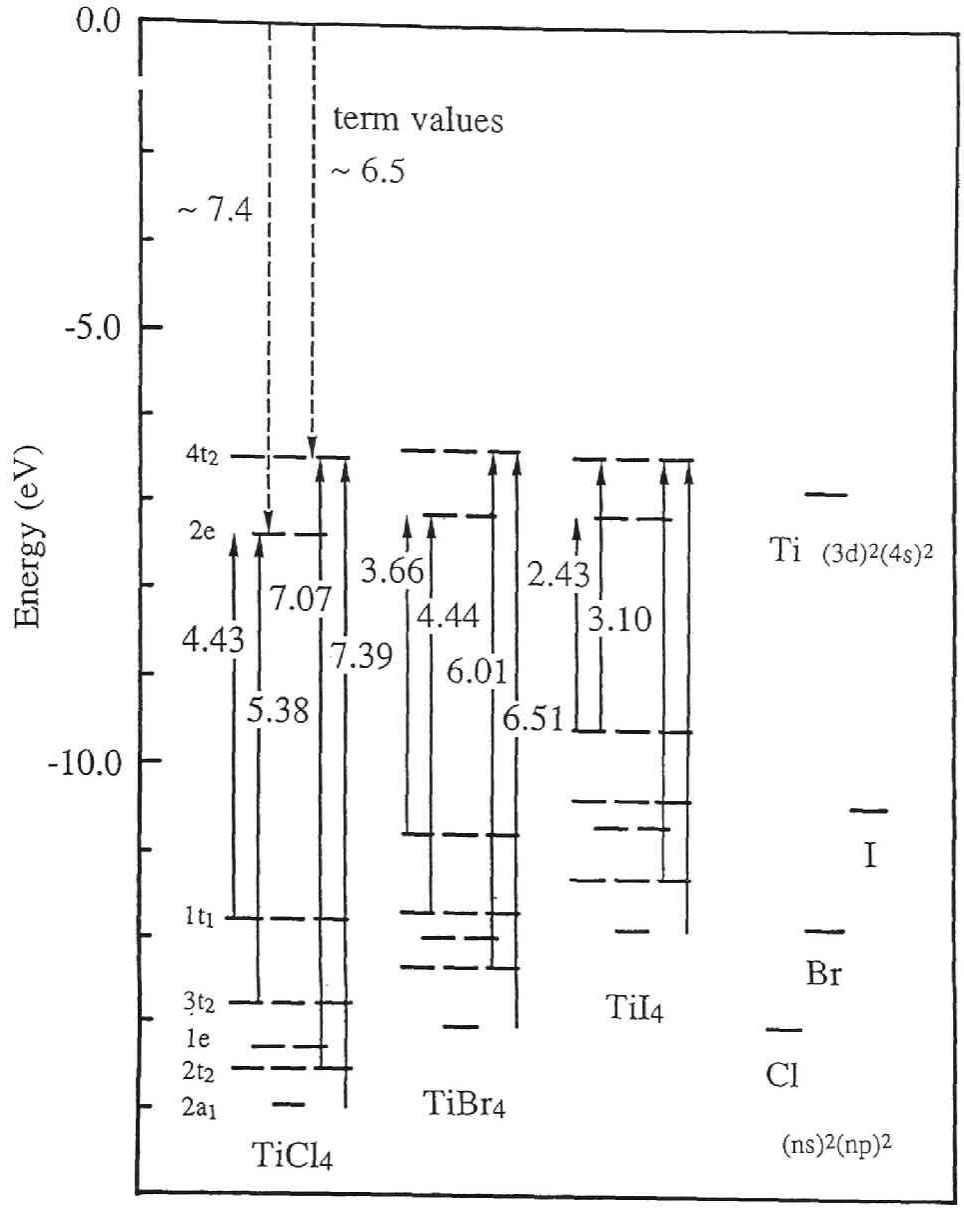

FIG. 3. Schematic energy diagram of TiX_4 (X=Cl, Br, I). Assignments of the present study are shown with experimental excitation energies (in eV). Experimental values are cited from references 2, 3, and 6a.

Since the $1T_2$ and $2T_2$ states are characterized as $1t_1 \rightarrow 2e$ and $1t_1 \rightarrow 4t_2$, energy separation between these states gives the $(2e)$-$(4t_2)$ separation. In the present calculation, e-t_2 separations are estimated as to be 0.80, 0.53, and 0.43 eV for $TiCl_4$, $TiBr_4$, and TiI_4, respectively. The splitting reduces as the ligand becomes soft. This fact is related to the IP's of the ligands.

V. IONIZED STATES

Ionization spectra of TiX_4 are divided into outer and inner valence region.[5] In the outer valence region, there are five different electronic states; namely, $(1t_1)^{-1}$, $(3t_2)^{-1}$, $(1e)^{-1}$, $(2t_2)^{-1}$, and $(2a_1)^{-1}$ states. These states lie in a low energy region and do not interact with the shake-up states. Therefore, Koopmans picture is valid for these states. On the other hand, $(1a_1)^{-1}$ and $(1t_2)^{-1}$ states correspond to the ionizations from the ns orbitals of the ligands and are located in the inner valence region. These states interact with many two electron shake-up processes through final state correlation and show breakdown of Koopmans picture. Calculated splitting pattern in the inner valence region of $TiBr_4$ and TiI_4 is similar to that of $TiCl_4$.[5] In this paper, we concentrate our discussion on the assignments of the outer valence region.

The experimental ionization spectra of TiX_4 (X=Br, I) have complicated structure compared to that of $TiCl_4$ even in the outer valence region. This is due to the spin-orbit interaction in the ligands and the Jahn-Teller distortion. We examine the former effect, which is lager than the latter, in the present study. With the inclusion of the spin-orbit interaction, doublet ionized states in the Td point group are transformed into the states in spinor double group Td* as follows:[4,23]

$^2A_1 \rightarrow E'(2)$

$^2A_2 \rightarrow E''(2)$

$^2E \rightarrow U'(4)$

$^2T_1 \rightarrow U'(4), E'(2)$

$^2T_2 \rightarrow U'(4), E''(2)$

where the numbers in the parentheses shows the degree of degeneracy.

Theoretical outer valence ionization potentials of TiX_4 (X=Br, I) are compared with the experimental values in Tables VIII and IX. Monopole intensities and the weight of degeneracy are also given. Theoretical IP's are given with including first

TABLE VIII. Outer valence ionization potential of $TiBr_4$ (in eV).

	Exptl.[a]				SAC-CI						
	ΔE	Assignment by EHMO	Band area He(I)	Band area He(II)	ΔE[b]	ΔE (S-O(1)[b])	ΔE (S-O(2)[c])	Δ[d]	Assignment	(Degeneracy)	Intensity[e]
a	10.55 10.63	U'($t_1(\pi)$)	2.0	2.0	10.13	10.050	10.039	-0.51	U'($1t_1^{-1}$)	(4)	0.94
b	10.86	E'($t_1(\pi)$)	1.0	1.3		10.290	10.277	-0.57	E'($1t_1^{-1}$)	(2)	
c	11.68	U'($t_2(\pi)$)	2.5	3.0	11.51	11.461	11.444	-0.24	U'($3t_2^{-1}$)	(4)	0.92
		E''($t_2(\sigma)$)				11.609	11.576		E''($3t_2^{-1}$)	(2)	
d	12.00	U'($t_2(\sigma)$)	5.1	7.6	11.96	11.960	11.940	-0.06	U'($1e^{-1}$)	(4)	0.92
	12.31	E''($t_2(\pi)$)			12.28	12.280	12.313	+0.00	E''($2t_2^{-1}$)	(2)	0.90
	12.42 12.55(s)	U'($e(\pi)$)				12.281	12.328	-0.09	U'($2t_2^{-1}$)	(4)	
e	13.04	E'($a_1(\sigma)$)	0.7	1.2	12.64	12.640	12.653	-0.39	E'($2a_1^{-1}$)	(2)	0.91
average descrepancies								0.27			

[a] Reference 3
[b] Without spin-orbit correction
[c] First order correction is included. see text.
[d] First and second order correction is included. see text.
[e] Deviation from the experimental value
[f] Monopole intensities without including initial state correlation.

TABLE IX. Outer valence ionization potential of TiI_4 (in eV).

	Exptl.[a]				SAC-CI						
	ΔE	Assignment by EHMO	Band area He(I)	He(II)	ΔE[b]	ΔE (S-O(1)[b])	ΔE (S-O(2)[c])	Δ[d]	Assignment	(Degeneracy)	Intensity[e]
a	9.22(s) 9.32	U'($t_1(\pi)$)	2.0	2.0	8.82	8.657	8.619	-0.60	U'($1t_1^{-1}$)	(4)	0.94
b	9.77	E'($t_1(\pi)$)	1.1	1.3		9.145	9.102	-0.67	E'($1t_1^{-1}$)	(2)	
c	10.23(s)	E''($t_2(\sigma)$)	5.2	9.2	10.24	10.113	10.064	-0.17	U'($3t_2^{-1}$)	(4)	0.92
	10.45	U'($t_2(\pi)$)				10.494	10.363	-0.09	E''($3t_2^{-1}$)	(2)	
	10.68	U'($t_2(\sigma)$)			10.56	10.560	10.490	-0.19	U'($1e^{-1}$)	(4)	0.92
d	11.19(s)	E''($t_2(\pi)$)	3.4	5.8	10.93	10.879	11.010	-0.18	E''($2t_2^{-1}$)	(2)	0.90
	11.34	U'($e(\pi)$)				10.956	11.111	-0.23	U'($2t_2^{-1}$)	(4)	
e	11.92	E'($a_1(\sigma)$)	0.9	1.7	11.59	11.590	11.613	-0.30	E'($2a_1^{-1}$)	(2)	0.91
average descrepancies							0.30				

[a] Reference 3
[b] Without spin-orbit correction
[c] First order correction is included. see text.
[d] First and second order correction is included. see text.
[e] Deviation from the experimental value
[f] Monopole intensities without including initial state correlation.

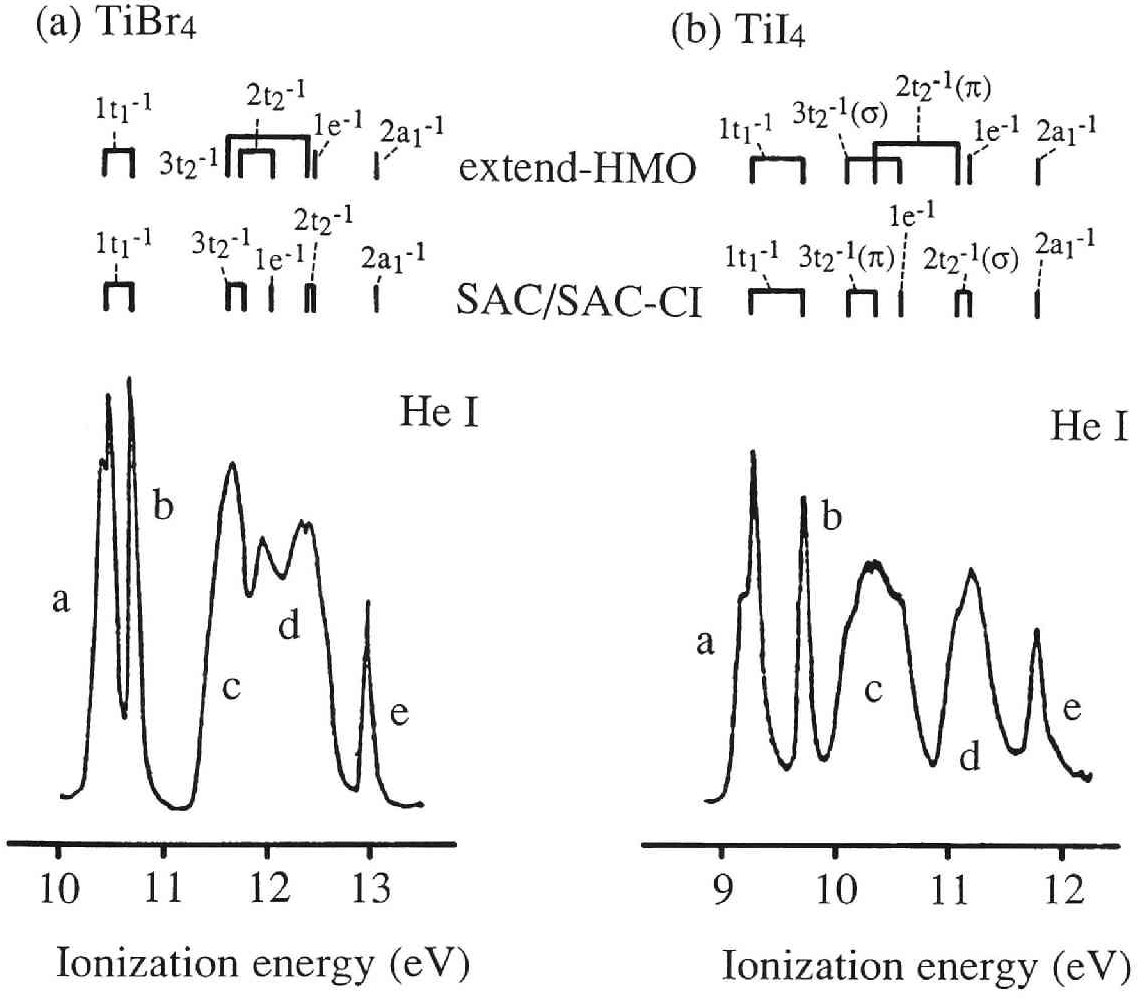

FIG. 4. Ionization spectra in the outer valence region and their theoretical assignments of (a) $TiBr_4$ and (b) TiI_4.

TABLE X. Spin-orbit splitting of the $^2T_1$ and $^2T_2$ states of TiX_4 (X=Br,I) (in eV).

State	$TiBr_4$				TiI_4		
	Exptl.		Calc.		Exptl.[b]	Calc.	
	Edgell[a]	Green[b]	S-O (1)[c]	S-O (2)[d]		S-O (1)[c]	S-O (2)[d]
$(1t_1)^{-1}$	0.24	0.23, 0.25[e]	0.240	0.238	0.45, 0.54[e]	0.488	0.482
$(3t_2)^{-1}$	0.10	-	0.148	0.133	0.22	0.381	0.289
$(2t_2)^{-1}$	-0.15	-0.11	-0.001	-0.014	-0.15	-0.077	-0.102

[a] Reference 3
[b] Reference 4
[c] First order correction is included. see text.
[d] First and second order correction is included. see text.
[e] Splitting due to vibronic coupling

and up to second order effect of spin-orbit interaction as S-O(1) and S-O(2), respectively. The present assignments of the spectra are schematically shown with the experimental spectra in Fig. 4. The calculated spin-orbit splitting values of the $^2T_1$ and $^2T_2$ states are summarized in Table X. The splitting pattern of the triply degenerated states, $^2T_1$ and $^2T_2$, is as follows; the U' state is more stable than the E' and E" states in the case of $(1t_1)^{-1}$ and $(3t_2)^{-1}$ states, because they are all hole states. However, the ordering between U' and E" state is reversed in the $(2t_2)^{-1}$ state.

A. $TiBr_4$

Here we discuss the outer valence region of $TiBr_4$. Edgell et al. assigned their experimental photoelectron spectra of TiX_4 (X=Br, I) using extend Hückel MO's.[3] Following the notation of experimental spectrum,[3] band a and b are assigned to U' and E' states split from $(1t_1)^{-1}$ state. The spacing between these components is calculated to be 0.238 eV, which is in good agreement with the experimental value 0.24 eV. As for band c, the relative intensity of the experimental spectrum indicates that this band is composed of four-hold states and two-hold states. $U'(3t_2^{-1})$ and $E'(3t_2^{-1})$ components correspond to this band in our calculation. Edgell et al. assigned this band to $U'(3t_2^{-1}(\pi))$ and $E'(2t_2^{-1}(\sigma))$ states. Our assignment is different from theirs since our estimated splitting value of $(3t_2)^{-1}$ state (0.133 eV) is smaller than theirs. The reason of this contradiction will be discussed in later. In the same way, we propose different assignment for band d; U'(1e), $E'(2t_2^{-1})$ and $U'(2t_2^{-1})$ states contribute to this overlapping band. Band e is attributed to the $E'(2a_1^{-1})$ state. Relative intensity of band d and e show remarkable increase under He(II) excitation in the experimental spectra. It is reported that the ionizations from the MOs having metal s or d components have large cross sections under the He(II) excitation.[3,6f] Accordingly, 1e and $2t_2$ orbitals has metal d character and $2a_1$ orbital has metal s character.

In summary, the present assignments are different from theirs in the following two points:

(1) the ordering of the $(1e)^{-1}$ and $(2t_2)^{-1}$ states.

(2) the spin-orbit splitting of the $(3t_2)^{-1}$ and $(2t_2)^{-1}$ states.

The difference between two assignments are clearly shown in Figure 4 and Table VIII. As discussed in the previous paragraph, our assignments are consistent with the

experimental spectra in the following points. (a) The weight of degeneracy in our assignment explains the ratio of the relative band area. (b) The change in the ionization cross section for each band under He(II) excitation is consistent with our results. (c) The average discrepancy between theory and experiment for the ionization spectra of $TiBr_4$ is only 0.27 eV

Next we analyze the effect of spin-orbit interaction stepwisely. We firstly investigate the first order effect which determines a large part of the spin-orbit splitting. It is well-known that the first order effects of the spin-orbit interaction on the T_2 and T_1 terms are similar to that on the P term. In this sense, Green et al. proposed an explicit form of the effective S-O coupling constants ζ_{eff} as[4]

$$\zeta_{t2} = C_{t2p}^2\zeta^M_p - C_{t2d}^2\zeta^M_d + \frac{1}{2} C'_{t2\pi}(C'_{t2\pi} - 2\sqrt{2}\, C'_{t2\sigma})\zeta^L_p$$

$$\zeta_{t1} = \frac{1}{2} (1+\chi_{t1\pi})^{-1}\zeta^L_p$$

$$C'_{t2k} = (1+\chi_{t1k})^{-1/2}C_{t2k}$$

where ζ^M_p, ζ^M_d, and ζ^L_p denote the spin-orbit coupling constants for the valence p and d orbitals of the metal atom M and the ligand L. C and χ are the MO coefficients and the overlap term, respectively. Though our approach is apart from these coupling constants, interpretation of the spin-orbit splitting is performed with these useful constants. According to these effective coupling constants, ζ_{t1} is approximated as $\frac{1}{2}$ ζ^L_p and our calculation also reproduce t_1 splitting (0.238 eV for $TiBr_4$). This is also obtained in the previous studies.[3,4] On the other hand, our estimation of the splitting of the $(3t_2^{-1})$ state is different from the previous one as mentioned above. Edgell et al. calculated the splitting value fairly large for this state. This is because their $3t_2$ MO is composed of both σ and π components of the ligand p-AO's.(see Appendix B of ref.4). We examine the nature of the $3t_2$ MO for the AB_4 system as shown in Appendix B and find that the $3t_2$ MO of TiX_4 (X=Br, I) has pure π components. Therefore, our estimated splitting values are relatively small compared to the previously estimated ones. However, the nature of the $3t_2$ MO is somewhat dependent on the basis set used, so that the estimation of the spin-orbit splitting for the t_2 symmetry is very delicate.[23] In the same way, the $2t_2$ MO has pure σ-bonding nature between metal and ligand.

Therefore, the third term in the ζ_{t2} becomes small and has negative sign, resulting the ordering between the E and U states being reversed. The effect of d-AO on Ti atom are small since the valence MO is dominated by ligands and the coupling constant ζ^{M}_{d} is small (0.073 eV).

Secondly, we consider the effect of the second order correction, that is the interaction between different irreducible representations of the Td point group, but the same ones in the Td* group. With this interaction, the $(1t_1)^{-1}$ and $(3t_2)^{-1}$ states are stabilized, while the other states are destabilezed. Energy perturbations for the U' states are smaller than those for the E' and E" states. Therefore, the E' state is stabilized compared to the U' state with the result that the splitting of the $(1t_1)^{-1}$ state becomes small. On the other hand, the E" state split from the $(2t_2)^{-1}$ state is calculated unstable compared to the U' state. This second order interaction works to destabilized these states. So the splitting of the $(2t_2)^{-1}$ state is enlarged through this interaction.

B. TiI_4

The ordering of the outer valence ionization potentials of TiI_4 is also the same as that of $TiCl_4$.[5] Band a, b are assigned to U' and E' $(1t_1^{-1})$ states with the spin-orbit splitting calculated as 0.482 eV. The splitting of band a is due to the Jahn-Teller distortion as reported by Edgell et al[3] Band c is composed of one four-hold states and one two-hold state from the consideration of the relative band area. We assign $(3t_2)^{-1}$ and $(1e)^{-1}$ states to this band. Split band d is attributed to $(2t_2)^{-1}$ state. The separations between U' and E" are small compared to the previous studies as explained in $TiBr_4$. Band e correspond to $(2a_1)^{-1}$ state. All the calculated ionization potentials underestimate the experimental values, especially for $(1t_1)^{-1}$ and $(2a_1)^{-1}$ states. The average discrepancy between theory and experiment for the ionization potentials of TiI_4 is 0.30 eV

VI. SUMMARY

Theoretical study of the excited and ionized states of TiX_4 (X=Br, I) are reported based on the SAC and SAC-CI theories. The effects of spin-orbit interaction of the ligand p-AO and Ti d-AO are examined both for the excited and ionized states.

Excitation spectra in the valence region are investigated and theoretical

assignments are proposed. Lowest 49 states are calculated in the valence region; namely two A_1, two A_2, five E, seven T_1 and eight T_2 states for singlet and triplet states. With including the spin-orbit effect, these states split into nine A_1, ten A_2, twenty E, thirty T_1 and T_2 states. Dipole-allowed T_2 states are generated from $^3A_2$, ^3E, $^3T_1$, and $^3T_2$ states and have certain oscillator strengths through the interaction with $^1T_2$ states. This effect is important especially for TiI_4 molecule. The shift of excitation energies according to the substitutions of the ligands is explained by the shift in the ionization potentials of these molecules. Furthermore, the change in the ionization potentials of TiX_4 is explained by that of the ligand atom. Theoretical results reproduce well the experimental spectra with the average discrepancies of 0.09 and 0.22 eV for $TiBr_4$ and TiI_4, respectively.

The present results also show good agreements with the experimental ionization spectra in the outer valence region. The ordering of the ionized states in the outer valence region is $(1t_1)^{-1} < (3t_2)^{-1} < (1e)^{-1} < (2t_2)^{-1} < (2a_1)^{-1}$, which is the same as that of $TiCl_4$.[5] Koopmans picture is valid for these states. The spin-orbit splitting of the peak in the present calculation explains the ratio of the relative band area in the experimental spectra. The change in the ionization cross section observed in the He(I) and He(II) excitation spectra is also consistent with our results. The spin-orbit splitting of the $^2T_2$ states is related to the natures of the ionized MO's. In the case of TiX_4 (X=Br,I) system, $2t_2$ MO has pure σ-bonding nature, while $3t_2$ MO is pure π-bonding between metal and ligand. Therefore, our estimated splitting values are relatively small compared to the previous study.[3]

ACKNOWLEGMENTS

The calculations have been carried out with the FACOM M780 computer at the Data Processing Center of Kyoto University and the HITAC M-680H and S-820 computer at the Institute for Molecular Science. This study has been supported by the Grant-in-Aid for Scientific Research from the Japanese Ministry of Education, Science, and Culture.

Appendix A.

The calculation of spin-orbit interaction is performed using one-electron one-

center approximation. We neglect spin-other-orbit terms and cross-integrals on different centers. The expression of the spin-orbit hamiltonian is

$$H_{IJ} = E_I \delta_{IJ} + < I \mid H^{so} \mid J >$$

$$H^{so} = \sum_i \sum_A \zeta(r_{iA})\, l_{iA}\, s_i$$

where $\zeta(r_{iA})$ is the spin-orbit coupling constants of atom A and l_{iA} denote the orbital angular momentum operator centered at atom A for i-th electron. E_I is the SAC-CI energy and the matrix element $< I \mid H^{so} \mid J >$ is calculated considering the spin-orbit interaction of the titanium d-AOs and the ligand p-AOs. All the symmetries of the sub-group C_{2v} are included for the state functions because of the degeneracy in the Td point group. State functions I, J are approximated by the singly excited configuration part of the excited state and by the Koopmans state for the ionized states. For valence excitations, the squares of the norms of the singly excited part in the linked terms are 0.95-0.93. The calculated monopole intensities are also large (0.94-0.90) for the ionized states in the outer valence region as shown in Tables VIII and IX. These facts support the validity of the present approximation in the calculation. The spin-orbit coupling constants are estimated from the experimental spectral data;[20] those of the 3d AO of Ti^+, 4p AO of Br, and 5p AO of I are 0.011, 0.305, and 0.628 eV, respectively.

Appendix B.

The spin-orbit splitting values for the $(2t_2)^{-1}$ and $(3t_2)^{-1}$ states of TiX_4 are estimated rather small in comparison with those in the previous works.[3,4] Since the present system shows complicated splitting structure, we refer to the ionization spectra of CBr_4 and $SiBr_4$. The splitting pattern of these molecules is clear because $2a_1$ and $2t_2$ orbitals are dominated by 2s and 2p AOs of the central carbon atom. The experimental photoelectron spectra for those molecules show large splitting for $(3t_2)^{-1}$ state (about 0.45 eV). Therefore, we examine the spin-orbit splitting of $^2T_1$ and $^2T_2$ terms for CBr_4 and $SiBr_4$. Results are summarized in Table XI.

The splitting value of the $(3t_2)^{-1}$ state of CBr_4 is calculated as 0.451 eV in good

agreement with the experimental value 0.46 eV.[4] The splitting values of CBr_4 are calculated so large compared to those of $TiBr_4$ system. We explain this fact in terms of the bonding natures of the ionized MO. The $2t_2$ and $3t_2$ MOs of CBr_4 molecule are C-L bonding and ligand non-bonding MO, respectively, like TiX_4 system. However, π- and σ- components of the ligand p-AOs mix in both MOs of CBr_4. In other words, both $2t_2$ and $3t_2$ MOs of CBr_4 still keeps the degeneracies of the p-AO of the bromine atom. Therefore, as seen from the expression of the effective coupling constant in the text, the splittings of the $(2t_2)^{-1}$ and $(3t_2)^{-1}$ states of CBr_4 becomes large. The same is true for the spin-orbit interaction of $SiBr_4$. On the other hand, $2t_2(3t_2)$ MO of TiX_4 has pure $\sigma(\pi)$ components of the ligand AOs, therefore, the splitting of the T_2 term becomes small. Thus, we see that the difference in the spin-orbit splitting between $TiBr_4$ and CBr_4 comes from their difference in the bonding character.

TABLE XI. Spin-orbit splitting of the $^2T_1$ and $^2T_2$ states of ABr_4 (A=C, Si) (in eV).

	CBr_4		$SiBr_4$	
State	Exptl.[a]	Calc.[b]	Exptl.[a]	Calc.[b]
$(1t_1)^{-1}$	0.26, 0.35[c]	0.270	0.27, (0.36)[c]	0.255
$(3t_2)^{-1}$	0.46, 0.64[c]	0.451	0.42, 0.53[c]	0.389
$(1t_1)^{-1}$		-0.091	-	-0.124

[a] Reference 4
[b] First and second order correction is included. see text.

REFERENCES

[1] M. B. Robin, *Higher Excited States of Polyatomic Molecules* (Academic, New York, 1975), Vol. 2.

[2] L. DiSipio, G. DeMichelis, E. Tondello and L. Oleari, Gazz. Chim. Ital. **96**, 1785 (1966).

[3] R. G. Egdell and A. F. Orchard, J. Chem. Soc. Faraday Trans. 2 **74**, 485 (1978).

[4] J. C. Green, M. L. H. Green, P. J. Joachim, A. F. Orchard and D. W. Turner, Phil. Trans. Roy. Soc. Lond. **A268**, 111 (1970).

[5] H. Nakatsuji, M. Ehara, M. H. Palmer and M. F. Guest, J. Chem. Phys. **97**, 2561 (1992).

[6] (a) C. A. Becker, C. J. Ballhausen, and I. Trabjerg, Theoret. Chim. Acta **355**, 13 (1969);
(b) John S. Tse, Chem. Phys. Lett. **373**, 15 (1981);
(c) A. A. Inverson and B. R. Russell, Spectrochimica Acta **A29**, 715 (1973);
(d) Aniko E. Foti, Vedene H. Smith, Jr., and M. A. Whitehead, Mol. Phys. **45**, 385 (1982);
(e) W. von Niessen, Inorg. Chem. **26**, 567 (1987);
(f) G. M. Bancroft, E. Pellach, and J. S. Tse, Inorg. Chem. **21**, 2950 (1982).

[7] (a) Y. Morino, U. Uehara, J. Chem. Phys. **45**, 4543 (1966);
(b) M. F. A. Dove, J. A. Creighton and L. A. Woodward, Spectrochim. Acta **18**, 267 (1962);
(c) J. K. Wilmshurst, J. Mol. Spectr. **5**, 343 (1960).

[8] H. Nakatsuji and K. Hirao, J. Chem. Phys. **68**, 2053 (1978).

[9] H. Nakatsuji, Chem. Phys. Lett. **59**, 362 (1978); **67**, 329, 334 (1979).

[10] H. Nakatsuji, Acta Chim. Hungarica **129** 719 (1992).

[11] H. Nakatsuji and S. Saito, J. Chem. Phys. **91**, 6205 (1989).

[12] H. Nakatsuji and S. Saito, Intern. J. Quantum Chem. **39**, 93 (1991).

[13] H. Nakai, Y. Ohmori, and H. Nakatsuji, J. Chem. Phys. **95**, 8287 (1991).

[14] H. Nakatsuji and M. Ehara, J. Chem. Phys. **98**, 7179 (1993).

[15] S. Huzinaga, J. Andzelm, M. Klobukowski, E. Radzio-Andzelm, Y. Sakai and H. Tatewaki, *Gaussian basis sets for molecular calculations* (Elsevier, Amsterdam, 1984).

[16] P. J. Hay and W. R. Wadt, J. Chem. Phys. **82**, 299 (1985).

[17] H. Nakatsuji, Chem. Phys. **75**, 425 (1983).

[18] M. Dupuis, J. D. Watts, H. O. Viller, and G. J. B. Hurst, Program System HONDO7, Program Library No. 544, Computer Center of the Institute for Molecular Science, (1989).

[19] H. Nakatsuji, Program system for SAC and SAC-CI calculations, Program Library No.146(Y4/SAC), Data Processing Center of Kyoto University, 1985;

H. Nakatsuji, Program Library SAC85 (No.1396),
Computer Center of the Institute for Molecular Science, Okazaki, 1986.

[20] (a) Nakatsuji, Y. Matsuzaki, and T. Yonezawa, J. Chem. Phys. **88**, 5759 (1988);
(b) C. A. Masmanidis, H. H. Jaffe, and R. L. Ellis, J. Phys. Chem. **79**, 2052 (1975);
(c) S. Kato, R. L. Jaffe, A. Komornicki, and K. Morokuma, J. Chem. Phys. **78**, 4567 (1983).

[21] C. J. Ballhausen and H. B. Gray, *Molecular Orbital Theory*
(Benjamine Press, Inc., New York, 1964).

[22] The 3^1A_1 state is calculated in very high energy region. To assertain this fact, we performed SE-CI calculation with the active space of 12 highest occupied MOs and 5 lowest unoccupied MOs for $TiBr_4$ molecule. In that SE-CI calculation, the 8^1T_2 state is calculated at 8.78 eV, while the 3^1A_1 state is calculated at 16.57 eV. Furthermore, small calculation with the active space I indicates that corresponding valence excited state of A_1 symmetry is located at 9.87 eV. We remove this state from the present results because (1) Rydberg states exist from 7.4 eV and (2) this state will have small effect on the other states after including the spin-orbit interactions.

[23] C. E. Moore, *Atomic Energy Levels* (National Bureau of Standards, Washington, D.C., 1971), Vol. 1, 2, 3.

[24] J. S. Griffith, *The theory of transition metal ions* (Cambrige University Press).

[25] B. D. Bird and P. Day, J. Chem. Phys. **49**, 392 (1968).

[26] The spin-orbit splitting values of the $(2t_2)^{-1}$ and $(3t_2)^{-1}$ states are dependent on the nature of the ionized MO. Firstly, we examine the effects of the polarization functions on Ti atom. We adopt the exponents of 0.09 and 0.03 proposed by Huzinaga instead of the present polarization functions. In the case of $TiBr_4$, splitting value of the $(1t_1)^{-1}$ state is calculated to be 0.238 eV, which is same as the result with the present basis sets. However, splitting values of the $(3t_2)^{-1}$ and $(2t_2)^{-1}$ states are estimated as 0.078 and 0.048 eV, respectively. Nextly, we examine the polarization function (ζ_d = 0.389) on Br atom. Splitting values are caluclated to be 0.238, 0.144, and -0.016 eV for the $(1t_1)^{-1}$, $(3t_2)^{-1}$, and $(2t_2)^{-1}$ states, respectively. The nature of MO's with t_2 symmetry seems to depend on the polarization functions of Ti atom. We believe present polarization functions are appropreate since the excitation spectrum of Ti^{3+} is well reproduced.

PART III

Theoretical Studies on the Collision Induced Absorption Spectra of CsRg System (Rg=Xe, Kr, Ar, Ne)

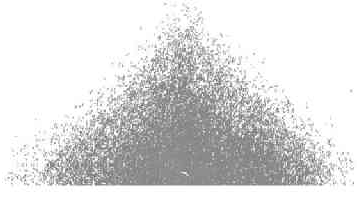

Chapter 6

Collision induced absorption spectra of CsXe system calculated by the SAC-CI method with ECP potentials

Abstract

Collision induced absorption spectra of Cs-Xe system is studied theoretically by SAC-CI (symmetry adapted cluster-configuration interaction) theory. The origin of 6S-5D dipole-induced transition is an existence of 5d Σ and 5d Π quasi-molecular states. Quasistatic model is used for calculations of reduced absorption coefficients. The calculated profiles of the collision induced absorption spectra reproduce well the experimental spectra. Since they sensitively reflect fine details of the potential energy curves of the ground and excited states, this agreement guarantees the reliability of the present theoretical potential curves of the ground and excited states of CsXe calculated by the SAC-CI method.

The optical s-s and s-d transitions of alkali atoms are dipole forbidden. However, when noble gas is admitted into alkali vapour, collisional interaction between alkali atom and noble gas makes these transitions dipole allowed and a new absorption band is observed near the position of the originally forbidden line [1-4]. This phenomena is called collision induced absorption. The position and the profile of the collision induced absorption sensitively reflect interatomic potentials of the ground and excited states of the alkali-noble gas system and the (induced) transition moments between them. We are very interested in this aspect of the collision induced absorption. Moe *et al.* [1] reported detailed absorption spectra for the Cs-noble gas and Rb-noble gas systems.

Elucidations of the mechanisms and theoretical evaluations of the line profiles have been carried out by several workers [5-11]. For Cs-Xe system, Gallagher *et al.* [6] investigated line core region by a perturbative method. Pascale *et al.* [8] calculated adiabatic potential energy curves of alkari-noble gas systems using a semiempirical model of Baylis [9] and investigated the wing region. Oscillator strengths for the induced dipole transitions were also reported by Pascale [10]. However, their calculated spectra are somewhat different from the experimental ones for the Cs-Xe system [11].

In this paper, we study the collision induced absorptions of Cs-Xe system by an *ab initio* method including electron correlations. This system shows relatively strong interactions and its spectra represent most of the features common to the alkali-noble gas systems [1]. We are interested in the Cs-Xe interactions in a relatively shorter ($R_{Cs\text{-}Xe} < 10$Å), i.e., so called wing region where van der Waals interactions, overlap interactions, and repulsive interactions cooperatively determine the interatomic potentials. We do not study very long-range ($R_{Cs\text{-}Xe} > 10$Å) interactions which are reflected in the line core region of the spectra. Since the spectral profiles depend very sensitively on the potential energy curves of the ground and excited states and on the induced transition dipole moments between them, we need a theory which is able to describe both ground and excited states in a considerable accuracy.

As such a theory we use SAC (symmetry adapted cluster) [12] and SAC-CI [13] theories. The details and the reliability of the SAC/SAC-CI method have been reported elsewhere [12-16]. The basis set we use is fairly flexible. The relativistic

effective core potential [17] is used for the cores of both the Cs and Xe atoms. The outermost nine and eight electrons of the Cs and Xe atoms, respectively, are explicitly treated. The Cs basis consists of (12s5p)/[3s4p] set of Hay and Wadt [17] augmented with a primitive (6s1p) set taken from Langhoff *et al.* [18] and three d functions whose exponents are the same as those of the outer three primitives of the [4p] set. The Xe basis set is (3s3p)/[1s2p] [17] augmented with the primitives (3s2p) of Ermler *et al.* [19] and the (2d) set of Huzinaga [20]. The final set is written as [8s5p3d] for Cs and [4s4p2d] for Xe. We select all of the 8 occupied valence orbitals ($5s_{Xe}$ $5p_{Xe}$ $5s_{Cs}$ $5p_{Cs}$ $6s_{Cs}$) and the lower 41 unoccupied orbitals as an active space. In the SAC-CI step, we do not do configuration selection for linked terms and the resultant dimensions of SAC-CI are 3961 (Σ states), 3370 (Π states) and 2788 (Δ state) for all the nuclear separations. Calculations are carried out at the Cs-Xe distances of 3.0, 3.5, 3.75, 4.0, 4.25, 4.5, 4.7, 5.0, 5.25, 5.5, 5.75, 6.0, 6.5, 7.0 and 10.0 Å. The SCF orbitals are calculated with the program GAMESS [21] and the SAC/SAC-CI calculations are performed by the program SAC85 [22]. In the quasistatic model [6, 23-25] , the reduced absorption coefficients is given by

$$\frac{k(\lambda)}{n_G n_A} = \sum_{Rc} \frac{4\pi^3}{3\lambda} | D(R_c) |^2 \left(\frac{4\pi R_c^2}{| d[Ve(R)-Vg(R)]/dR |_{Rc}} \right) \exp\left[- \frac{Vg(R_c)-Vg(\infty)}{k_B T} \right]$$

where n_G and n_A are the density of the perturber Xe and the absorber Cs, D(R) the induced transition dipole moment at the Cs-Xe distance R, and V_g and V_e the potentials of the ground and excited states, respectively. The temperature T is 371 °C according to the experimental condition of Moe *et al.*

Fig. 1 shows the potential energy curves of the Cs-Xe system calculated by the SAC-CI method. We have calculated the ground and excited states which are correlated to the 6S(ground), 6P, 5D and 7S states of the Cs atom. Within the several basis sets examined here, we failed in getting a proper ordering of the 5D and 7S states of the Cs atom. So in Fig. 1 the potantial curve of the 7sΣ state is shifted upwards, in order to avoid an overlap with the 5D state. The excitations to the 5D and 7S states are dipole forbidden in an atomic limit, but their intensities are induced through the Cs-Xe interaction. The 5D state of the Cs atom splits into Σ, Π, and Δ states by the interaction, while the 6P state into Σ and Π states. The 6pΣ and 5dΣ states have a

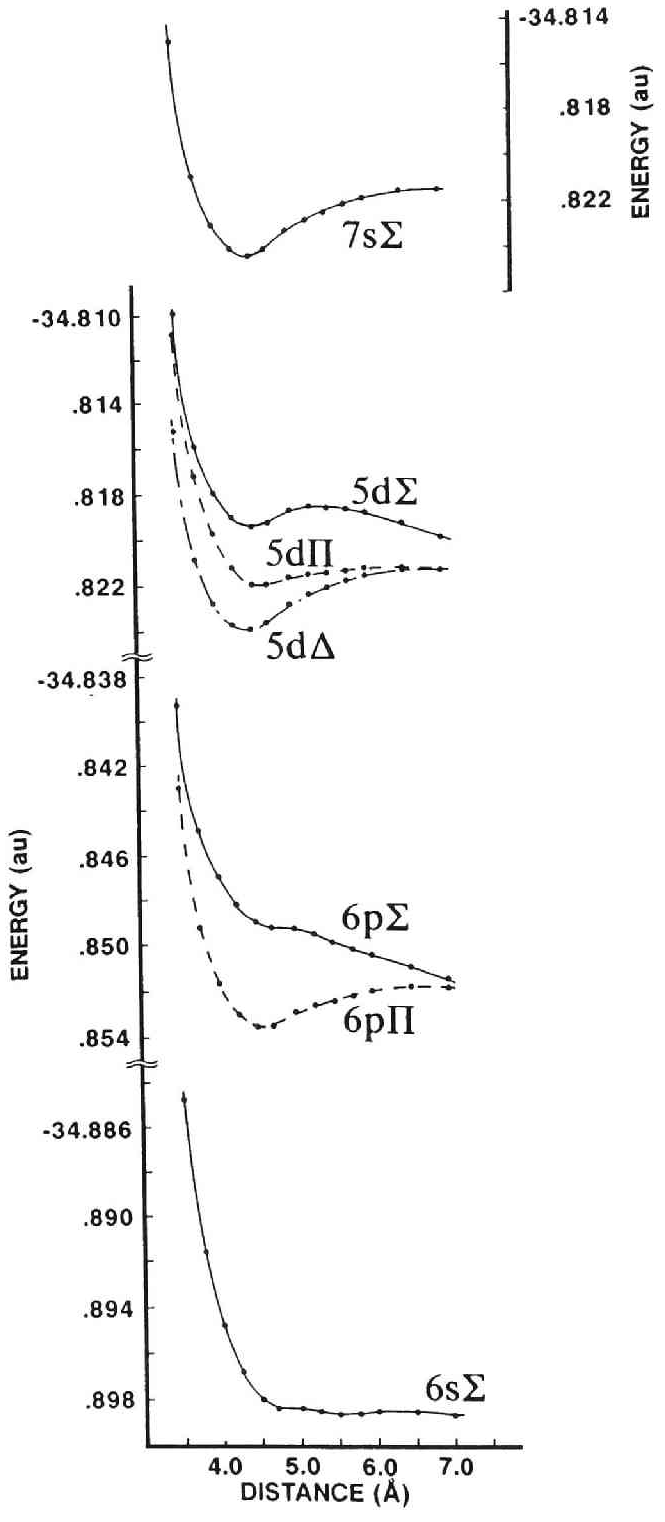

Fig. 1. Potential energy curves for the 6S, 6P, 5D and 7S states of CsXe without including spin-orbit coupling. The potential curve of the 7sΣ state is shifted upwards as noted in the text.

repulsive nature at large internuclear distances, and show a characteristic shoulder or hump near 5.0Å - 5.5Å. On the other hand, the 6pΠ, 5dΠ, 5dΔ and 7sΣ states are attractive and have a shallow minimum near 4.5Å. These two features of the potential curves are reflected in the positions and the profiles of the induced absorption spectra.

Fig. 2 gives induced dipole moments as a function of the internuclear distance. The transitions from 6sΣ to 7sΣ, 5dΣ and 5dΠ are induced at the intermediate nuclear distances of 4.3Å 7Å, since the Boltzmann factor for the ground state sharply decreases in shorter distances than 4.3Å. The 5dΔ transition is dipole-forbidden even after the interaction. The transition moment for the 5dΣ state is larger than those for the 7sΣ and 5dΠ states. This is reflected in the intensity of the observed induced absorption spectra shown below.

The present theoretical absorption spectra for the 5D states are compared in Fig. 3 with experiment. The 6S-5D transition energy of the Cs atom is calculated at 588 nm in comparison with the experimental value of 692 nm. Though this difference of 0.303 eV is not small, the essential features of the spectra seem to be properly reproduced. The experimental peak in the blue region of the atomic forbidden transition is attributed to the transition from the 6sΣ state to the 5dΣ state of the collision complex. The experimental band has a steep cusp, and correspondingly, the calculated band also shows a steep peak, which is due to the extremum in the excitation energy dependence on R. In the quasistatic theory, the absorption intensity diverges at this extremum [5,11]. Looking at the potential curves, we see that this extremum is due to the hump of the 5dΣ potential shown in Fig. 1, so that the cusp in the spectrum is assigned as being due to the hump of the 5dΣ potential. In the theoretical spectra, R denotes, in a classical picture, a internuclear distance of the collision complex at which the absorption of the light of a given wavelength occurs. The experimental spectra has a broad shoulder at 650 - 670 nm, but the theoretical spectra does not have such a feature. So we do not know the origin of this shoulder. Though the calculated intensity of the spectra is about a order of magnitude smaller than the experimental one, the experimental determination of the intensity itself is rather difficult. Our intensity is similar to the theoretical one due to Sayer *et al.* [11].

The present result shows that the 6sΣ-5dΠ transition would appear in a red region of the atomic forbidden absorption. The calculated profile shown in the right-hand

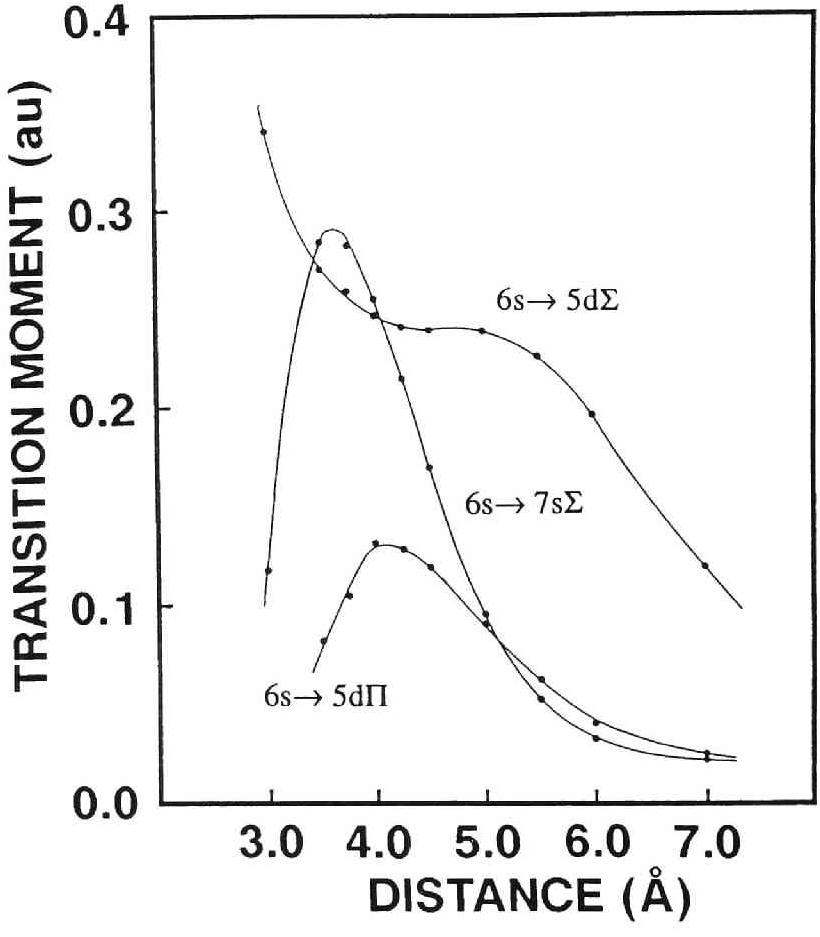

Fig. 2. Dependence of transition dipole moments on the CsXe distance for the 6S-7S and 6S-5D transitions.

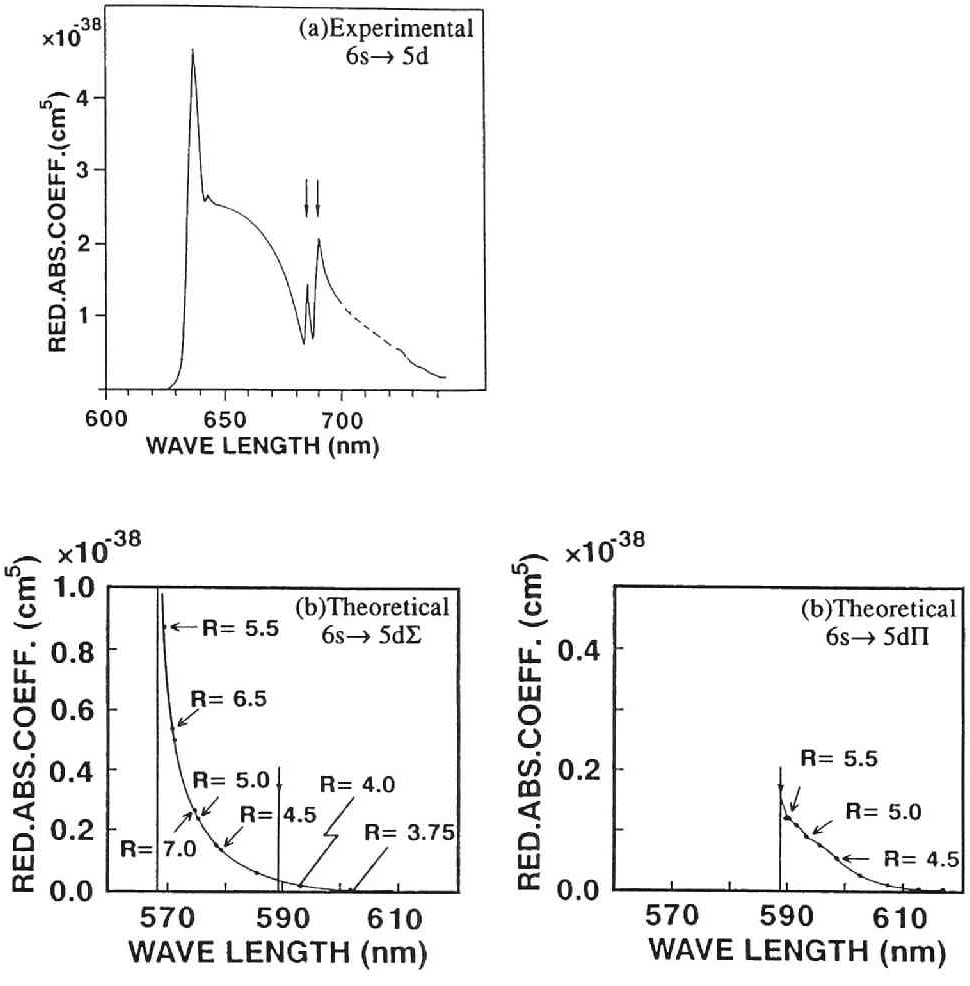

Fig. 3. (a) Experimental [1] and (b) theoretical reduced absorption coefficients for the 6S-5D transitions. In the theoretical spectra, R denotes the Cs-Xe distance in Å.

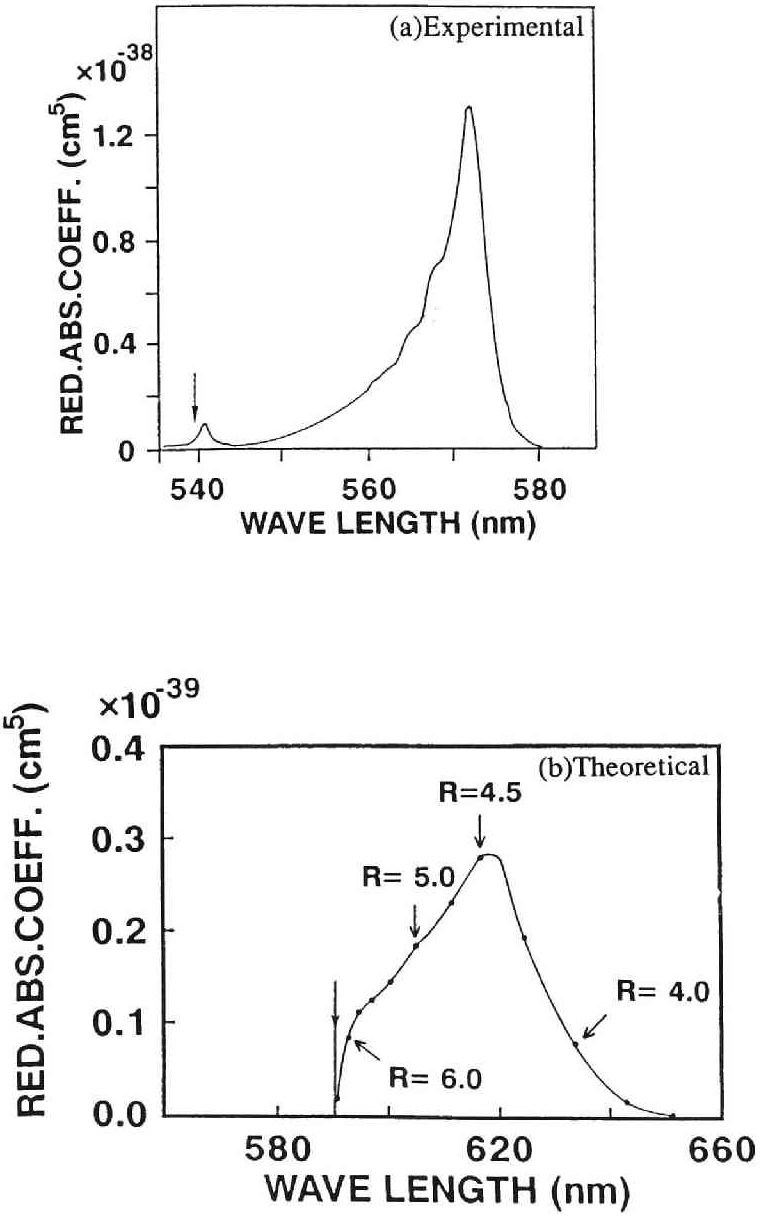

Fig. 4. (a) Experimental [1] and (b) theoretical reduced absorption coefficients for the 6S-7S transition. In the theoretical spectrum, R denotes the Cs-Xe distance in Å.

side of Fig. 3 compare well with the experimental profile observed in the red region of the forbidden line shown by the arrows (two arrows indicate spin-orbit splitting). In this red region, the 6sΣ-5dΣ transition also contributes as shown in the left-hand side of Fig. 3. However, the absorption intensity of this transition in the red region is small because the Boltzmann factor of the ground state in the region R < 4.0Å is very small. The experimental profile is the sum of the 6sΣ-5dΠ and 6sΣ-5dΣ transitions, the former being the main contribution.

In Fig. 4 we compare the experimental and theoretical collision induced absorption spectra associated to the 6S-7S transition of the Cs atom. The experimental spectrum [1] has a vibrational structure which indicates an existence of an attractive potential well for the excited state. The depth of the potential well of the 7sΣ state shown in Fig. 1 is 0.078 eV. The position of the calculated atomic forbidden transition differs by 0.196 eV from the experimental value. Both experimental and theoretical induced absorptions appear in the red region of the atomic transition, though the shapes of the profiles are somewhat different. The induced transition moment should increase more rapidly as the Cs-Xe distance becomes smaller. In shorter distances, the Boltzmann factor of the ground state rapidly diminishes, so that the induced absorption intensity falls off very rapidly.

More details of the present study and the results for the 6S→6P transitions will be published elsewhere in the literature.

Acknowledgments

The conversations with Prof. Y. Sato of Tohoku University were stimulating for this study. The calculations have been carried out with the FACOM M780 computer at the Data Processing Center of Kyoto University and the HITAC M-680H computer at the Institute for Molecular Science. This study has been supported by the Grant-in-Aid for Scientific Research from the Japanese Ministry of Education, Science, and Culture, and by the Kurata Foundation.

References

[1] G. Moe, A. C. Tam and W. Happer, Phys. Rev. **A14** (1976) 349.

[2] A. C. Tam, G. Moe, B. R. Bulos and W. Happer, Opt. Commun. **16** (1976) 376.

[3] A. C. Tam, G. Moe, W. Park and W. Happer, Phys. Rev. Letter **35** (1975) 85.

[4] R. T. M. Su, J. W. Bevan and R. F. Curl Jr., Chem. Phys. Lett. **43** (1976) 162.

[5] For review articles, see, J. F. Kielkopf and N. F. Allard, Rev. Mod. Phys. **54** (1982) 1103. ; P. R. Brooks, Chem. Rev. **88** (1988) 407.

[6] Alan Gallagher and T. Holstein, Phys. Rev **16** (1977) 2413.

[7] G. Alber and J. Cooper, Phys. Rev. **A33** (1986) 3084.

[8] J. Pascale and J. Vandeplanque, J. Chem. Phys. **60** (1974) 2278.

[9] W. E. Baylis, J. Chem. Phys. **51** (1969) 2665.

[10] J. Pascale, J. Chem. Phys. **67** (1977) 204.

[11] B. Sayer, J. P.Visticot and J. Pascale, J. Phys. (Paris) **39** (1978) 361.

[12] H. Nakatsuji and K. Hirao, J. Chem. Phys. **68** (1978) 2053.

[13] H. Nakatsuji, Chem. Phys. Lett. **59** (1978) 362.; **67** (1979) 329, 334.

[14] H. Nakatsuji, Chem. Phys. **75** (1983) 425.

[15] H. Nakatsuji, Theor. Chem. Acta. **71** (1987) 201.

[16] Y. Mizukami and H. Nakatsuji, J. Chem. Phys. (in press).

[17] W. R. Wadt and P. J. Hay, J. Chem. Phys. **82** (1985) 284.

[18] S. R. Langhoff, C. W. Bauschlicher and H. Partrige, J. Phys. **B18** (1985) 13.

[19] W. C. Ermler, Y. S. Lee, K. S. Pitzer and N. W. Winter, J. Chem. Phys. **69** (1971) 716.

[20] S. Huzinaga, J. Andzelm, M. Klobukowski, E. Radzio-Andzelm, Y. Sakai and H. Tatewaki, *Gaussian basis sets for molecular calculations* (Elsevier, Amsterdam, 1984).

[21] B. R. Brooks, P. Saxe, W. D. Laidig, and M. Dupuis, Program System GAMESS, Program Library No. 481, Computer Center of the Institute for Molecular Science, (1981).

[22] H. Nakatsuji, Program system for SAC and SAC-CI calculations, Program Library No.146(Y4/SAC), Data Processing Center of Kyoto University, 1985; H. Nakatsuji, Program Library SAC85 (No.1396), Computer Center of the Institute for Molecular Science, Okazaki, 1986.

[23] J. Holmtzmark, Ann. Phys. (leipzig) **58** (1919) 577.

[24] A. Jablonski, Phys. Rev. **68** (1945) 78.

[25] S. Y. Chen and M. Takeo, Rev. Mod. Phys. **29** (1957) 20.

Chapter 7

Collision induced absorption spectra of CsRg system (Rg=Xe, Kr, Ar, Ne) calculated by the SAC-CI method with all-electron basis sets

ABSTRACT

Collision induced absorption process of Cs-Rg system (Rg= Xe, Kr, Ar, and Ne) is studied theoretically by the SAC-CI (symmetry adapted cluster-configuration interaction) method. The potential energy curves of the CsRg system which correlate to the 6S, 6P, 5D, and 7S states of the Cs atom and the oscillator strengths are calculated. The reduced absorption coefficients are estimated by the quasistatic approximation. The results of the calculated shift values and intensities agree well with the experimental data. The monotonic shift of the spectral peaks with substituting the rare gas atom is confirmed to be related to the shift of the avoided crossing point between 7sΣ and 5dΣ states. The absorption intensities are calculated to decrease as the rare gas atom is substituted from Xe to Ne, which reproduces the feature of the observed spectra. The intensities of 6sΣ-5dΣ transitions are calculated to be larger than those of 6sΣ-7sΣ ones, which is attributed to the fact that the former transitions are induced in larger internuclear distances than the latter ones. The broadening of 6P resonance line is also investigated by the present method.

I. INTRODUCTION

Chemical reactions in the optical fields have been received much attention in recent years with the developments of the spectroscopies.[1] The spectral broadening and shift observed in the absorption or emission spectra have the informations of transient species of such photo-assisted reactions. As the primary examples of such reactions, electronic spectra of the alkali atoms purturbed by the rare gas atoms have been widely observed and investigated.[2-6] Especially, Cs-rare gas (Cs-Rg) systems show relatively strong interactions and therefore, the spectra have large broadening, shift and asymmetry. Dipole forbidden transitions, S-S and S-D excitations of the Cs atom, are induced during the collision between the Cs and rare gas atoms.[2,3] This phenomenon is called as collision induced absorption process and the induced absorption spectra of the CsRg systems were observed by Moe *et al.*[2] The broadening and peak shift of the resonance lines are also observed for these systems. Hedges *et al.*[5] and Kielkopf *et al.*[6] reported the detailed spectra associated to 6S-6P emission and 6S-nP absorption lines of the Cs atom.

Several theoretical works are also performed in order to elucidate the mechanism of this induced transition and line broadening.[7-10] The line broadening of the 6S-6P transition for the alkari-rare gas systems was researched by Baylis[7] with the semiempirical potential curves. Pascale *et al.* calculated the potential energy curves[8] and oscillator strengths[9] of the alkari-rare gas systems using the semiempirical potential model of Baylis[7] and investigated the collision induced absorption process. However, orbital relaxations caused by the interaction during the collision were considered only for the Cs atom in their calculations and their results seem to contradict with the experimental spectra in some points for the Cs-Rg system.[10]

In the preceding study, we investigated the collision induced absorption process of the Cs-Xe system with *ab initio* method.[11] However, the ordering of 5D and 7S levels of the Cs atom was not properly reproduced in that calculation. In the present article, we overcome this problem with using refined basis sets and investigate this phenomenon systematically with the perturber substituted by the other rare gas atoms. Since we are interested in the interactions in the intermediate nuclear distances, the far wing region of the spectrum is investigated. The SAC(symmetry adapted cluster)/SAC-CI method[12,13] is used for the calculations of the van der Waals (vdw)

interactions of the open-shell Cs-Rg systems. The method has been applied successfully to large number of molecular spectroscopies[14] including vdw systems such as Ar_2[15] and Kr_2.[16] The reduced absorption coefficient, which is directly determined by the experiment, is estimated by the quasistatic approximation.[6,17-19]

II. CALCULATIONAL DETAILS

The flexible basis sets are extremely important for the description of the vdw interactions. In the preceding study,[11] we adopted the RECP with including outermost core orbitals of Hay and Wadt[20] and diffuse functions proposed of Langhoff *et al.*[21] on Cs. However, we failed in getting proper energy ordering between the 5D and 7S states of the Cs atom with those basis sets, even though the core polarization effects are included. The relative positions and the interactions of these states in the Cs-Rg systems were found to be quite important and therefore, all-electron basis sets of Huzinaga[22] are examined. The excitation energies at the dissociation limit of the systems (15.0Å) calculated with the present basis sets are summarized in Table I and are compared with those in the previous study in Fig. 1. The energy ordering of the excited states of the Cs atom is successfully reproduced and the deviations from the experimental values are within to 0.25 eV. The f-function seems not to have considerable effects on the excitation energies as shown in Fig. 1 and therefore, is not included in the present study.

TABLE I. Excitation energy of the Cs atom (eV).

Transition	Exptl.[a]	SAC-CI[b]
6S → 6P	1.386, 1.455	1.18
6S → 5D	1.798, 1.810	1.78
6S → 7S	2.298	2.04
6S → 7P	2.699, 2.721	2.68
6S → 6D	2.800, 2.806	2.70

[a] Reference 26
[b] Atomic excitation energies are estimated for CsRg system with the internuclear distance of 15.0 Å.

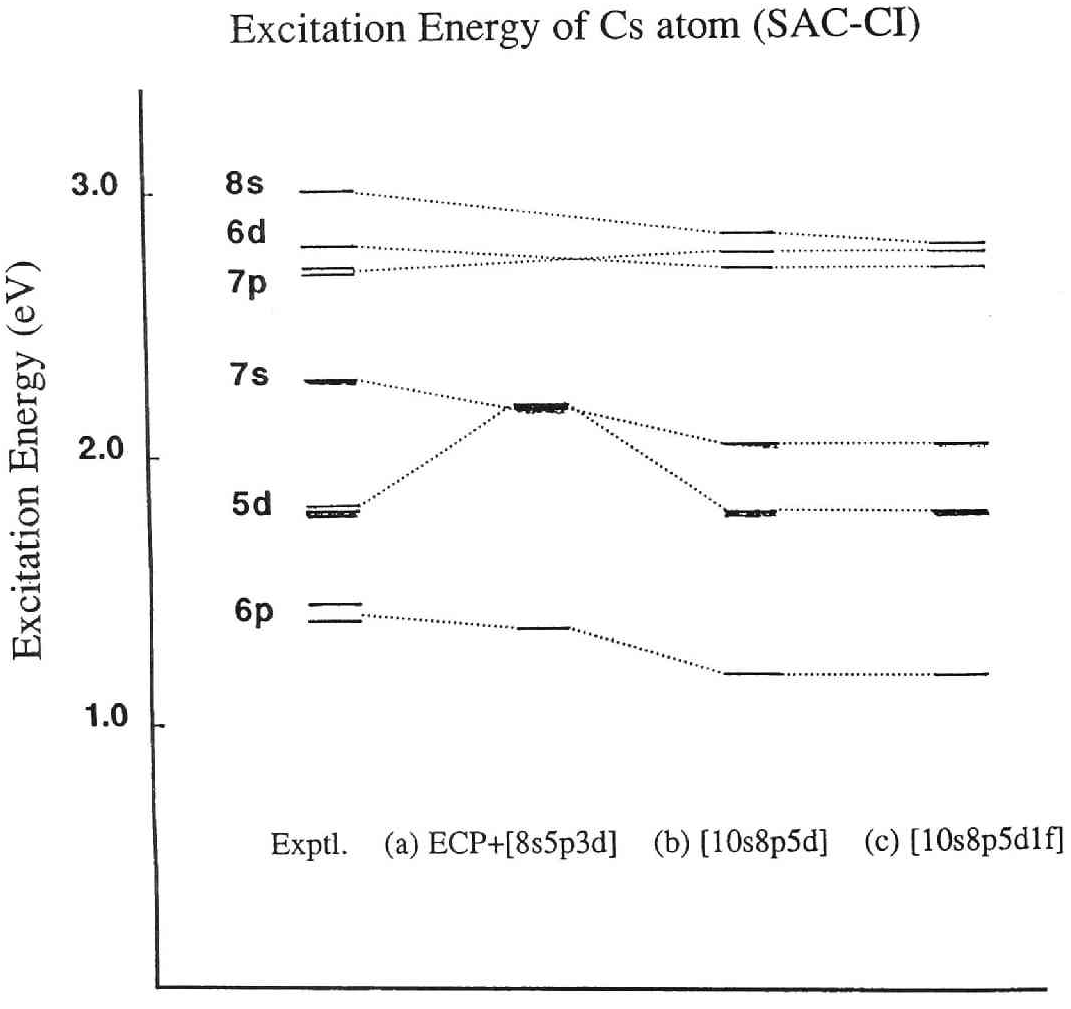

FIG. 1. Excitation energies of Cs atom calculated using various basis sets. (a) Basis sets used in Reference 12 (b) Basis sets used in the present study (c) f-AO proposed in Reference 19 is added to the basis sets (b)

As the results of the basis set examinations, the basis sets proposed by Huzinaga[22] are adopted and all electrons are explicitly treated for both the Cs and Rg atoms. The basis set of Cs is composed of [7s5p2d] set for valence part and augmented with primitive sets (3s3p3d) of Langhoff *et al.*[21] for Rydberg part. The Xe basis set is derived from [6s5p2d] set of Huzinaga[22] augmented with the primitives (3s2p) of Ermler *et al.*[23] plus polarization functions of (2d) sets of Huzinaga.[22] Basis sets of other rare gas atoms are selected as similar quality to Xe; namely the Rg basis set is derived from [ns(n-1)p(n-4)d] [n=5(Kr), n=4(Ar), and n=3(Ne;3s3p)] set of Huzinaga[22] augmented with the diffuse functions of (2s2p) plus (2d) sets of Huzinaga.[22] The final sets of the form [10s8p5d]/[ns(n-1)p(n-4)d] are selected for CsRg [n=8(Xe), n=7(Kr), n=6(Ar), and n=6(Ne)]. The resultant SCF dimensions are 117, 107, 97, and 93 AOs for CsXe, CsKr, CsAr, and CsNe, respectively. Relativistic effects are not included in the present calculation. Calculations are carried out at appropriate 13 points from 3Å to 15Å of Cs-Rg distance.

The SAC-CI method[13] is used for the calculations of the electron correlations. Details of the SAC[12] and SAC-CI[13] theories have been reported elsewhere. The $CsRg^+$ system is solved by the SAC method and then the wave function of CsRg is constructed by the SAC-CI method. The valence orbitals of eight occupied MO's ($5s_{Xe}$ $5p_{Xe}$ $5s_{Cs}$ $5p_{Cs}$ $6s_{Cs}$) and the lower 41 unoccupied MO's are adopted for the active space for the CsXe system. In the SAC step, configuration selection[24] is performed with the threshold of $\lambda_g=1\times10^{-5}$ au for the linked operators. In the SAC-CI step, no configuration selection is performed for the linked terms, because weak interaction of the vdw system should be calculated. The resultant dimensions of the SAC-CI are 3961(Σ states), 3370(Π states) and 2788(Δ state) for all the nuclear distances. For other CsRg systems, the calculations of the similar accuracy to those of CsXe system are performed. The SCF orbitals are obtained with the program HONDO7[25] and the SAC/SAC-CI calculations are performed by the program SAC85.[26]

For the discussions of the fine structures observed in the 6P-state, the spin-orbit interactions are estimated by the method reported earlier.[27] The spin-orbit coupling constant of ζ_p= 369.4 cm^{-1} is estimated by the experimental data.[28]

The basis set superposition error (BSSE) is taken into account. The BSSE of atom

A is defined as

$$\delta_A = E_A(\phi_A \cup \phi_B) - E_A(\phi_A)$$

where ϕ_A and ϕ_B denote the basis sets centered at A and B, respectively. The total correction of the BSSE is estimated as

$$\delta = \delta_A + \delta_B$$

and the BSSE of the excited state is assumed to be the same to that of the ground state.

Quasistatic approximation[17-19] is adopted for the calculations of reduced absorption coefficients. Though there exist more elaborate treatments,[29] this approximation seems to be reliable for calculating spectra and is also useful for the understanding of the mechanism of the collision induced absorption process. Assuming binary collisions between the Cs and Rg atoms and canonical distributions, the reduced absorption coefficient is given by[19]

$$\frac{k(\lambda)}{n_G n_A} = \sum_c \frac{4\pi^3}{3\lambda} D(R_c)^2 \left(\frac{4\pi R_c^2}{d[V_e(R)-V_g(R)]/dR \mid_{R_c}} \right) \exp\left[- \frac{V_g(R_c)-V_g(\infty)}{k_B T} \right],$$

where n_G and n_A are the densities of the perturber Rg and the absorber Cs, respectively, D(R) denotes the induced transition dipole moment at internuclear distance R, and V_g and V_e are the energies of the ground and excited states, respectively.

III. RESULTS AND DISCUSSIONS

A. Potential energy curves

We have calculated the ground and excited states of the Cs-Rg system which are correlated to the 6S(ground), 6P, 5D and 7S states of the Cs atom. Among these states, the excitations to the 5D and 7S states are originally dipole forbidden and their intensities are collisionally induced through the interaction between the Cs and rare gas atom. For allowed transition, 6S→ 6P, collisional perturbation by the rare gas atom leads to the broadening of the resonance line.

First, the potential curves of the CsXe system are discussed. Fig. 2 shows the calculated potential curves for the 6S, 6P, 5D, and 7S states of the CsXe system. Hund's case a, which is suitable in the internuclear distance of the present interest, is adopted for these states.[2] The calculated spectroscopic constants for the bound states of CsRg system are summarized in Table II. The potential curve of the ground state

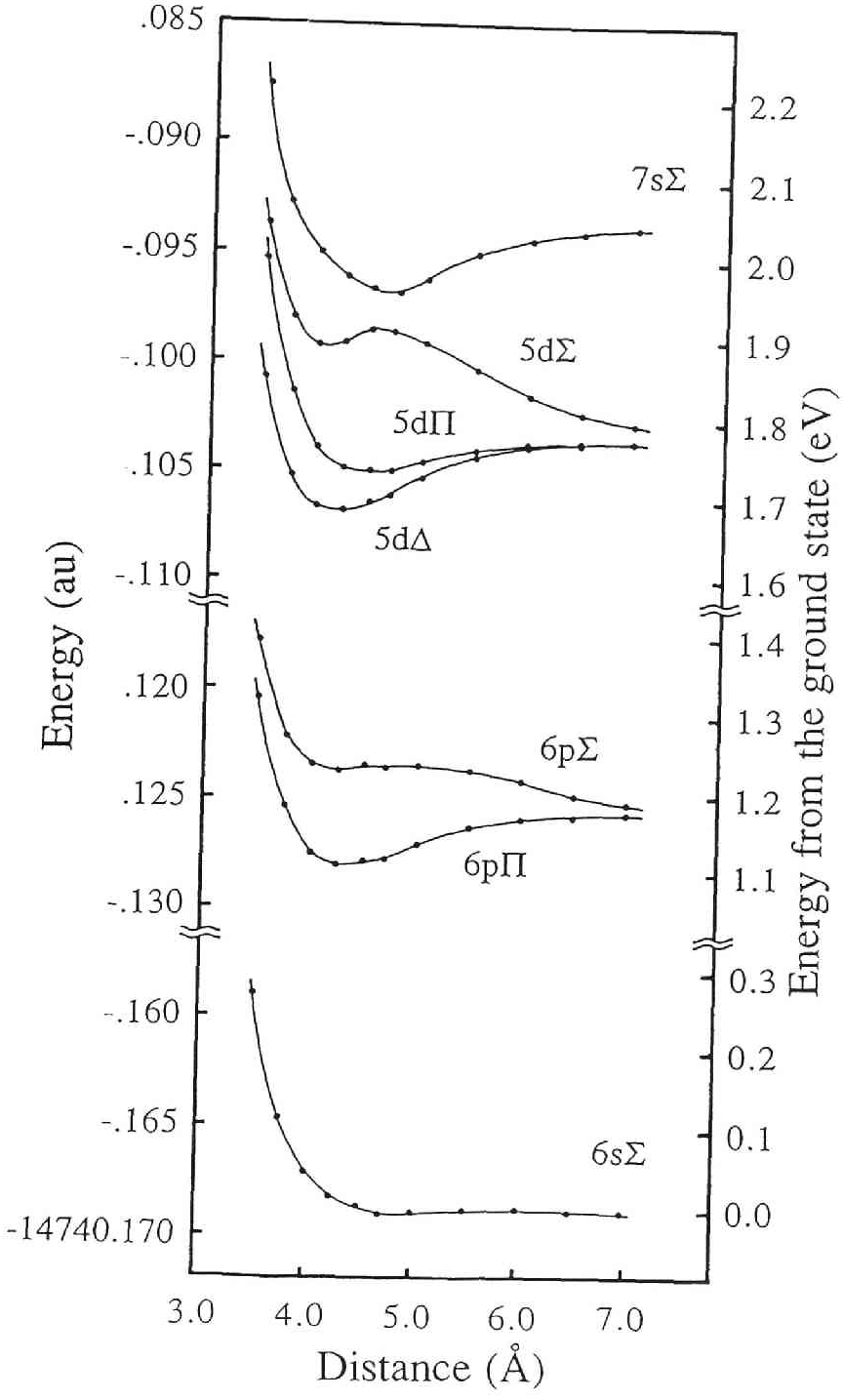

FIG. 2. Potential energy curves for the 6s, 6p, 5d and 7s states of CsXe without including spin-orbit coupling.

TABLE II. Spectroscopic constants for the bound states of CsRg (Rg=Xe,Kr,Ar).

		Exptl.	SAC-CI		
Molecule	State	D_e (cm^{-1})	D_e (cm^{-1})	R_e (Å)	ω_e (cm^{-1})
CsXe	$6s\Sigma$ (Ground)		30	4.97	
	$5d\Delta$		698	4.20	33.2
	$5d\Pi$		280	4.48	23.5
	$7s\Sigma$	~ 890[a]	662	4.61	33.8
	$6p^2\Pi_{1/2}$	~ 430[b]	425	4.27	32.5
	$6p^2\Pi_{3/2}$	~ 500[b]	538	4.33	32.4
CsKr	$5d\Delta$		441	3.90	46.2
	$7s\Sigma$		322	4.35	22.3
	$6p^2\Pi_{1/2}$	~ 300[b]	163	3.95	35.1
	$6p^2\Pi_{3/2}$	~ 350[b]	283	3.98	38.3
CsAr	$5d\Delta$		340	3.69	-
	$7s\Sigma$		113	4.27	-

[a] Reference 2
[b] Reference 6

of CsXe has flat shape with a shallow minimum of 30 cm^{-1} calculated at 4.97 Å, while the atomic scattering experiment gives the well of 110 cm^{-1} at 5.45 Å.[30] For other complexes, no potential minima are calculated in the ground state, though the shallow wells are observed in the ground state of CsKr and CsAr.[30]

As for the 6pΣ and 5dΣ states, since they are characterized as the excitations from 6s non-bonding MO to weakly anti-bonding 6pσ and 5dσ MO's which direct along the molecular axis, system becomes unstable and the potential curves become repulsive. The repulsive interaction of the 5dΣ state appears to be more effective than that of the 6pΣ state starting from large internuclear distance. Both the 6pΣ and 5dΣ states have characteristic shoulder or hump at $R_{shoulder}$= 5.0 Å and R_{hump}= 4.6 Å, respectively in their potential curves. Those features were also obtained in the semiempirical calculation.[8] Remarkable hump in the potential curve of the 5dΣ state is caused by the avoided crossing with the 7sΣ state and the natures of the potential curves are reversed at this internuclear distance. In the following discussions, upper curve is called as the 7sΣ state and lower one as the 5dΣ state for convenience. Pascale *et al.*[8] explained the hump in the 6pΣ state is occurred by the interaction with the neighboring states of the same symmetry; namely $5D_{3/2}$ and $5D_{1/2}$ levels in their dissociation limits. We also get configuration mixing of 6s→ 5dσ component in the 6pΣ state, which causes the shoulder in the potential curve.

The 6pΠ, 5dΠ, and 5dΔ states have shallow minima in their potential curves. Rydberg orbitals in these states of the Cs atom do not direct toward the rare gas atom. Ion core of the Cs atom polarizes the rare gas atom, which is responsible for these bound states. As for the CsXe system, potential wells and equilibrium distances are calculated to be D_e=538 cm^{-1} with R_e=4.33 Å, D_e=280 cm^{-1} with R_e=4.48 Å, and D_e=698 cm^{-1} with R_e=4.20 Å for the 6pΠ, 5dΠ, and 5dΔ states, respectively. Since the Rydberg orbital of the 5dΠ state slightly directs along the CsRg axis, the 5dΠ state feels repulsive force more than the 6pΠ and 5dΔ states. Therefore, the equilibrium distance R_e of the 5dΠ state is calculated larger than those of the 6pΠ and 5dΔ states and D_0 of the former is smaller than those of the latter. The potential curve of the 7sΣ state also has a well (662 cm^{-1}) at 4.61 Å and this state suffers avoided crossing with the 5dΣ state, as noted above.

The potential energy curves of the 5dΣ, 5dΠ, 5dΔ and 7sΣ states of the CsRg

systems are shown in Fig. 3. All the potential curves of different systems are depicted as they converge to the same atomic dissociation limits for comparison. The attractive wells of the 5dΠ, 5dΔ and 7sΣ states become shallower and the equilibrium distances become shorter, as the rare gas atoms are replaced from Xe to Ne. For example, the attractive well and equilibrium distances of CsKr are calculated to be 441 cm^{-1} with 3.90Å and 332 cm^{-1} with 4.35Å for the 5dΔ and 7sΣ states, respectively, and the 5dΠ state is almost flat. These features are clearly due to the polarizability and the vdw radii of the rare gas atoms. According to these changes, the avoided crossing points between the 5dΣ and 7sΣ states change their relative positions; namely, more unstable in energy and shorter in their nuclear distances as the rare gas atoms are substituted from Xe to Ne. (R = 4.6Å, 4.3Å, and 4.1Å for CsXe, CsKr, and CsAr, respectively). The observed peak of the collision induced absorption shows monotonic shift; namely, peak shift of the red band associated to 7S becomes small, while that of the blue band associated to 5D becomes large, as the rare gas atoms are substituted from Xe to Ne. It is confirmed that the monotonic shift of the peaks with substituting rare gas atoms are related to this changes of the relative positions of the avoided crossing points.

Fig. 4 shows the dependence of the excitation energies of the 5dΣ, 5dΠ, 5dΔ and 7sΣ states on the internuclear distance (difference potential). The difference potential gives the absorption energy at the corresponding nuclear distance. It is clear that the 5dΣ states are responsible for the absorption bands in the blue regions and the 7sΣ and 5dΠ states are related to those in the red regions relative to atomic forbidden lines. The 6sΣ-5dΣ transitions clearly have extrema in their difference potentials. The corresponding internuclear distances of these extrema are calculated to be 4.69, 4.39, 4.19, and 3.68 Å for CsXe, CsKr, CsAr, and CsNe, respectively. These values reflect the positions of the hump in the 5dΣ states caused by the avoided crossing between the 5dΣ and 7sΣ states. The semiempirical calculation also gives the extremum at 4.34Å for CsXe system.[8] On the other hand, excitation energies of the 7sΣ and 5dΠ states monotonically decrease at the large internuclear distances and there exist flat regions at small distances. Existence of these flat region coincides with an interpretation of the experimental 6sΣ-7sΣ absorption spectra by Moe *et al.*[2] as seen later. In a classical picture, these extrema or flat regions in the difference potentials correspond to the peaks of the shifted bands. Tables III and IV give these frequency shifts of the peaks

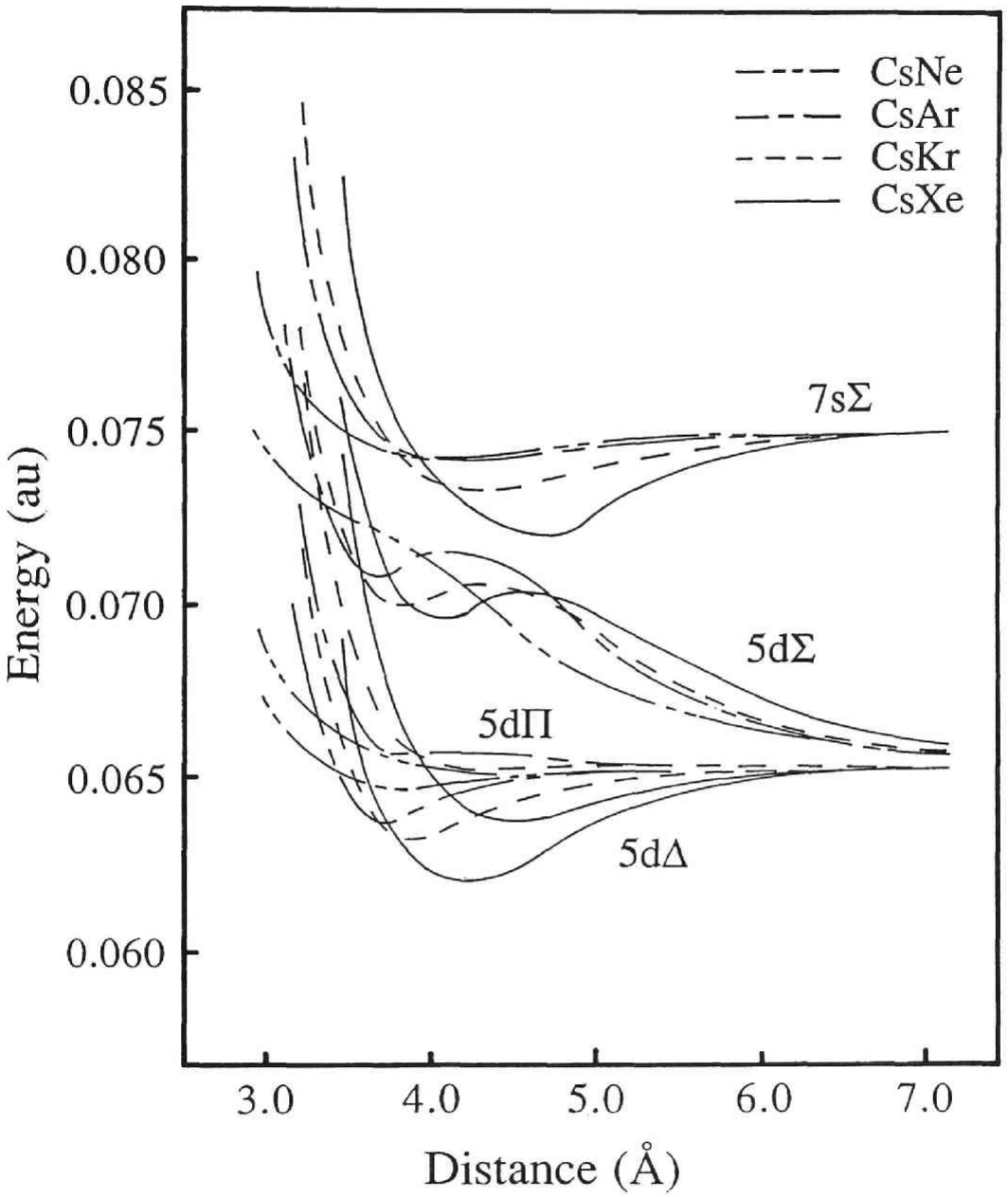

FIG. 3. Potential energy curves for the 5d and 7s states of CsRg without including spin-orbit coupling.
——:CsXe, – – – –:CsKr, —·—:CsAr, and —··—:CsNe.

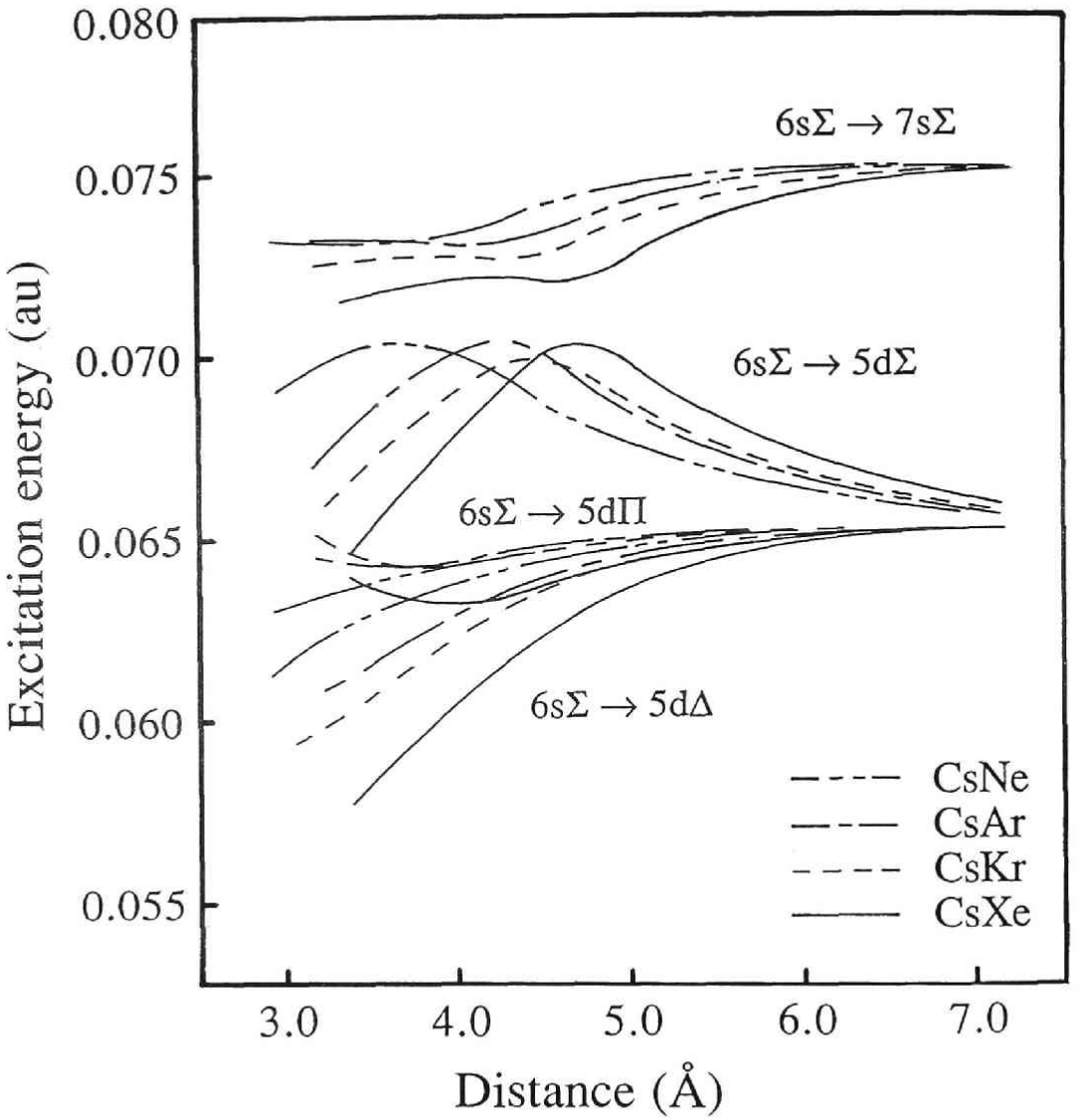

FIG. 4. 6s→ 5d and 6s→ 7s excitation energy vs. Cs-Rg distance.
———:CsXe, - - - - - :CsKr, —·—:CsAr, and —··—:CsNe.

TABLE III. Energy shift of the 6sΣ-7sΣ excitation relative to the 6S-7S excitation of the Cs atom (in cm^{-1}).

Molecule	Exptl.[a]	SAC-CI[b]	Semi-empirical[c]
CsXe	-1061	-630	-136
CsKr	-829	-480	-676
CsAr	-741	-420	-
CsNe	-500	-370	217

[a] Reference 2
[b] Energy shift is estimated at the extremum of the difference potential.
[c] Reference 9

TABLE IV. Energy shift of the 6sΣ-5dΣ excitation relative to the 6S-5D excitation of the Cs atom (in cm^{-1}).

Molecule	Exptl.[a]	SAC-CI[b]		Semi-empirical[c]
		Shift	Distance(Å)	
CsXe	1082	1130	4.69	3153
CsKr	1204	1030	4.39	2696
CsAr	1478	1100	4.19	1759
CsNe	1585	1150	3.68	3378

[a] Reference 2
[b] Energy shift is estimated at the extremum of the difference potential.
[c] Reference 9

which are associated to the 7S and 5D lines, respectively. The shift values are discussed in details in Sec. III-C.

B. Transition moments

The induced dipole moments are shown in Fig. 5 as a function of the internuclear distance. The transitions of 6S→5D and 6S→7S are originally dipole forbidden. These dipole-forbidden transitions are induced by the intra-atomic orbital mixing of p-components of the Cs atom, which is cased by the reduction of the space symmetry of the system. Transitions from 6sΣ to 7sΣ, 5dΣ, and 5dΠ are induced at the intermediate nuclear distances from 3Å to 7Å. The 5dΔ state not having the induced transition dipole moments gives no contribution to induced absorption.

Induced transition moment is important factor which determines the intensity of the induced absorption. Overall behavior of these transition moments is similar for all the CsRg systems. The transition moment of 6sΣ-5dΣ is induced at the larger internuclear distance than that of 6sΣ-7sΣ. Taking into accounts of the boltzmann distributions of the ground state, this tendency agrees well with the experimental spectra, where the observed reduced absorption coefficients of 6sΣ-5dΣ are larger than those of 6sΣ-7sΣ.[1] Magnitude of the transition moment is replaced between the 5dΣ and 7sΣ state at the corresponding nuclear separation of the avoided crossing point. Therefore, p-component of the Cs atom seems to interact with 5dΣ component more than 7sΣ component of the system. Transition moment of 6sΣ-7sΣ shows the oscillatory structure, which is also obtained by the semi-empirical calculation of Pascale.[9] This structure is assumed to correspond to the node of the p-component mixed in the 7sΣ wave function from the analysis of the CI coefficients. Because of this node, for example CsXe system, vdw complex of Cs-Xe distance of 5-6Å has small contribution to the collision induced absorption around 7S line. The calculated transition moments seem to be underestimated in comparison with the experimental results, as seen later.

C. Absorption spectra

The experimental and theoretical absorption spectra of the 7S band of the CsRg system are compared in Fig. 6. Experimental absorption spectra have broad

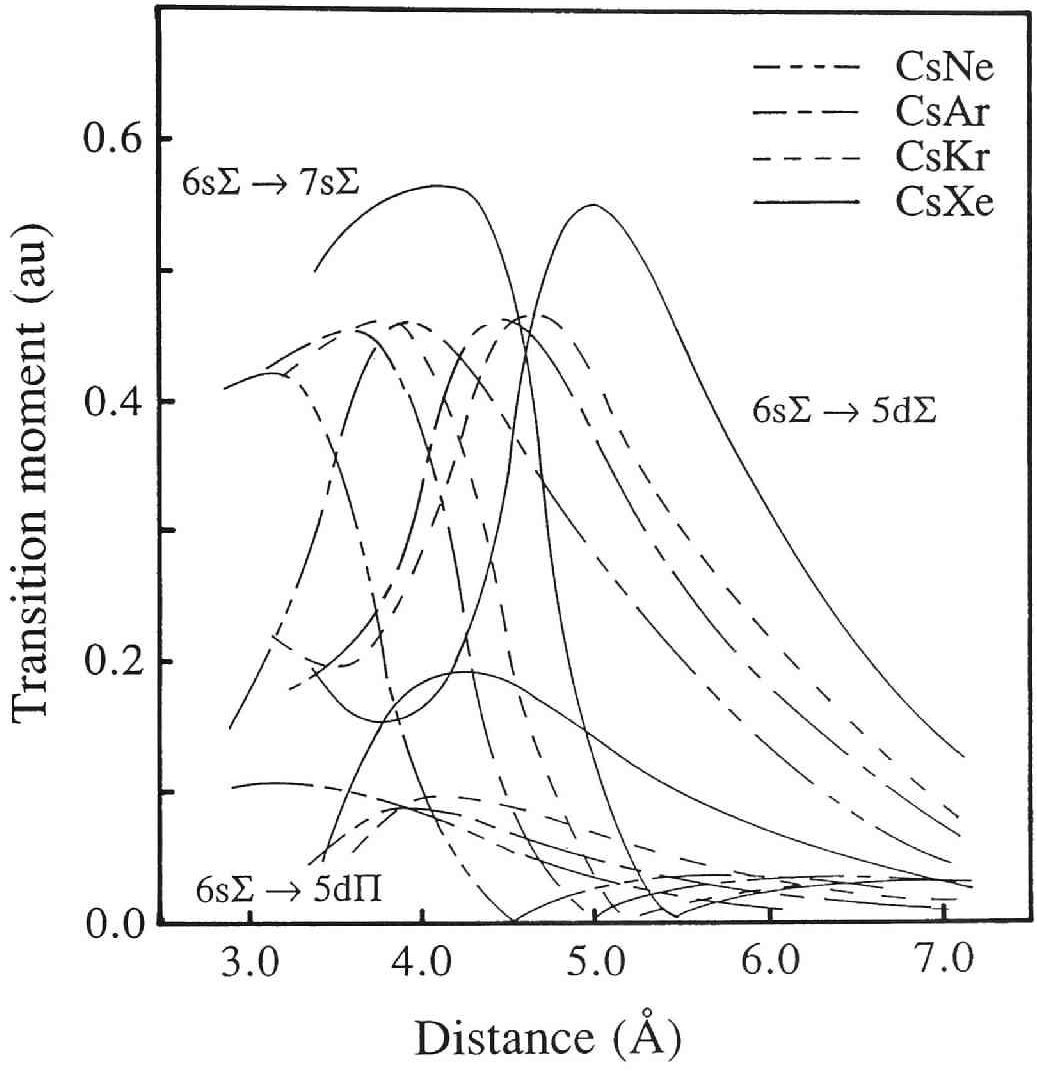

FIG. 5. Transition dipole moments of 6sΣ→ 5dΣ, 6sΣ→ 5dΠ, and 6sΣ→ 7sΣ excitation vs. internuclear distance.
———:CsXe, - - - - - :CsKr, — · —:CsAr, and — · · —:CsNe.

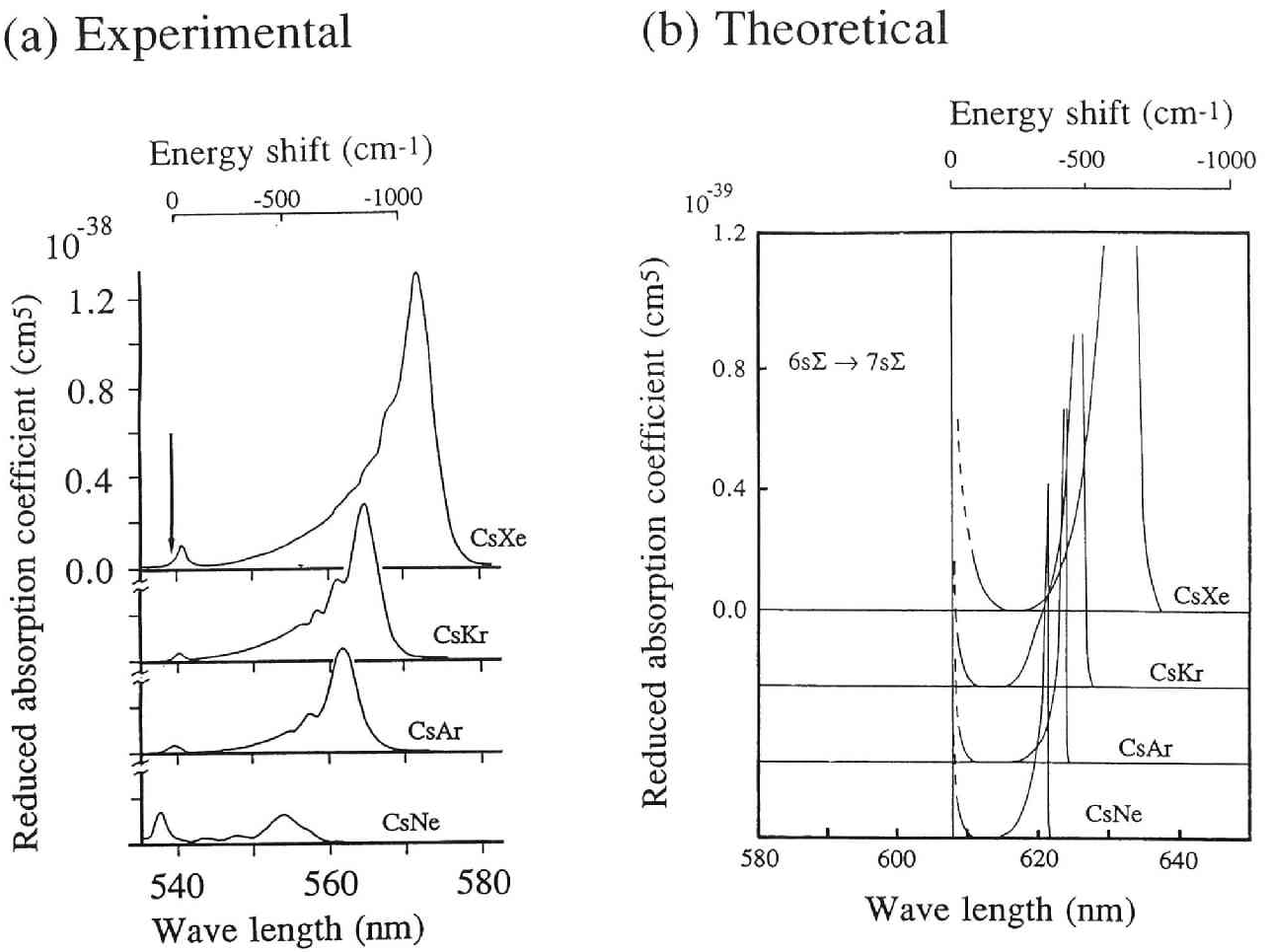

FIG. 6. (a) Experimental and (b) theoretical reduced absorption coefficients for 7s state of Cs-Rg. Experimental spectra are cited from Reference 1

continuous bands located in the red regions of the atomic forbidden lines for all species. The energy shift of the peak maximum and the band intensity become small as the rare gas is substituted from Xe to Ne. Absorption band has vibrational structure, which indicates the existence of the attractive well in the excited state and the vertical electron transition. The calculated potential curves of $7s\Sigma$ have attractive wells of D_0= 662, 322, 113 cm^{-1}, for CsXe, CsKr, and CsAr, respectively, reflecting the polarizabilities of the rare gas atoms. Moe *et al.* proposed[2] the potential well of the $7s\Sigma$ state for CsXe as ~ 890 cm^{-1} from the analysis of the absorption spectrum. They also reported[2] that the spectral shapes and the peak shifts do not change with varying temperature, therefore this red-shifted band occurs by the mechanism similar to the satellite observed in the dipole-allowed transition. Accordingly, there exist flat regions in the difference potentials of the $6s\Sigma$-$7s\Sigma$ transitions for all species, as noted in Sec. III-A. Classical treatment comes to breakdown at this point and the calculated absorption intensities show divergence at the corresponding energy region. These energy shift values are given in Table III. Our calculated results explain the $6s\Sigma$-$7s\Sigma$ transitions show red shift for all species, while those of semiempirical calculation do not. The red shift values of $6s\Sigma$-$7s\Sigma$ is calculated to be -630 cm^{-1}, -480 cm^{-1}, -420 cm^{-1}, and -370 cm^{-1} for CsXe, CsKr, CsAr, and CsNe, respectively, which reproduce the monotonic change of the peak shift observed in the experiment. The calculated absorption intensities also reproduce the experimental trends, though the absolute values are underestimated; the absorption intensities decrease as the rare gas is substituted from Xe to Ne.

In Fig. 7, we compare the collision induced absorption spectra associated to the 6S-5D forbidden transition. Absorption band of the 6S-5D transition has complex shape in comparison with those of the 6S-7S one. This is due to the fact that there exists $5d\Sigma$ and $5d\Pi$ states which contribute to the induced absorption. The peak shift of the blue band becomes large as the rare gas atom is substituted from Xe to Ne, while the intensity of the band becomes small in the experimental spectra.

As shown in Fig. 5, the difference potential of the $6s\Sigma$-$5d\Sigma$ excitation has an extremum for all species. The calculated energy shift values of the $6s\Sigma$-$5d\Sigma$ excitation are compared with the experimental values and those calculated by Pascale *et al.*[8] in Table IV. The peak shift of CsXe is calculated to be 1130 cm^{-1}, which is compared to

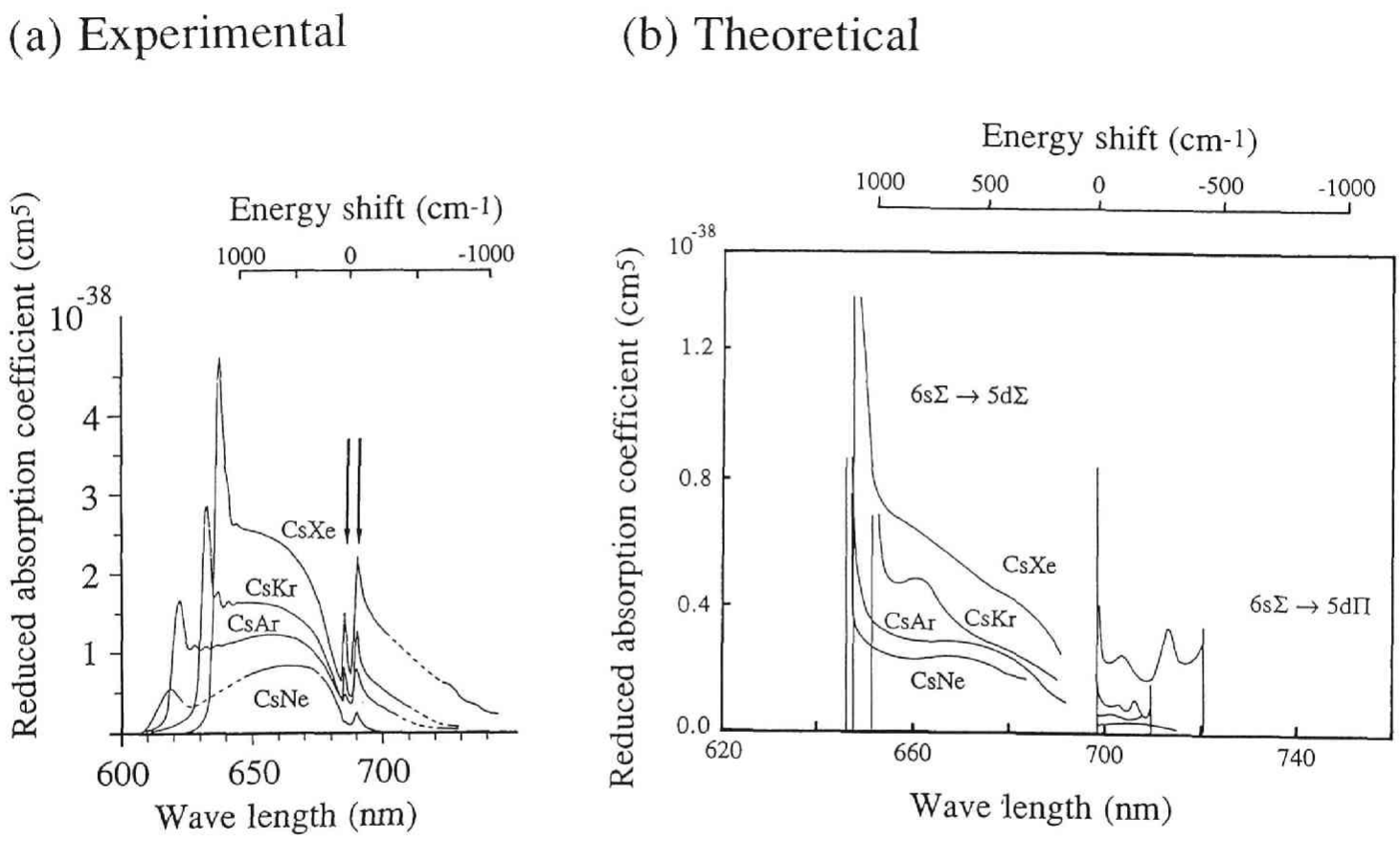

FIG. 7. (a) Experimental and (b) theoretical reduced absorption coefficients for 5d state of Cs-Rg. Experimental spectra are cited from Reference 1.

the experimental value of 1082 cm^{-1}. The calculated peak shifts of $6s\Sigma$-$5d\Sigma$ do not reproduce the experimental ordering according to the substitution of the rare gas atoms. This is because energy separation between the 5D and 7S state of the Cs atom is underestimated. The $6s\Sigma$-$5d\Pi$ excitation also has induced transition dipole moment. This transition is calculated to have small intensity relative to that of $6s\Sigma$-$5d\Sigma$ and to be located in the red region of the forbidden line. Experimental spectrum also has absorption band in the red side of dipole forbidden line and the band seems to decrease gradually as separating from the 6s-5d quadrupole transition. However, this band partially overlaps with Cs_2, so it was noted that more precise analysis of this profile seems to be difficult by the experiment.[2] On the other hand, calculated difference potentials have flat region as shown in Fig. 4, therefore theoretical spectra have limit in their red shifted bands. Observed absorption bands have some structures in this energy region before the intensity of Cs_2 is subtracted.[2]

D. Broadening of 6P emission line

The broadening of 6P resonance line is due to the $6p\Sigma$ and $6p\Pi$ states of the CsRg system. Hedges et al.[5] analyzed the far wing regions of the emission spectra of 6P line and determined the $A\Pi_{1/2}$, $A\Pi_{3/2}$, $B\Sigma_{1/2}$ potentials for the CsRg system using quasistatic approximation.

Fig. 8 gives the potential curves of the $6p^2\Sigma_{1/2}$, $6p^2\Pi_{1/2}$ and $6p^2\Pi_{3/2}$ states of the CsXe system with including spin-orbit effects. For the CsXe system, our potential curves of the $6p^2\Pi_{1/2}$ and $6p^2\Pi_{3/2}$ states show good agreements with those experimentally determined by Hedges *et al.*[6] with respects to D_0 and R_e. The dissociation energies and equilibrium distances are calculated to be D_0=538 cm^{-1} with R_e=4.27Å and D_0=425 cm^{-1} with 4.33Å for $6p^2\Pi_{1/2}$ and $6p^2\Pi_{3/2}$ states, respectively, which is compared to the experimental values of D_0= ~500 cm^{-1} and D_0= ~430 cm^{-1}.[5] As for the CsKr, those states are calculated to have shallow potential wells of D_0=283 cm^{-1} and D_0=163 cm^{-1} in comparison with the experimental results of D_0= ~350 cm^{-1} and D_0= ~300 cm^{-1}.[5] The calculated potential curve of the $6p^2\Sigma_{1/2}$ state has a small hump at R_{hump}= 5.1Å(CsXe), which is also reported by Pascale et al.[8] However, the potential curve determined by the experiment has no such a shoulder or hump.[5]

The calculated and experimental emission spectra of the CsXe system associated

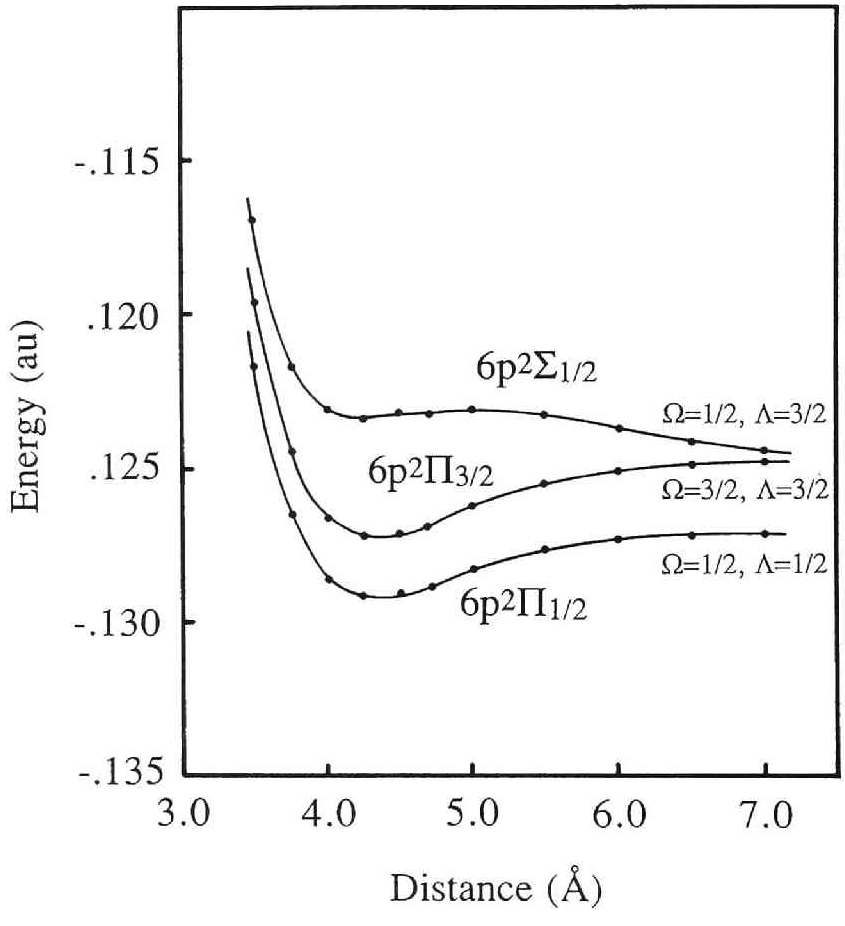

FIG. 8. Potential energy curves of 6p states for CsXe with including spin-orbit effects.

to 6P-6S line are compared in Fig. 9. The difference potential of $6s\Sigma$-$6p^2\Sigma_{1/2}$ also has a extremum like $6s\Sigma$-$5d\Sigma$, therefore, calculated emission band shows divergence in the blue region. Accordingly, the experimental spectrum also has the limit of the emission band in the blue region. The calculated shift values and the nuclear distances of the flat region for $6s\Sigma$-$6p^2\Sigma_{1/2}$ transitions of the CsRg system are summarized in Table V. The energy shifts are calculated to be about 400 cm^{-1}, while those are observed as about 200 cm^{-1}. The blue shift values of $6s\Sigma$-$5d\Sigma$ are calculated larger than those of $6s\Sigma$-$6p\Sigma$ for all the system. This trend is also observed in the experimental spectra.[2,5] This is due to the fact that the $5d\Sigma$ state feels more repulsive interaction than the $6p\Sigma$ state.

The $6p^2\Pi_{1/2}$ and $6p^2\Pi_{3/2}$ states are related to red band and their band intensities gradually fall off as separated from the 6S-6P atomic line. However, the calculated emission bands in the red wing have small spires which are due to the boltzmann distribution in the upper bound states. These spires are less clear in the experimental spectra.

TABLE V. Energy shift of the $6s\Sigma$-$6p^2\Sigma_{1/2}$ excitation relative to the 6S-6P excitation of the Cs atom (in cm^{-1}).

Molecule	Exptl.[a]	SAC-CI[b]	
		Shift	Distance(Å)
CsXe	~ 150	400	5.00
CsKr	~ 150	350	4.75
CsAr	~ 200	430	4.50
CsNe	~ 230	420	4.00

[a] Reference 6
[b] Energy shift is estimated at the extremum of the difference potential.

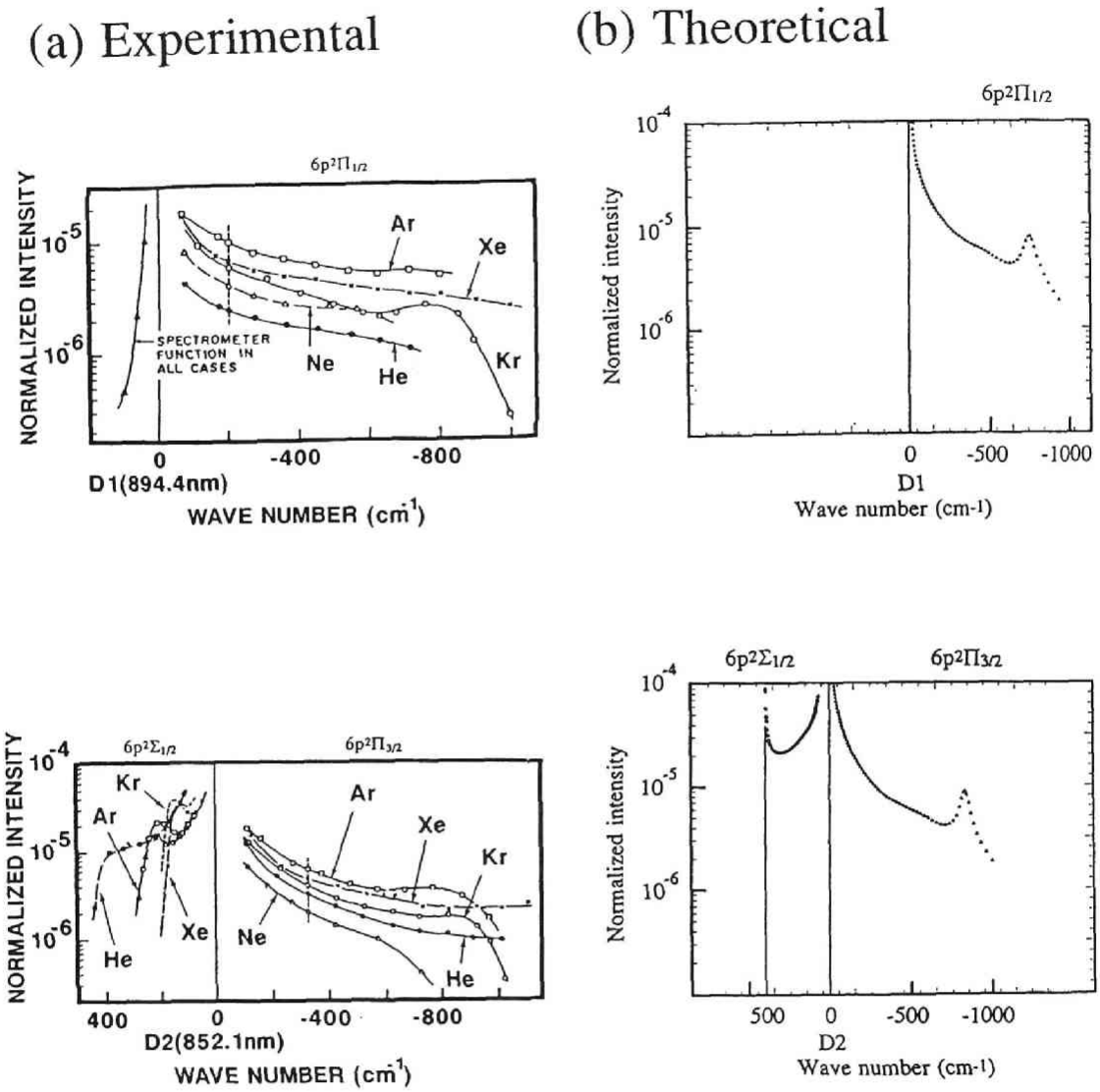

FIG. 9. (a) Experimental and (b) theoretical emission spectra of 6s→ 6p excitations for CsXe. Experimental spectra are cited from Reference 6.

IV. CONCLUSION

We have applied the SAC-CI method to the calculations of the potential curves and transition moments of the CsRg system (Rg= Xe, Kr, Ar, and Ne). The collision induced absorption processes associated to the 5D and 7S lines and the broadening of the 6P resonance line of this system are investigated. The reduced absorption coefficients of the induced transitions, which is directly observed by the experiment, are calculated by the quasistatic approximation. The spectroscopic constants of the bound states are also calculated.

The relative positions and the interactions of the 5dΣ and 7sΣ states are important for the descriptions of the collision induced absorptions of this system. The excitation energies of the Cs atom are reproduced with the errors less than 0.25 eV and the avoided crossing between the 5dΣ and 7sΣ states are correctly calculated. The calculated direction and magnitude of the band shifts agree well with the experimental data. The monotonic shift of the spectral peaks with substituting the rare gas atom is confirmed to be due to the relative positions of the avoided crossing points between the 5dΣ and 7sΣ states.

The intensities of the 6sΣ-5dΣ transitions are calculated to be larger than those of the 6sΣ-7sΣ ones, which is attributed to the fact that the former transitions are induced in larger internuclear distances than the latter ones. The absorption intensities are calculated to decrease as the rare gas atom is substituted from Xe to Ne, which reproduces the feature of the observed spectra.

ACKNOWLEDGMENTS

The authors thank Dr. K. Ueda and Professor N. Sato in Tohoku University for valuable discussions. They also thank Dr. T. Momose in Kyoto University for letting them use the program for calculating the transition moments. The calculations have been carried out with the FACOM M780 computer at the Data Processing Center of Kyoto University and the HITAC M-680H at the Institute for Molecular Science. This study has been supported by the Grant-in-Aid for Scientific research from the Japanese Ministry of Education, Science, and Culture.

REFERENCES

[1] P. R. Brooks, Chem. Rev. **88**, 407 (1988).

[2] G. Moe, A. C. Tam and W. Happer, Phy. Rev. **A14**, 349 (1976).

[3] A. C. Tam, G. Moe, B. R. Bulos and W. Happer, Opt. Commun. **16**, 376 (1976).

[4] A. C. Tam, G. Moe, W. Park and W. Happer, Phys. Rev. Lett. **35**, 85 (1975).

[5] R. E. Hedges, D. L. Drummond, and Alan Gallagher, Phys. Rev. **A6**, 1519 (1972).

[6] J. F. Kielkopf and N. F. Allard, J. Phys. **B13**, 709 (1980); Rev. Mod. Phys. **54**, 1103 (1982).

[7] W. E. Baylis, J. Chem. Phys. **51**, 2665 (1969).

[8] J. Pascale and J. Vandeplanque, J. Chem. Phys. **60**, 2278 (1974).

[9] J. Pascale, J. Chem. Phys. **67**, 204 (1977).

[10] B. Sayer, J. P.Visticot, and J. Pascale, J. Phys. (Paris) **39**, 361 (1978).

[11] H. Nakatsuji and M. Ehara, Chem. Phys. Lett. **172**, 261 (1990).

[12] H. Nakatsuji and K. Hirao, J. Chem. Phys. **68**, 2053 (1978).

[13] H. Nakatsuji, Chem. Phys. Lett. **59**, 362 (1978); **67**, 329, 334 (1979).

[14] H. Nakatsuji, Acta Chim. Hungarica **129** 719 (1992).

[15] Y. Mizukami and H. Nakatsuji, J. Chem. Phys. **92**, 6084 (1990).

[16] Y. Mizukami and H. Nakatsuji, Chem. Phys. **92**, 6084 (1990).

[17] W. R. Wadt and P. J. Hay, J. Chem. Phys. **82**, 284 (1985).

[18] S. R. Langhoff, C. W. Bauschlicher, and H. Partrige, J. Phys. **B18**, 13 (1985).

[19] S. Huzinaga, J. Andzelm, M. Klobukowski, E. Radzio-Andzelm, Y. Sakai and H. Tatewaki, *Gaussian basis sets for molecular calculations* (Elsevier, Amsterdam, 1984).

[20] W. C. Ermler, Y. S. Lee, K. S. Pitzer, and N. W. Winter, J. Chem. Phys. **69**, 716 (1971).

[21] H. Nakatsuji, Chem. Phys. **75**, 425 (1983).

[22] M. Dupuis, J. D. Watts, H. O. Viller, and G. J. B. Hurst, Program System HONDO7, Program Library No. 544, Computer Center of the Institute for Molecular Science, (1989).

[23] H. Nakatsuji, Program system for SAC and SAC-CI calculations, Program Library No.146 (Y4/SAC), Data Processing Center of Kyoto University, 1985; H. Nakatsuji, Program Library SAC85 (No.1396), Computer Center of the Institute for Molecular Science, Okazaki, Japan, 1986.

[24] (a) H. Nakatsuji, Y. Matsuzaki, and T. Yonezawa, J. Chem. Phys. **88**, 5759 (1988);
(b) C. A. Masmanidis, H. H. Jaffe, and R. L. Ellis, J. Phys. Chem. **79**, 2052 (1975);
(c) S. Kato, R. L. Jaffe, A. Komornicki, and K. Morokuma, J. Chem. Phys. **78**, 4567 (1983).

[25] C. E. Moore, *Atomic Energy Levels* (National Bureau of Standards, Washington, D.C., 1971), Vol. 2

[26] J. Holmtzmark, Ann. Phys. (leipzig) **58**, 577 (1919).

[27] A. Jablonski, Phys. Rev. **68**, 78 (1945).

[28] S. Y. Chen and M. Takeo, Rev. Mod. Phys. **29**, 20 (1957).

[29] G. Alber and J. Cooper, Phys. Rev. **A33**, 3084 (1986).

[30] U. Buck and H. Pauly, Z. Physik **208**, 390 (1968).

LIST OF PUBLICATIONS

PART I.

Chapter 1. "SAC-CI (symmetry adapted cluster-configuration interaction) Method Applied to High-Spin Multiplicity."
H. Nakatsuji and M. Ehara, J. Chem. Phys. **98**, 7179-7184 (1993).

Chapter 2. "Hyperfine Splitting Constants Studied by the SAC-CI (symmetry adapted cluster-configuration interaction) Method."
H. Nakatsuji and M. Ehara, to be submitted to J. Chem. Phys.

Chapter 3. "Exponentially Generated Configuration Interaction (EGCI) Method Applied to High-Spin Multiplicity."
M. Ehara and H. Nakatsuji, J. Chem. Phys. **99**, 1952-1961 (1993).

PART II.

Chapter 4. "Theoretical Study on the Excited and Ionized States of Titanium Tetrachloride."
H. Nakatsuji, M. Ehara, M. H. Palmer, and M. F. Guest, J. Chem. Phys. **97**, 2561-2570 (1992).

Chapter 5. "Theoretical Study on the Excited and Ionized States of $TiBr_4$ and TiI_4."
H. Nakatsuji and M. Ehara, to be submitted to J. Chem. Phys.

PART III.

Chapter 6. "Collision-Induced Absorption Spectra of CsXe System Studied by SAC-CI Theory."
H. Nakatsuji and M. Ehara, Chem. Phys. Letters **172**, 261-264 (1990).

Chapter 7. "Collision-Induced Absorption Spectra of CsRg System (Rg=Xe, Kr, Ar, and Ne) Studied by SAC-CI Theory."
H. Nakatsuji and M. Ehara, to be submitted to J. Chem. Phys.

Other publications not included in the present thesis.

(1) "Multiphoton Ionization of Rb_2 in the Wavelength Range 620-670 nm"
H. Suemitsu, H. Kitaura, R. Yokoyama, M. Ehara, and H. Nakatsuji,
J. Phys. B.: Atomic, Molecular and Optical Physics **25**, 4507-4517 (1992).

(2) "Quantum Chemical Studies of the Molecule in the Excited States"
H. Nakatsuji and M. Ehara, Annual Report of Research Institute
for Organic Synthetic Chemistry **6**, 115-129 (1992).